Categorisation and Discrimination of Automotive Glass Fragments by Laser Ablation Inductively Coupled Plasma Mass-Spectrometry (LA-ICP-MS) for Forensic Purposes

THE UNIVERSITY OF
WAIKATO
Te Whare Wānanga o Waikato

A thesis submitted in partial fulfilment

of the requirements for the degree

of

Master of Science in Chemistry

at

The University of Waikato

by

MEGAN NICOLE CLARE GRAINGER

The University of Waikato
2010

Abstract

Glass is one of the most common types of trace evidence found at crime scenes and on suspects. Refractive index is presently used for matching recovered and control samples of glass. However, increased quality control in manufacture has substantially reduced the spread of RI values and many samples can no longer be distinguished. Therefore analysis of glass by elemental techniques is required if samples are to be distinguished.

This research project was carried out on behalf of the Institute of Environmental Science and Research (ESR), Auckland. The aim was to develop a method to analyse automotive glass fragments by laser ablation inductively coupled plasma mass spectrometry (LA-ICP-MS), and create a database which can be used to categorise samples into country of origin and to distinguish samples. 244 glass samples were obtained from ESR which contained 162 laminated and 82 toughened samples from a range of vehicle makes and models manufactured between 2002 and 2006.

Two calibration standards (NIST 612 and FGS 2) were compared for their ability to calibrate float glass. FGS 2 is a better standard due to its closer composition to float glass and was used for this research. 23 elements were initially analysed and assessed for accuracy, precision and long term stability. This was cut down to 15 elements for the final method. The relative accuracy and precision of these elements was less than 5 % when compared to the literature values. An inter-laboratory comparison study showed most elements had less than 10 % bias between laboratories when analysing float glass. However, Sn had over 25 % bias between the two laboratories.

A homogeneity study of three panes showed no spatial variation for most elements. However, the three Pb isotopes showed spatial variation in the windscreen. In addition, outliers were found for replicates of some database samples and the pooled standard deviation for the database was very large, indicating Pb is not homogeneous in glass.

Multivariate analysis was used to investigate the natural splitting of the data. The splitting was influenced by the country of origin from which the raw materials were sourced from for glass manufacture. Australian samples had a clear separation from all samples originating from the Northern Hemisphere. A multiclass classifier correctly categorised 86.87 % of samples into the vehicles' country of origin. Correct classification was not higher due to importation of some glass. For example, Australia imports glass from Thailand for the Falcon and Commodore ranges.

Statistical methods were compared in their ability to discriminate fragments. The elemental composition range overlap method allowed 80.39 % (164/204) discrimination between samples. Only small elemental variation between Australian samples was observed. With Australian data removed, 93.59 % (146/156) of samples could be distinguished. A three-step method was created to increase the distinguishing power; this used a combination of elemental composition and RI. This procedure was able to distinguish 84.31 % (172/204) samples from the entire database and 94.87 % (148/156) samples with Australian data removed. This method decreased the occurrence of type II errors.

Acknowledgements

Firstly I would like to thank my supervisor Merilyn Manley-Harris. Who knows where I would have ended up if you hadn't decided to take a chance and invite me to work in your lab as a first year student! Your faith in me has helped me get to where I am today. I appreciate all the opportunities you have presented me with and all the doors you have helped to open. Even though you seem to have more graduate students than fingers, you always find the time for me, whether it be lightning-fast proof-reading and e-mail replies or juggling your day for a meeting. I have enjoyed the last five years and I am looking forward to working with you for my PhD thesis.

Sally Coulson, thank you for initiating this project and giving your supervision throughout it. Your e-mail replies were always very prompt even when you weren't in the office! I appreciate all the time that you have put into helping me improve my thesis.

To Steve Cameron, thank you for your tireless effort in maintaining the LA-ICP-MS in good working order. Thank you for your weekend calls into the instrument room. Your help has been appreciated.

To Ray Littler, from the University of Waikato Statistics department, thank you. Without your help I would still be staring at a screen of numbers trying to figure out what to do next. Thank you for the time that you spent and the patience you showed while you were helping me get my head around statistics. I learnt a lot and I think you also learnt more than you bargained on in helping me out!

A very large part of this thesis could not have been completed without the donation of the float glass standard from Stefan Becker. Thank you to Brad Gibson from Mitsi World, Novus in Frankton, Hamilton, Te Rapa Parts, Hamilton and Keith Jones for your contributions of glass samples.

Christopher May (Centre for Forensic Science, University of Western Australia), thank you for your interest in my research and offering to help with the inter-laboratory comparison. The time you have taken has been much appreciated.

Dale Fletcher, thank you for your help with the Weka analysis. I appreciated the extra time you have spent thinking about my research.

Thank you to Cheryl Ward, the librarian who is only an e-mail away. You have gone above and beyond the call of duty to help me. Your help has been much appreciated, not only throughout my Masters research, but undergraduate degree as well. I am very grateful to you for taking on the huge task of proof reading.

I am very thankful to have received scholarships to help me through this part of my journey of study. With these contributions I have been able to focus on my research without needing to find a night job. My sincere thanks go to ESR, University of Waikato, Todd Foundation Trust, Woman's Graduate Trust and Bonded Merit for their financial support. Thank you to New Zealand Institute of Chemistry (NZIC) for helping with travel costs to attend a conference in Australia.

To Gwenda Pennington, thank you for your continual help for scholarship applications and for being a friend and mentor. I always enjoy our enlightening conversations. Thank you for taking the time to set up a mock interview to help me through the real one.

Thank you to all the Chemistry staff, technicians and students at The University of Waikato including, in no particular order, Jolene Brown, Maria Revell, Cody Wright, Simon Williams, Sam Pachal, Nicky Cameron and Jacob Jaine. You have all made this journey an exciting one. Being part of the Chemistry department is like being a part of a large dysfunctional family, but I wouldn't change one thing about it. Thank you for all the conversations (serious and otherwise), laughs, fun and memories.

Cody, thank you for all your advice to my never ending questions and for stating the obvious when I was in too deep to see it myself!

Jake, thank you for reminding me that there is a whole world out there which doesn't involve my thesis, without it the last six months would have existed between the lab and my computer. Thank you for helping me to take a step back every so often and relax. Your support and encouragement has been unwavering.

The last thanks are saved for the most important people in my life. This is the first time I can acknowledge my parents, Roy and Wendy, in print for all their love and support they have given me continuously throughout my life. Mum, thank you for always being there with advice, to proof read or just to listen. Also thank you for looking after me when I was lost in the world of 'thesis'. Dad, thank you for your unwavering support, encouragement and ability to instantly cheer me up. Thank you both for believing in me, even when I didn't believe in myself. You have never given up on me. Thank you for always being by my side through all the highs and lows. My appreciation and love for your both is beyond words.

Table of Contents

List of Figures

List of Tables

List of Abbreviations

σ	standard deviation
µ-XRF	Micro x-ray fluorescence
AFM	Atomic force microscopy
alr	Additive-log ratio
AMU	Atomic mass unit
ANOVA	Analysis of variance
ASTM	American Society for Testing and Materials
BKA	Bundeskriminalamt
CFS	Centre for Forensic Science
CI	Confidence interval
clr	centred-log ratio
cps	Counts per second
CRM	Certified reference material
CSV	Comma separated values
DRC	Dynamic reaction cell
EC	External calibration
ENFSI	European Network of Forensic Science Institutes
EPG	European Paint Group
ESR	Institute of Environmental Science and Research
FGS	Float glass standard
FI	Fractionation index
GLITTER	Gemoc Laser ICP-MS Total Trace Elemental Reduction
ICP-AES	Inductively coupled plasma atomic emission spectroscopy
ICP-MS	Inductively coupled mass spectrometry
ID	Isotope dilution
IS	Internal standard
ISO	International Organization for Standardization
LA-ICP-MS	Laser ablation inductively coupled mass spectrometry
LCL	Lower confidence limit
LF	Left front
LIBS	Laser-induced breakdown spectroscopy
LOD	Limit of detection

LOQ	Limit of quantification
LTSA	Land Transport Safety Authority
LR	Left rear
LRQ	Left rear quarter
MDL	Minimum detection limits
Nd:YAG	Neodymium-doped yttrium aluminium garnet
NFI	Netherlands Forensic Institute
NIST	National Institute of Standards and Technology
NITECRIME	Natural Isotopes and Trace Elements in Criminalistics and Environmental Forensics
PCA	Principal component analysis
PI	Prediction interval
PIXE	Particle induced X-ray emission
ppb	Parts per billion
ppm	Parts per million
QC	Quality control
R	Rear
RF	Right front
RI	Refractive index
RR	Right rear
RRQ	Right rear quarter
RSD	Relative standard deviation
SEM-EDS	Scanning electron microscopy energy dispersive spectroscopy
SRM	Standard reference material
SEM-EDX	Scanning electron microscopy energy dispersive x-ray
TRA	Time resolved analysis
UCL	Upper confidence limit
UoW	University of Waikato
Weka	Waikato environment for knowledge analysis
WS	Windscreen
WS_F	Windscreen front (pane)
WS_B	Windscreen back (pane)
XRF	X-Ray fluorescence

1 Introduction

1.1 Glass

Glass is an ubiquitous material. It has a number of uses due to its inert, non-porous nature[1]. Glass can be referred to as a 'solid liquid'[2]. This is due to the high disorder at the submicroscopic level. Above two atoms the ordering is random[3]. Glass becomes a solid without undergoing crystallisation during cooking[2]. The American Society for Testing and Materials (ASTM) define glass as 'an inorganic product of fusion that has been cooled to a rigid condition without crystallising'[4,p.1.].

Glass has an interesting history dating back to 3000 B.C. The first manufactured glass was not translucent or transparent and was manufactured for aesthetic purposes, such as glaze on ceramic vessels[5, 6]. There are many references which discuss the history of glass in detail[5, 7, 8].

1.2 Glass categories

The chemical composition of glass determines its physical properties. Glass can be manufactured to suit specific niches[1].These are generally divided into one of four categories – soda-lime glass, borosilicate glass, lead glass and speciality glass[3]. There are numerous sub-categories of glass which include flat glass, glass containers, optical glass and fibreglass[6].

1.2.1 Soda-lime glass

More than 90 % of all glass is soda-lime glass, which is comprised of silica sand (SiO_2, 63-74%), soda ash (Na_2CO_3, 12-16%) and limestone (CaO, 7-14%)[3, 9]. It has a relatively fixed composition making it easy to recycle. The raw materials are inexpensive and found throughout the world. The glass is strong, easy to melt, simple to shape and has good chemical durability[3, 6]. Pure sand is able to form glass on its own. However, soda ash and potassium oxides are added to lower the

melting point. Limestone is used to give glass its insoluble properties in water and increase chemical durability[9]. Soda-lime glass is used for the manufacture of flat glass. This includes most bottle-,sheet-, and window- glass as it is suited to automatic-machine forming methods[3]. Soda-lime glass is of most interest to forensic examination.

1.2.2 Sodium borosilicate glass

Sodium borosilicate glass was originally developed early last century to stop hot railway-signals shattering when exposed to cold rain. It has high chemical durability and low thermal expansion, making it ideally suited to demanding industrial and domestic use, such as in chemistry labs, for cookware and pharmaceutical ware[3]. *Pyrex* is a type of sodium borosilicate glass. It has very small thermal expansion due to approximately 12% wt B_2O_3[1].

1.2.3 Lead glass

Lead glass is comprised of silica sand and lead oxide. It is expensive due to the cost of the raw materials and the vigilance required to exclude air bubbles when melting the glass. It is easy to mould by hand due to the slow rate of increase in viscosity with decrease in temperature[3].

Lead glass has a high refractive index (RI) due to lead oxide replacing the calcium content of glass, which makes it visually appealing. It is often used in high quality art and table ware. Lead glass also has high electrical resistivity. Therefore it is also used in special electrical applications[3].

Lead crystal tableware contains silica (55.7 %), alumina (0.2 %), iron oxide (0.02 %), lime (0.2 %), soda (0.1 %) and lead oxide (31.4 %). However, some lead glass can contain up to 92 % lead oxide[7].

1.2.4 Speciality glass

There are many types of speciality glass. Each is manufactured to have properties to suit a specific niche. They have clearly defined chemical and physical properties[10]. A brief outline of two speciality glasses, laser glass and fibre glass will be touched on for interest.

1.2.4.1 Laser glass

The random structure of glass allows broad emission and absorption which provides higher efficiency, more energy storage and greater energy per pulse than any other material. Thus it is ideally suited as a host material for lasers. Neodymium is the only rare earth ion used in commercial applications[3].

1.2.4.2 Fibre glass

There are three types of fibre glass; insulation wool which are short-fibres used for thermal and acoustic insulation, continuous fibres which are used in electrical insulation, cement and plastic reinforcement and special purpose fibres which are used for heat resistance and light-weight materials[11]. In 1991 fibre glass accounted for 9 % of all glass produced[10].

1.3 Glass manufacture

The production of glass is a sophisticated process[12]. Raw materials are selected according to their oxide content, purity and grain size. Regardless of the type of glass being produced, the raw materials are accurately weighed and mechanically mixed to form a homogenous batch[3]. Recycled glass or cullet (waste glass from a previous batch) is added. This prevents wastage and decreases the heat needed to melt the batch. The batch is transported to the furnace for melting. It is heated by gas or oil and melts between 1425 – 1600°C depending on the composition[6]. Figure 1.1 depicts the float glass manufacturing process.

Most glass is melted using a continuous furnace. Molten glass is withdrawn from the working end, while batch and cullet are added continuously to replace the

glass that has been taken out. Once melted, the glass is ready to be shaped in one of four ways: blowing, pressing, drawing or casting[6].

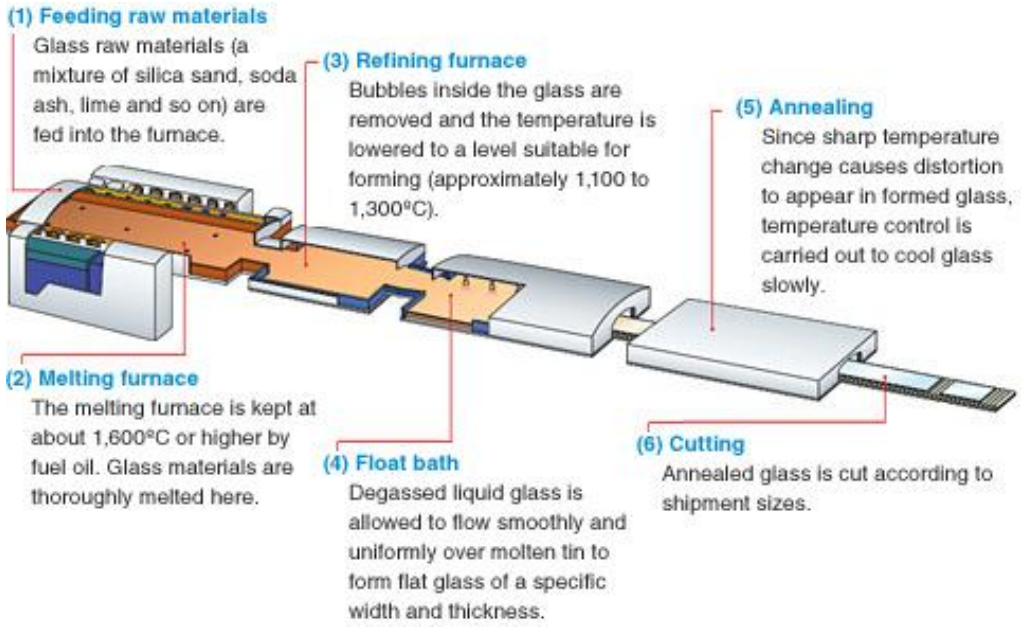

Figure 1.1 Float glass manufacturing process[13].

1.3.1 Sheet glass

Sheet glass is produced by continuously drawing glass vertically through a slotted refractory. It is ground and polished to remove any deformations[9].

1.3.2 Float glass

Most glass is produced using the float glass method which was developed by Pilkington brothers in 1952[9, 14]. There are about 169 glass manufacturing plants around the world which use the float glass process[15]. The molten glass floats across a bath of molten tin and cools to a temperature at which it is still rigid. Tin is denser than glass. Its melting point (232 °C) is lower than glass but its boiling point is much higher than the melting point of glass. Therefore it can be used as a stable, non-reacting liquid for the float glass process[16].

During manufacture, the non-float surface is exposed to a hot reducing N_2/H_2 atmosphere within the tin bath. This side ends up depleted in species such as Fe,

Na_2O, CaO and SO_3. Therefore it has a locally higher concentration in Si which decreases the RI value. In comparison, the float surface has a higher RI value due to Sn[17].

The float glass process forms even sheets of glass which require no polishing as imperfections are melted out by careful temperature control[3]. The sheets are annealed to eliminate tension due to uneven cooling and to strengthen the glass[6].

Float and container glass have similar Si and Na content (~34 % and ~10 % respectively) but different levels of Mg (~ 2.5 % compared to 0.5 %) and Al (~ 0.4 % and ~ 1 %)[18]. Iron oxides in float glass are approximately 0.07 to 0.16 % (w/w) and in containers are 0.03 to 0.15 %[19].

1.4 Secondary modifications in glass manufacture

1.4.1 Tempered glass

Tempered safety glass is a single sheet of glass which has been reheated until almost soft then chilled suddenly to make it stronger than the original glass[6]. This heating is in addition to the annealing process in the production of float glass. The rapid cooling causes the surface of the glass to be slightly less dense than the centre which puts the centre under extension and the surface under compression. An object breaks more easily under extension than compression so the glass must be subjected to a tough shock in order for it to break. The mechanical energy which was accumulated during tempering is aggressively released causing the glass to shatter entirely into small blunt fragments[1]. This property makes it suitable for use in side and rear windows of automobiles and glass doors[6].

1.4.2 Laminated glass

Laminated safety glass consists of a non-glass sheet placed between two sheets of glass. Originally celluloid, a cellulose nitrate plastic, was used. However, it was not the best choice of material; it required additional adhesive and sealer to bond with the glass, was not very resistant to impact and its strength was not uniform across the range of temperatures it was exposed to outdoors[7].

Presently a resin, such as polyvinyl butyral, is used to hold two sheets of glass together. The laminated glass is exposed to slightly increased temperature and pressure to bond the three sheets together [3].
When laminated glass is struck, the crack radiates from the centre of the impact. The broken pieces of glass remain firmly fixed to the plastic sheet. If there is a force on the window the plastic stretches and the glass fragments stay in place [6, 7]. Laminated glass is used for automobile windscreens.

1.5 Components and chemical modifications of glass

It is possible to have an unlimited number of glass compositions. However, in practice the basic mix is limited by the ease of melting, the temperature range over which the glass is malleable, its durability and the access of raw materials. These factors, in addition to increased precision in manufacturing processes, result in most manufacturing plants having very similar products[20, 21].

The chemical composition is ultimately determined by the overall glass manufacturing process, including the amount and kind of cullet added to the batch and the raw materials. Some elements and their concentrations may reflect the origin of the raw materials[22].

The chemical composition of glass has remained reasonably consistent for the last 30 years. Glass manufacturers are constantly making small adjustments to float glass to obtain desirable properties at the lowest possible cost. Increased Fe levels are now found in automotive glass to create thinner glass which is not compromised in strength or UV protection. The thickness of automotive glass has decreased from 6.5 mm to 4 mm over 30 years[23].

1.5.1 Major components

The composition of soda-lime glass has been relatively unchanged for hundreds of years. As previously stated, it is comprised of silica sand (SiO_2, 63-74%), soda ash (Na_2CO_3, 12-16%) and limestone (CaO, 7-14%)[3, 9].

1.5.2 Minor, trace and ultra-trace elements

As well as the major components, glass contains a broad array of minor, trace and ultra-trace elements, which are not monitored during glass manufacture processes. These include aluminium (Al), barium (Ba), calcium (Ca), iron (Fe), magnesium (Mg), manganese (Mn), strontium (Sr), titanium (Ti) and zirconium (Zr)[24].

Trace elements may be unintentionally added through impurities in the raw material. These elements are directly related to the site from which the material was collected[21]. Examples of impurities which can be used for discrimination of glass include iron and chromium introduced from sand, magnesium and aluminium oxides from lime, potassium oxides from soda ash and strontium from dolomite[9].

Cullet used in the manufacturing plant is mostly sourced from within the plant when producing sheet glass. However, some container plants use recycled consumer glass which adds some heterogeneity between batches from the same plant. Another source of unintentionally added elements is from corrosion of the inner surfaces of the furnace as they age; this leaches elements into the molten glass. Therefore glass from different sources will have widely varying elemental profiles which is fortuitous from a forensic point of view[25].

Alternatively, trace elements may be purposely added during the manufacturing process to alter properties, such as colour, of the glass[20]. Vibrantly coloured glass can be produced by adding different metals. Metals used include copper (red and blue-red), iron (black, brown and green), antimony (yellow), cobalt (blue, green, pink), manganese (purple), cerium (yellow), gold (red), titanium (purple, brown) and tin (white)[1, 25].

There is a natural correlation between lanthanum and cerium. However, this correlation may not be observed as Ce_2O_3 is added during manufacture as a decolourising agent. It dissociates at a high temperature. The release of oxygen increases the partial pressure of the gas and converts the metal to the stable tetravalent form, facilitating the oxidation of the ferrous ion to the colourless

ferric ion[26]. SbO, $NaNO_3$, $BaNO_3$, K_2SO_4 or $BaSO_4$ may also be used to decolourise glass[9].

Alkali metal oxides improve the melting properties of glass but lower its chemical resistance. Al_2O_2, CaO, MgO and BaO are stabilisers used in glass to increase chemical resistance[27]. To produce transparent glass the raw materials need to be of high purity and contain less than 0.1 wt % of iron oxides[1]. In addition Fe may alter furnace temperature during manufacture[19].

1.6 Sources of glass in New Zealand

1.6.1 Manufacture of glass

Large scale manufacture of bottles did not occur in New Zealand until 1922 when the Australian Glass Manufacturers Company opened in Penrose, Auckland. This was later renamed New Zealand Glass Manufacturers and is still producing bottles today[28, 29].

Up until the late 1950s, New Zealand imported flat glass. In 1961, the McKendrick Glass Manufacturing Company Ltd was opened but could not produce satisfactory glass and closed later in the year[30].

In 1963, Pilkington Brothers Ltd and Australian Consolidated Industries Ltd formed a partnership which set up a glass plant in Whangarei called New Zealand Window Glass Ltd. 30, 000 tonnes of glass were produced each year. By 1988, 40 % of the glass was exported to Australia, Japan and the Pacific. The plant closed in 1991. After this, importation of window glass into New Zealand was required[30].

A review of glass between 2004 -2007 by Koons stated that there is an increased globalisation of glass manufacture. New float glass plants were being constructed in countries including Russia, India and China at the time the review was published[23].

1.6.2 Automotive sources

From the 1960s to the 1990s, Toyota assembled cars in Thames and Christchurch. However, during the 1990s it moved to the importation of overseas assembled vehicles[31]. New Zealand no longer produces or assembles any makes of vehicles.

Land Transport Safety Authority (LTSA) has published information relating to the vehicles on New Zealand roads. The 2008 data shows that most imported cars originate from Japan (Table 1.1and Table 1.2). However, the country of previous registration refers to the country the car was last registered and may not reflect the country of manufacture of the vehicle.

Table 1.1 Main countries of manufacture of new cars (including ex-overseas)[32]

Country	2008, %	2003, %
Australia	7.12	8.27
Japan	67.30	75.77
United Kingdom	1.44	1.92
All others	24.13	14.04

Table 1.2 Main countries of previous registration of ex-overseas (used imported) cars[32]

Country	2008, %	2003, %
Australia	0.87	0.46
Japan	94.71	96.55
United Kingdom	0.64	0.29
All others	3.77	2.70

1.7 Glass in forensic situations

Glass is valuable case work evidence as it is commonly found at crime scenes, including car accidents, burglaries, assaults and vandalism. Fragments may be transferred to clothes, shoes and hair of people who were at the scene of crime. These fragments, which are frequently less than 0.5 mm in size, are persistent and are likely to go unnoticed. Therefore they can easily be carried to another site or

transferred to other people or items. This forms links to the crime scene[33, 34]. These samples can be recovered and analysed as glass is chemically stable and has physical and chemical properties which can be measured. Fragments from the source can be collected to use as control samples. These are compared with the recovered samples to find a match.

For forensic purposes, glass is generally classified into 5 categories: sheet (window or float glass), vehicle window, vehicle headlamp (borosilicate glass), container (bottle, jar) and tableware (including lead glass)[18]. As previously stated, soda-lime glass is of most interest for forensic examination[23].

The two main aims for forensic analysis of glass lie in classification of a glass fragment and comparison of two fragments. Comparison aims to determine whether two fragments of glass originated from the same glass object. Classification determines the type of glass fragment, for example, building, automotive window or headlight or container. Classification is important if no control sample is available. By categorising the sample, forensic investigators may be able to refine their search. Comparison of two samples may allow a suspect to be convicted or exonerated[33].

DNA fingerprinting and polymerase chain reaction (PCR), used to amplify DNA, were introduced in 1985[35]. Since the 1990s, there have been rapid advances of DNA interpretation for forensic purposes. Blood, semen and saliva are important DNA rich sources. This has become a routine technique for crime scene investigation and is widely accepted in court. In cases where DNA data is available, trace evidence analysis can be used to strengthen the case.

DNA is not always available and cannot answer all questions concerning a crime. Trace evidence, such as glass, paint, textile fabrics and soil, may be the only evidence with which to solve a crime in the absence of DNA and fingerprints. In addition, glass found on a victim from a hit-and-run may help to identify the vehicle involved. Elemental analysis is the final stage of glass comparison and is used to distinguish glass with similar RI values[18].

The first case in New Zealand to use glass as evidence for a crime was in 1933. Glass fragments were recovered from a person suspected of breaking a shop window. The tiny shards of glass were given to the Dominion Laboratory who carried out analysis using density and RI. 65 samples were compared to the recovered sample, with only the glass from the shop window matching the sample[9].

Until the early 1980s, only restricted information was obtained from glass. However, due to the advancement of analytical instrumentation quality information can now be obtained from glass fragments, allowing glass to become valuable evidence[27].

In 1999, 6 % of case work at the Australian Federal Police Forensic Services lab was reported to involve analysis of glass fragments[36]. In 2000, 20 % of casework in New Zealand involved glass work[9]; the majority of this being analysis of float glass[37].

1.8 Transfer and collection of glass

Nelson and Revell (1967) discovered that some glass disperses in the direction of the force when broken. This is known as back scatter. It is accepted that some fragments will hit anyone within close proximity of the shattering glass. In the majority of cases the fragments are small (usually between 0.1 to 2 mm) and irregularly shaped. Hit-and-run and ram raids may produce larger fragments[9].

From the late 1980s, New Zealand has applied a likelihood ratio and in recent times have also incorporated the continuous method to compare recovered and control glass fragments. The first step is to compare control and recovered fragments using a t-test (for two fragments) or Welch test (for > 2 fragments). The continuous method replaced the t-test and Welch test in the mid 1990s for determining the match/non-match of glass as it prevents a blunt match/non-match. The second step examines the evidential weight of the findings by using the likelihood ratio method which requires two hypotheses. The first is that the suspect is the person who committed the crime, and the second is that the suspect

did not commit the crime. For the second hypothesis to be true it is assumed the suspect has come from a random population. Therefore it is important to survey a population that will best represent the background level of glass found in the general population.

A critical question to consider is, "What is the probability of finding glass evidence on clothing given the defendant was not at the scene?" There are a wide range of publications examining the number of glass fragments on random populations. The results are variable; it has been reported that the population, geography, and method of analysis are all factors which influence the results[38].

In 1971, Pearsons *et al*. from Britain, researched this question and found numerous fragments of glass on clothing. The study used a non-bias sample set of men's clothing obtained from a dry cleaning business. However, they targeted pockets and cuffs, where glass is likely to accumulate. The findings of this study have been used in Australian courts as the background level of glass on a given member in the community[36].

Petterd *et al.* (1999) believed the findings from Pearsons *et al.* were not relevant to Australia in the 1990s. They conducted a study using the exterior of upper garments from people of all ages and backgrounds in Southern Australia. They report the natural level of glass fragments on clothing of members of the community as very low. Only 6 of the 2008 (0.3%) garments had glass fragments. Each garment only had one fragment, giving strength to the use of glass analysis. 3 of the 6 samples had RI values which corresponded to float glass, two samples may have been headlight glass[36]. If these results are reflective of populations other than Southern Australia, finding multiple glass fragments on a piece of clothing would be very noteworthy.

Many studies have been conducted to determine transfer rates of glass from the scene to a person and from a person to another area[39-41]. Hick's *et al.* studied the rate of glass transfer to clothing when the wearer broke a pane and how long the fragments stayed on the garment. The results were variable but they concluded the transfer depends on how many strikes and the distance the person is from the glass.

The retention depends on the time and weave of fabric[42]. Other studies report transfer is dependent on fabric type and size of particles[39].

Allen *et al.* have extensively studied the rate of transfer of glass in different circumstances, including transfer from a breaking window to someone in the vicinity[43], transfer of glass by various methods[44], transfer from a contaminated person to a non-contaminated person[45] and transfer from an item's surface to a person[46].

In Australia, around 235 glass cases are analysed each year. One third of these cases involve footwear. Roux *et al.* reported glass fragments were recovered from 7.3 % of shoes examined. 5.9 % were embedded in the sole while the remaining 1.9 % were found in the upper area. Less than 0.3 % of the samples contained fragments in both areas and the occurrence of matching fragments was very rare. Therefore it is significant to find glass on the sole and upper area when fragments match[47].

In New Zealand, Coulson *et al.* (2001) examined the frequency of glass on outer clothing (surface and pockets of garments and upper and soles of footwear). They examined clothing from people attending a gymnasium and compared the findings to people suspected of a breaking crime. They reported those suspected of a breaking crime had more fragments of glass on the surface of their clothes compared to the general public[38].

1.9 Techniques used for glass discrimination

Glass manufacture has improved considerably over the years and has become more controlled. Variation in optical and physical properties of glass has decreased and it is not uncommon for glass from different origins to have the same physical properties. The use of RI, the primary method of discrimination, is now limited. Therefore there is a requirement to develop a new technique for discrimination[12].

The samples may only differ at the trace element level of the glass samples. This variation can provide a unique elemental fingerprint which will allow for discrimination and comparison of samples. Due to the small size of most recovered fragments, the need to retain the evidence, and the increased control in the manufacturing process, techniques for analysis need to be selected wisely[48].

1.9.1 Physical and optical examination

In New Zealand, surface features of individual fragments are assessed as one method to analyse glass in a forensic situation[38]. Most physical examination can only be carried out on large fragments of glass[9]. This includes colour and fracture match and the density of the sample.

1.9.1.1 Colour match

Large fragments can be viewed through different light against a neutral or complementary background. However, this technique may be subjective and visible spectroscopy appears to have limited discrimination. Small fragments are unable to be analysed by colour as very small coloured fragments will appear clear[9].

1.9.1.2 Fracture match

Large fragments can also be analysed by the jigsaw approach. An unknown source can be matched to the control sample by piecing the edges together[9]. Broken fragments have a unique morphology which can be matched unambiguously to adjoining surfaces[23].

Guin and Wiederhom examined whether fracturing in silicate glass is brittle or ductile using atomic force microscopy, concluding glass is completely brittle. Therefore each fracture has a unique morphology[49]. However, the matching of two edges in casework samples is rare[25].

1.9.1.3 Density

The density of glass can be determined by the sink-float method. The most common density test is performed by placing the fragment in a tube with liquid that is approximately the same density. A miscible liquid is added until the glass floats[9]. However, toxic liquids are often required and at least 5 mg of sample is needed. In addition, measurements of small, irregular or dirty fragments may not be accurate. Density measurements have now been replaced by RI measurements[25].

1.9.1.4 Refractive index (RI)

RI is the primary method for analysis of glass in New Zealand. RI is able to detect changes of major elements in glass. The higher the mass density and/or atomic number of elements in a piece of glass, the higher its RI will be, due to the association with a greater electron density. Therefore glass with large proportions of heavy ions, such as Pb or Ba, have larger RI values. The density and therefore the RI, depends on the rate at which the glass has cooled through the transformation region. The change in RI is very small, affecting only the third decimal place[20].

In 1985, Stoney and Thornton reported the need for both RI and density data for interpretation of glass[39]. In the same year Brown reported a correlation between RI and density, with a correlation coefficient of 0.93. Therefore very little supplementary information is gained by using both RI and density methods. He reported RI as the quicker and easier method for glass determination[50].

Automated glass RI measurement (GRIM) is used for RI analysis. The RI of glass is the ratio of the velocity of light in a vacuum to the velocity of light in the glass fragment[51]. It is measured using the immersion method in silicone oil, which was first reported by Slater and Fong in 1982[52]. The measurement is limited by the contrast between the fragment and the oil it is immersed in. The edge of the sample is critical to the contrast. Decreased edge contrast increases RI variation. Recovered samples may be very small. Therefore low edge counts are obtained, compared with control samples[53].

In 1982, the variation of RI due to the structural stress of a glass pane was first reported. This allowed tempered glass to be distinguished from soda-lime glass due to the very noticeable RI difference between the bulk and surface caused by the intentionally added stress[52]. Since float glass has not been tempered the difference is a lot smaller. A set of RI data was obtained by English Forensic Science laboratories which showed that annealing produced a more uniform RI over the fragment[54]. Annealing is often used in forensic interpretation to relieve the structural stress before RI data is obtained[17]. However, in 1994 Cassita and Sandercock reported RI data after annealing may not be reliable[55]. Suzuki *et al.* reported a variation in RI of up to six times in glass which has been heated compared with the usual variation within a pane[56].

Early research showed variation of RI values in toughened, thicker non-toughened and container glass[53]. RI values have also been reported to vary between the surface and bulk of the glass. Around one third to half of recovered glass fragments are from the glass surface[37].

Glass is assumed to be homogenous for RI measurements. Locke and Hayes (1984) reported this may not hold true for toughened windscreen glass. Bennett *et al.* extended this research to float glass. They reported observable differences across the pane even though there were no systematic differences in RI[37].

While RI has simple sample preparation and short analysis time, there is a higher chance of incorrect matching of the sample and control fragments due to only one variable which can be evaluated[56]. In addition, with improved quality of manufacturing processes, the optical and physical properties of glass have been well regulated. Glass from a certain manufacturing plant has little variation between batches, reducing discriminating ability[9]. Glass manufacturers now target a certain RI to give the most favourable physical and optical properties. Therefore the deviation of the RI measurement in glass by the same manufacturer over time and different manufacturers is very small[57]. Glass measured by RI for an FBI database between 1964 and 1979 shows a large spread of RI values (Figure 1.2). A survey of a more recent period (1980-1997) has a much reduced spread of data, (Figure 1.3) with values that overlap each other, thus there is limited potential for

discrimination between fragments[58]. Stoecklien reported that more than 10 % of float glass examined from 32 plants could not be distinguished by RI and gave type II errors[‡15]. In 2008, RI of float glass in Australia was reported to lie between 1.5189 – 1.5194[17].

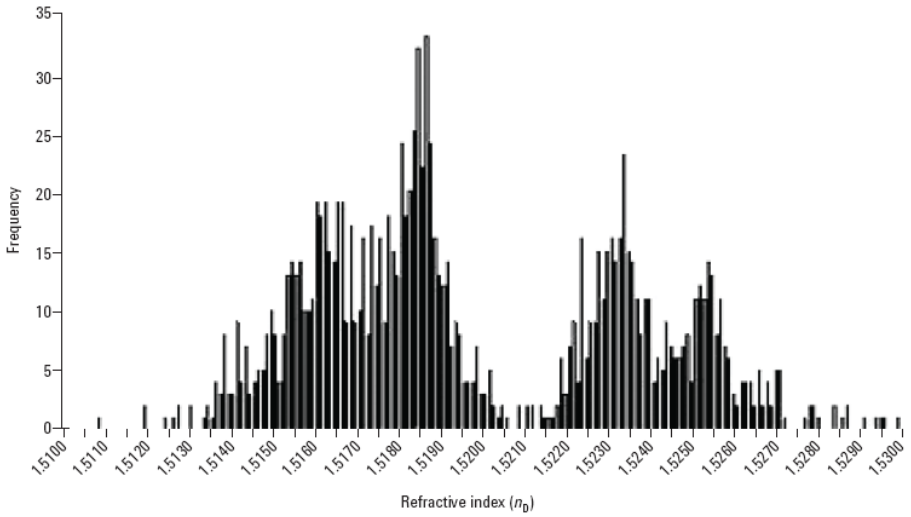

Figure 1.2 Distribution of RI values in a FBI database of flat glasses, 1964 to 1979 [58,p.2.]. There is a wide range of RI values making discrimination of glass samples possible.

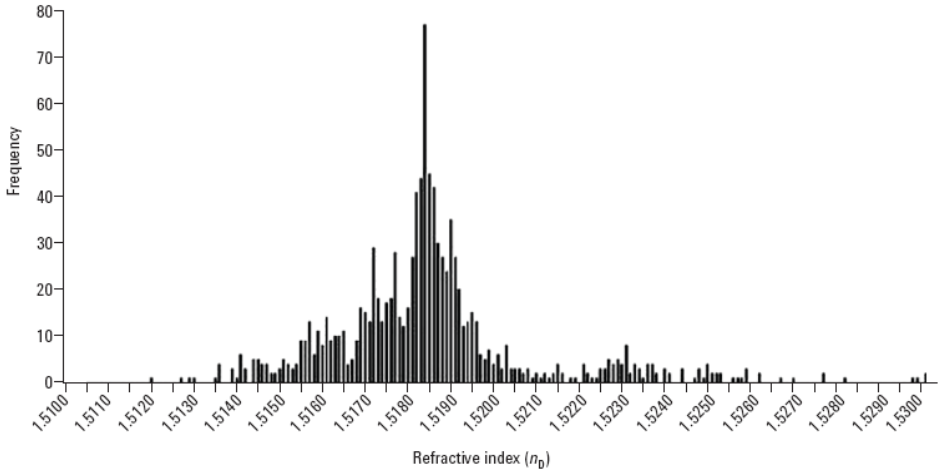

Figure 1.3 Distribution of RI values from a FBI database of flat glasses, 1990 to 1997 [58, p.2.]. The range of RI values is reduced as manufactures target a certain RI value. This has led to decreased discrimination of glass samples by RI.

‡ A type II error occurs when two samples are said to be the same, but are from different populations (false inclusion)

A similar observation was made by Coulson *et al.* who examined the RI of 246 samples (164 laminated glass and 82 toughened glass) from vehicles between the years 2002-2006. They reported that the RI measurements were moving from a bi-modal distribution (RI peaks at approximately 1.5199 and 1.5207) seen in their 1999-2001 study, to a uni-modal distribution (RI peak at approximately 1.5201). The same phenomenon was observed when the samples were divided into laminated and toughened glass categories[59].

At a 2005 conference, Becker and Dücking reported preliminary results of RI values of glass after they have been exposed to laser heating during LA-ICP-MS (213 nm) for elemental analysis. They reported RI values could not be readily measured on the immediate crater edge. In addition, RI measurements on the edges near the crater showed increased variability. However, this did not affect the mean of the samples[23].

Research has been conducted on using annealing as a discriminating technique. However, this has limited ability to further discriminate samples. Float glass has a wider spread of measurements after annealing. There was a decrease in the variation for toughened glass, but not enough to increase discrimination[60].

1.9.2 Elemental composition

RI can no longer provide enough information to associate or exclude fragments. Additional techniques, such as elemental analysis, are now used instead of, or in addition to RI, to enhance informing power of the comparison between fragments. The elemental composition of a sample can be used to detect differences which physical methods are unable to pick up[9]. Trace elements are not regulated during glass manufacture, so are valuable for analysis. Therefore minor variations in the elemental composition of the glass are seen between and within batches which act as a unique fingerprint for each sample. Comparison of multiple elements increases the probability of correctly matching an unknown fragment to a control sample[56]. In addition, glass is relatively homogeneous within a single pane which allows discrimination of fragments arising from separate sheets and association of fragments from the same source[25].

Since 2004 there has been a shift in published literature from RI to elemental characterisation which reflects active research[23]. Quantitative chemical analysis of small glass fragments has become accepted as a powerful tool for classification and discrimination. Early reports showed it as a useful supplement to other techniques[23].

A wide range of instruments have been trialled for elemental analysis of glass due to laboratories using machines which are available to them. Each machine has its own set of advantages and disadvantages[9].

1.9.2.1 X-Ray methods

X-ray is a common technique in forensic analysis due to its non-destructive nature, its minimal sample preparation and ability to provide multi-elemental data[23]. X-rays can be induced by X-rays (e.g. X-ray fluorescence (XRF)), electron beams (e.g. scanning electron microscopy coupled with an energy dispersive X-ray spectrometer (SEM-EDX)) or particle beams (e.g. particle induced X-ray emission (PIXE)). Traditional X-ray methods are well developed and accepted for glass analysis so there is not a lot of recent literature[23]. The following sub-sections will give an overview of different X-ray methods, and discuss their advantages and disadvantages.

1.9.2.1.1 Scanning electron microscopy energy dispersive x-ray (SEM-EDX)

SEM-EDX is used for many forensic elemental comparisons, including glass. SEM-EDX has been able to categorise samples, such as optical glass, from windows or car headlamps due to their vastly distinctive features. Optical glass was found to contain more potassium or barium since these elements enhance the optical properties of the glass[33]. SEM-EDX can only detect major and minor elements in glass (O, N, Ba, Al, Mg, Si, K, Ca, Fe) due to its high limit of detection on glass (1000 ppm)[25]. Trace elements such as Ti, Sr, Zr, Cr, Cu and Co are below the detection limits of the SEM-EDX method making it unsuitable for robust glass analysis[33]. In addition precision is poor and analysis is slow[25]. Therefore SEM-EDX is not a good method to use for discrimination of glass.

1.9.2.1.2 X-Ray fluorescence (XRF)

Nishiwaki and co-workers used total reflection X-ray fluorescence (TXRF) to differentiate 23 glass types by calculating the ratios of Mn, Pb, Rb, Ti and Zn to the Sr content with precision typically less than 8.1 %. TXRF uses grazing incidence for the incoming X-ray beam instead of 45°[18]. These samples were unable to be differentiated by RI. Less than 0.5 mg of sample was needed. This was dissolved in 100 µl of HNO_3/HF and condensed to 10 µl then dried onto a silicon wafer.

The group also used synchrotron radiation XRF to ratio 34 isotopes to Ba. The precision was less than 8.2 %. They reported Bi, Cs, Mo, Pd and Sb were the most discriminating elements[61].

Micro XRF (µ-XRF) spectrometry was commercially introduced in the early 2000s which led to an increase in publications concerning forensic characterisation of small particles[23].

Roedel *et al.* examined glass particles between 50 µm and ≥ 1 mm in size. Quantitative analysis with good precision and reproducibility was obtained for fragments ≥ 1 mm as they were adequately thick and had reduced morphological effects[62].

Up until 2004 most µ-XRF studies analysed data qualitatively as quantitation was difficult due to the unknown energy distribution of the excitation spectrum. In 2005 Padillia *et al.* used a standardless calculation to overcome this problem which they demonstrated using glass certified reference materials (CRM)[63].

XRF has reasonable precision and discriminating power for glass is fair. However, analysis time is slow, it requires more than 100 µm of sample and the limit of detection on glass is 100 ppm[25].

1.9.2.2 Laser-induced breakdown spectroscopy (LIBS)

Laser-induced breakdown spectroscopy (LIBS) is a fairly new technique and has been used for slightly over ten years. LIBS focuses a laser beam on a sample which produces atomic, ionic and molecular emission processes to determine elemental composition of a sample.

LIBS have fast sample preparation and high sample throughput. Its sensitivity is 10-50 ppb which allows small samples to be precisely measured[57]. In addition it is relatively non-destructive, portable and less expensive than LA-ICP-MS[23]. LIBS can be distinguished from conventional spectrochemical techniques by its simultaneous multi-element ability and low detection limits. However, it has poor precision (5-10 %) and shows matrix and spectral interferences[64]. LIBS are also limited by a high background continuum, line broadening and self-absorption. LIBS is best suited for relative elemental concentration determination in a sample rather than absolute determination[65].

One study using LIBS identified glass fragments by their unique fingerprints and statistical correlation methods. An unknown sample was identified by matching its spectra to one in the available database. The spectra from the fragments were also compared to verify if they were from the same source. The developed method was tested using 10 automotive glasses from a range of manufacturers between 2002-2007. 100 % identification was possible using a 95 % confidence interval[64].

Bridge *et al.* analysed 23 automobile float glass samples and reported 83 % discrimination using LIBS. They used 18 emission wavelengths to form 10 different ratios of emission intensities. Hourly analysis of a single sample revealed the daily % RSD variation to be between 0.8 and 15.0 %. Due to a small sample set and fast analysis, all samples were analysed over 12 hours to avoid the inter-day variation[65].

93 % of samples were discriminated at the 90 % CI and 82.2 % at the 99 % CI. By using both LIBS and RI data 98% of samples were discriminated at the 90 % CI and 95.6 % at 99 % CI[65]. The study was extended to four types of glass

(automotive windows, headlights, side mirrors and bottles) giving 87 % discrimination at the 95 % confidence interval[66].

1.9.2.3 Inductively coupled plasma atomic emission spectroscopy (ICP-AES)

Almirall *et al.* analysed clear container, vehicle and non-vehicle float glass and headlight glass collected between 1992-1997 in the US. They were analysed by RI and ICP-AES. Headlight glass had a considerably lower RI than the other three glass categories and was the only type which could be discriminated by RI alone. Container glass had a low Mg concentration (0.35 %) compared to float glass (2 %). Vehicle and non-vehicle float glass were identified by Fe content (0.3 % and 0.1 % respectively)[34]. Al, Br, Ca, Fe, Mg and Sr were used alongside RI values in Fisher's linear discrimination to classify glass into one of the four categories. 92 % of container glass was correctly assigned. All headlight samples and float glass samples were correctly assigned. However, the latter were not all correctly assigned as vehicle/non-vehicle[34].

ICP-AES has a detection limit <100 ppm in glass and has good precision. However, analysis time is slow and sample throughput is low. In addition, 5-8 mg of sample is required for each replicate[25].

1.9.2.4 Inductively coupled plasma mass spectroscopy (ICP-MS)

An argon inductively coupled plasma (ICP) joined to a quadrupole mass spectrometer was first developed in 1980. The ICP-MS became commercially available in 1983-84 and its popularity rapidly increased. ICP-MS has a wide dynamic range. Nine orders of magnitude can be obtained when the detector is used in the pulse-analog mode. A quadrupole mass filter is most commonly used, which allows fast scanning over the mass spectrum[67].

One of the first reports of ICP-MS as a technique for glass analysis was in 1990. 15 elements were used to discriminate glass from different origins. Glass from USA and Australia was also able to be categorised[68]. ICP-MS has been used at the Forensic Science Institute of the Bundeskriminalamt (BKA), Germany, for glass analysis since 1992[15].

Duckworth *et al.* used ICP-MS to find the best elements to discriminate glass fragments. They studied the variance due to sample population, sample dissolution and replicate measurements. They found dissolution affected B, Cu, Ag and Ni the most[69].

Early work on ICP-MS was able to determine 48 elements with a RSD of 4 % or less. Australian window glass was successfully discriminated from USA glass[68]. ICP-MS has been applied to elemental analysis of 13 elements with RSDs less than 3.2 % for bottle glass. The ICP/RI analysis was superior to RI alone and could differentiate the 13 pairs that RI alone could not[70].

Montero *et al.* analysed glass evidence from a crime where a person broke 15 vehicle windows. Glass from the suspect and vehicles were analysed using ICP-MS. All samples were differentiated and four control samples were matched to those from the suspect. The traditional methods (density, RI and thickness) were unable to correctly associate all the samples[12].

A review of elemental techniques has found ICP-MS offers the most information. It has 10 – 100 times the sensitivity of ICP-AES, allowing ultra-trace element detection. In addition, it has low detection limits, ability to analyse a wide range of elements and isotopic information can be gained[69]. ICP gives better detection limits and discriminating power than other elemental techniques, for example XRF and scanning electron microscopy energy dispersive spectroscopy (SEM-EDS)[71].

ICP-MS is the preferred method of detection when glass may have been exposed to high temperatures from fire in illegal entry as there is no significant variation when analysed[56].

ICP-MS is a reasonable technique for glass analysis as it has excellent precision and discriminating power as well as low detection limits (< 2 ppm in glass). However, there are factors which prevent it from being a top technique for glass analysis. It has low sample throughput and analysis is slow. Aqueous analysis is limited by a minimum sample mass for digestion, which glass fragments are not

likely to meet[72]. 2 mg of sample per replicate is required for analysis. In addition, dissolution of glass may result in the loss of elements (Hg, Cd, Se, As, Th, Ga, Ge, Bi) by volatilisation. Other elements (Zr, Hf, Ta, Nb, Ti, Th, U) may be chemically inert giving incomplete dissolution. The rare earth elements form insoluble fluorides in HF preventing quantitative analysis unless they are broken down. Also the stability of elements vary significantly once they are in solution. Some elements require high concentrations of acid (for example 20 % v/v hydrochloric) to stay in solution. Some elements which require these conditions are Nb, Hf, Ta, Sn and Ti[21].

1.9.2.5 Laser ablation inductively coupled plasma mass spectrometry (LA-ICP-MS)

ICP-MS has been utilised for over 25 years. However, from 2004 the number of publications using solution based ICP-MS as an analytical technique for glass analysis declined due to the increase in LA-ICP-MS. During the period 2004-2007 several hundred publications involved LA studies for glass.

LA-ICP-MS is the instrumental technique that was used for this research. A detailed account is given below.

1.10 LA-ICP-MS

Although ICP has many advantages, problems such as long preparation times and contamination from solvents led to the development of alternative methods for sample introduction. One of these is the use of laser ablation (LA) to analyse solid samples[73]. Coupling of a laser to an ICP-MS originated because the instrument possessed high sensitivity which was a requirement for analysis of the small quantity of sample which is ablated[74].

Laser ablation involves focusing a laser beam onto a sample in an airtight ablation chamber. When the laser strikes the solid sample it is converted to a fine dense aerosol[75]. A carrier gas, for example He or Ar, sweeps the material into the ICP-MS where the sample is introduced to the plasma and ionised. The resulting ions

are passed through the interface and guided through the mass analyser for mass to charge separation, then passed to the detector[76].

An assortment of parameters can be varied on the laser to optimise the ablation for a given sample. This includes spot diameter, laser power, ablation mode, ablation chamber gas type and flow rate[77].

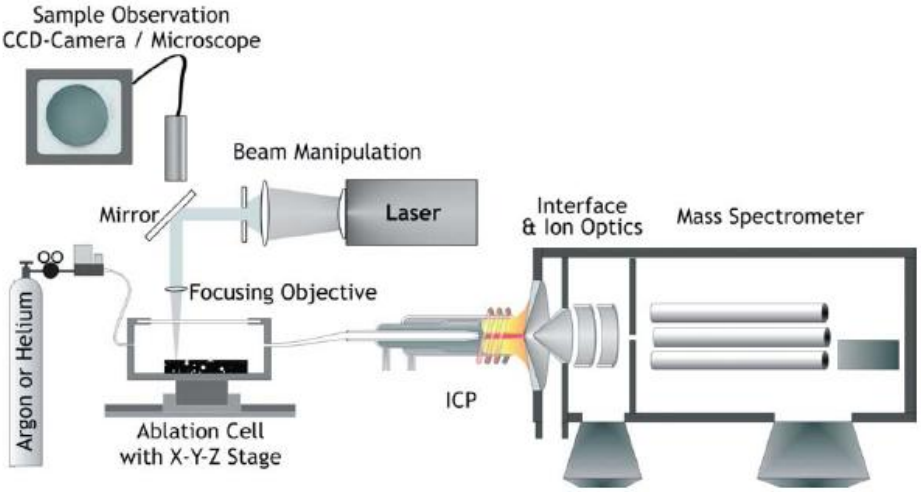

Figure 1.4 Schematic set-up of LA-ICP-MS[67, p. 256].

The operating principle of LA remains virtually unchanged since it was introduced in 1985 by Alan Gray. However, the wavelength of the laser, pulse to pulse stability and optical set-up have been notably modified[74]. The first lasers (1985) were based on solid-state ruby lasers (694 nm), but were unsuccessful.

Neodymium-doped yttrium aluminium garnet (Nd:YAG) lasers are the most common laser source for LA-ICP-MS due to their reliability, ease of use and affordability[78]. Nd:YAG lasers operating at 1064 nm, did not have potential in the analytical community as they have been found to interact differently with diverse matter due to the samples absorbing light differently. The absorption of silicate-based glass is variable depending on the chemical composition at this wavelength. This discovery was followed by the development of lasers which emit in the ultra violet region[79].

In the last 20 years most available laser wavelengths have been combined with ICP-MS. The wavelength used has decreased due to advantages of a shorter

wavelength[67]. It was not until the 1990s that the frequency was doubled (532 nm), quadrupled (266 nm) and quintupled (213nm) by using optical components[76]. The 213 nm laser became commercially available in 1999[78].

1.10.1 Advantages of analysis by LA-ICP-MS

Laser ablation is an efficient method which has many advantages over other analytical techniques. It has the advantages associated with ICP-MS with the added benefit of solid sampling. Only about 280 ng of sample is used per analysis which makes it relatively non-destructive[48]. This is 10,000 times less sample than needed for digestion (2-5 mg). This is valuable for forensic cases where very small quantities of sample are recovered and sample consumption needs to be minimised. The sample can then undergo further analytical methods to strengthen the discrimination process and is preserved for evidence in court[19, 33, 75]. Analysis of samples that are difficult or impossible to digest is also made possible.

In dissolution work, contamination may prevent samples from being differentiated by elevating the background level and masking low level elements in the sample, thus reducing the number of elements which can be used for discrimination[21]. The limit of detection in LA-ICP-MS is < 1 ppm[25]. Samples analysed by LA-ICP-MS can be examined with no prior preparation thus there is less chance of contamination by acid sample handling[75]. Also, without acid, spectral interferences, such as $^{40}Ar^{35}Cl^{+}$, are reduced. This allows better detection of the ion of interest[73]. An additional bonus is that 80 % of overall analysis time is eliminated[71].

LA-ICP-MS allows simultaneous detection of elements and isotopes, detecting all major, minor and trace elements (0.02 wt %) in a single measurement allowing maximum discriminating power in minimum time. A central attribute of LA-ICP-MS is its sensitivity as many elements are detected at very low levels with excellent precision[22, 67]. The detection of a wide range of elements improves the discrimination power[21]. Each sample takes approximately two minutes, giving high throughput. It has time resolved analysis, which allows instant feedback on

data[72]. Additional data, such as the lateral distribution of elements, can also be obtained[15] .

1.10.2 Analysis of glass using LA-ICP-MS

The use of LA-ICP-MS as a technique for forensic glass analysis has been reported since the early nineties. A research group at Florida International University has been studying the elemental composition of glass for forensic purposes for over a decade. Organisations such as the European Natural Isotopes and Trace Elements in Criminalistics and Environmental Forensics (NITECRIME) have taken time to develop a standardised method using LA to quantitatively analyse glass[80]. Early work by Moenke-Blankenburg *et al.* showed LA-ICP-MS of major elements had good accuracy and precision. They reported it showed the promise of replacing traditional wet-chemical methods of analysis[81].

Almirall *et al.* (Florida, Miami) analysed 46 automotive windscreens and side windows, which were actual casework samples provided by the Centre of Forensic Sciences (CFS), Toronto Canada. This consisted of 18 windscreens and 28 side or rear windows. They also analysed 45 headlights from a range of vehicles over a 20 year range collected from wrecking yards. The results were compared with external calibration (EC) ICP-MS, isotope dilution (ID) ICP-MS and RI. 1035 comparison pairs were made for the windows. 471 pairs were indistinguishable by RI, but only 3 were indistinguishable when combined with LA-ICP-MS data. This is comparable to EC-ICP-MS and ID-ICP-MS which had only one indistinguishable pair[71].

Trejos *et al.* also analysed glass from CFS[I]. They used isotopic ratios to compare samples to eliminate inter-day variation between samples. 45 % of automotive pairs could not be discriminated by RI alone. Analysis of the same samples by LA-ICP-MS resulted in only 0.7 % indistinguishable pairs. When coupled with RI, 0.3 % of pairs were indistinguishable (3 of 1035 pairs). They compared this to

[I] This research was carried out at the National Centre for Forensic Science and Department of Chemistry, University of Central Florida

external calibration and isotopic dilution methods using ICP and reported LA had superior accuracy and precision[82].

Bridge *et al.*(Orlando, Florida) analysed 23 automotive float glass samples using a raster[II] sequence[83]. LA-ICP-MS was able to discriminate 100 % of samples without requiring the data to be coupled to RI measurements. When analysed by LIBS only 83 % of the samples could be discriminated.

Berends-Montero *et al.* validated a method using LA-ICP-MS. Glass was obtained from a float glass manufacturer in the Netherlands, a Dutch supplier and a local shop window in the Netherlands. They tested ruggedness of the method by testing laser energy, energy output, crater diameter and nebuliser flow at two different levels. Out of all the elements tested, only Zn was affected at a confidence level of 99 %. The variation of the results between different parameters over a range of days was found to be no larger than that for samples in the same experiment. They used the method to analyse fragments from building windows. Precision and accuracy were less than 10 % for all samples analysed and the limits of detection were in the order of ppm[84].

Naes *et al.*[III] analysed 41 automotive fragments ranging from 1995 – 2005 from wrecking yards in Miami, Florida. Isotopes with similar responses were ratioed to diminish the effect of pulsating carrier gas flows (e.g. $^{7}Li/\ ^{53}Cr$ and $^{23}Na/\ ^{24}Mg$)[57].

Zurhaar and Mullings tested Australian and USA glass by ICP-MS and found they could be distinguished. However, they only used three samples from the USA and four from Australia[68].

1.11 Calibration and standards for LA-ICP-MS

Calibration is very important for all analytical techniques. Laser ablation is no exception. Quantification of data from LA-ICP-MS involves three areas of concern:

[II] Raster – A pattern of parallel lines
[III] Naes is from National Centre for Forensic Science and Department of Chemistry, University of Central Florida

1) Calibration of the mass response of the ICP-MS, as it has been found to be an unstable instrument requiring frequent recalibration.
2) Correction for difference in ablation yield of standard and sample, due to the different responses.
3) Correction of non-stoichiometric effects which occur due to the different volatility of elements causing fractionation[85].

One disadvantage of LA is optimisation of the laser as the parameters change depending on the matrix. Method development is therefore dependent on the matrix of the sample. Calibration of the laser using solid standards can be problematic as it is difficult to get matrix matched standards.

There are a variety of methods which can be used for calibration. At present, LA-ICP-MS is commonly calibrated on liquid solution before coupling to the laser. However, there are reports of problems associated with liquid ablation and simultaneous feeding of both dry and wet aerosol into the plasma. Gunter *et al.* reports the use of simultaneous solution aerosol with a drying system and laser-induced aerosol to diminish the formation of oxides and polyatomic species[86].

1.11.1 External standards

External standards are the most commonly applied form of calibration for LA-ICP-MS. Matrix-matched standards are necessary for calibration as the amount of sample ablated per laser pulse is dependent on the matrix. Matching the standard and sample helps to avoid fractionation difficulties[75]. The use of external calibration by itself is not ideal due to fluctuations in the laser output caused by small differences in the target matrix[82].

The NIST standards manufactured by National Institute of Standards and Technology are the most widely used standards for calibration of LA-ICP-MS. However, these have been reported to have heterogeneity for at least 25 of the trace elements due to areas of depleted volatile and siderophile[IV] elements, and

[IV] Element commonly found in metallic phases e.g. Ni and Co.

enrichments of Cu, Cd, Fe and Mn. These areas occur near the rim and also in irregular streaks throughout the disk[85].

NIST 610 and 612 (400 mg kg^{-1} and 40 mg kg^{-1} respectively) are commonly used standard reference materials (SRM) for laser ablation. However, their composition differs slightly to that of float glass. The weight % of each can be seen in Table 1.3. Latkoczy *et al.* reported variation of up to 60 % in results when using NIST 610 and 612[87].

Table 1.3 Composition of float glass and NIST standards

Compound	Float glass, wt %	NIST 610 and 612, wt %
SiO_2	72	72
NaO_2	13	14
CaO	8	12
MgO	4	mg/kg level
Al_2O_3	-	2

New float glass standards were produced in 2002 by SCHOTT, Germany; these are FGS 1 and FGS 2. They have 16 elements and are closer to the composition of soda-lime glass than are the NIST standards. Their composition is the same as soda-lime glass, but differs by a factor of five, based on the concentration by previous elemental analysis using ICP-MS. Latkoczy *et al.* reported improved results with the use of new glass standards. This reduced the variation to < 10 %[87].

Smith *et al.* reported FGS 2 gave more accurate results than NIST 612 for float glass, but for analysis of container glass there was less significance in the difference of the results when either NIST 612 or FGS 2 were used[80].

1.11.2 Internal standards

For a quantitative result the amount of aerosol entering the ICP must be known; however, this is rare. Therefore using an internal standard along with an external standard improves the quality of the data and makes the method more robust[85].

Internal standards are also able to correct for matrix suppression or enhancement and instrumental drift. The element chosen for the internal standard is the least abundant isotope of a major element[80]. The concentration is usually determined by another technique. The Si content is high and invariable in glass[87, 88]. ^{30}Si, the least abundant isotope (3.09 %) is interfered with by NO^+. Therefore ^{29}Si (4.7 %) is commonly chosen as the internal standard[57, 80].

Reports of ^{42}Ca as the internal standard have been documented. Latkoczy *et al.* reported Ca gave enhanced accuracy and precision for Sr, Zr, Ba, La and Ce. However, Si was the element of choice due to its constancy[87]. Montero reported that Ca gave better results for the analysis of NIST 612, but when the matrix was changed Si gave better results. She suggested that this was due to the assumption that the internal standards were constant in all glasses and equal to the ones in NIST 612[89].

Using an internal standard for quantitation is preferred compared to using isotopic intensities as fluctuations within the signal, as well as systematic errors, can be corrected for. The internal standard also minimises inter- and intra- day variation[57].

1.11.3 Aspirated solutions

Calibration using aspirated solutions has been reported; the carrier gas from the laser is joined to an aerosol from solution nebulisation. The introduction of liquid into the plasma eliminates the advantage of a dry plasma and also introduces contamination which can raise the background level and increase polyatomic interferences[85, 86]. Desolvation can reduce polyatomic problems. However, it gives non-quantitative results for some elements. Therefore solution calibration has limited use[85].

1.11.4 Liquid ablation

Liquid ablation has been reported as a viable calibrating procedure for solid sample analysis. Liquid standards are placed in a well and covered with a thin

film for ablation. It has the advantage of use when solid standards are not suitable[85].

1.11.5 Normalisation of totals to 100 %

Normalisation of totals to 100 % is an alternative to normalising concentrations to a single internal standard. All concentrations are calculated and normalised to 100 % which corrects for differences in standards and samples without prior knowledge of the sample's chemistry. However, all significant elements must have their concentration accurately determined[85].

1.11.6 Fractionation

Elements behave differently during laser ablation, which can lead to elements fractionating relative to each other and to production of signal intensities which are not representative of the target material[85]. There are two types of fractionation; absolute and time dependent. Absolute fractionation occurs when the aerosol composition does not chemically match the solid sample. In time dependent fractionation, the aerosol chemical composition alters during repeated ablation of a sample[90]. Ablation, transport and excitation contribute to elemental fractionation[91].

Fractionation by the laser is also an issue. It can occur during drilling mode due to the change in diameter-to-depth ratio[90]. There are a lot of studies dedicated to examining this phenomenon. While these are not directed purposely at forensic glass analysis, they use NIST glass standards making the results applicable[23].

Fractionation indices have been calculated to give a fractionation index (FI) which is a comparative measure of fractionation relative to Ca. Günther has reported the relative values of FI are independent of the matrix and operation conditions. However, these affect the absolute degree to which fractionation occurs. Therefore if an element has a different FI to the internal standard, the wrong ratio will be measured and inaccurate results given. This can be overcome by closely matching sample and standard matrices as well as parameters for analysis.

Elements analysed which have a similar FI to the internal standard will give accurate results regardless of the matrices and parameters. Si is the best internal standard for the transition metals[85].

Fractionation has been reported to lessen when using short wavelength UV lasers since all matrices tend to absorb with the same efficiency[85].

1.12 Method development in LA-ICP-MS

LA-ICP-MS was first used as an analytical method to quantitatively distinguish between glass samples by Becker and colleagues[15].

In the past ten years, there has been an increase in the published research concerning quantitative elemental analysis of glass using LA-ICP-MS. Organisations such as NITECRIME have spent time developing a method by which to analyse glass samples from crime scenes. Various factors, such as size of fragments, sample preparation and laser conditions have been studied in depth.

Netherlands Forensic Institute (NFI) were the first crime lab to validate a protocol using LA-ICP-MS according to the ISO/IEC17025 standards. The Bundeskriminalamt (BKA) have also validated a method similar to that of NFI[23].

A protocol for quantitative analysis of glass fragments was produced in 2005, by NITECRIME. Due to ongoing development, this was revised in 2007[87]. The European Network of Forensic Science Institutes (ENFSI) released a manual for analysing glass fragments in February 2009[15].

1.12.1 Samples

Glass fragments recovered from crime scenes and suspects vary greatly in size (>3 mm and 0.1 – 1 mm respectively). Therefore the way the samples are handled is important. Work has been done to ensure a small sample is representative of an entire window.

1.12.1.1 Sample preparation

Sample preparation is kept to a minimum across the literature. Smith *et a.l* reported washing fragments in methanol followed by 10 % nitric acid and rinsing with deionised water before analysis[80]. Trejos *et al.* scratched the glass surface with 3600 mesh sandpaper and washed with water then nitric acid before analysis[82]. Bridge *et al.* wiped glass surfaces with a Kimwipe® prior to analysis[65]. Other reports used no washing before analysis[92].

1.12.1.2 Mounting samples

Berends-Montero *et al.* chose to embed the fragments into an epoxy stub when possible. This achieved higher precision (1.4-5.5 % RSD) compared to those which were not embedded and held by double sided tape (6.8-14 % RSD). However, both sample preparation methods showed no significant differences for the means of all elements analysed, allowing for results to be used even if samples are not embedded[84].

Many articles report embedding their samples in resin for analysis[21, 87]. However, many fragments retrieved from crime scenes are very small and are unable to be embedded as this may cause damage or loss of the sample. Double sided tape, blu-tack™ and clay have been reported to hold small fragments for ablation[92, 93].

1.12.1.3 Homogeneity

Prior studies conducted using ICP-OES demonstrated mg-size samples were homogenous when used in dissolution methods. However, there was concern that the tiny samples used in laser may show heterogeneity. In 2005, Trejos and Almirall addressed this problem; they reported no spatial heterogeneity within samples using a 266 nm laser and 50 µm spot size[23, 88]. Becker analysed 34 fragments from a pane and reported there were no systematic changes in elemental concentration[15].

May analysed the float, bulk and anti-float portions of a float glass pane. He reported that the float surface is enriched in tin, but is depleted of other elements

and recommended the bulk of anti-float surface should be analysed[94]. This has also been reported elsewhere[57, 87, 93].

Float glass has been reported to have internal homogeneity. However, Montero reported LA can detect small variations of trace elements within a single pane. Montero reported glass from the same pane could be determined as two separate panes if the discrepancy of trace elements is not accounted for (when using LA)[95]. Therefore a number of samples from the control need to be collected in order to form a representative sample set[37, 89]. Bernerds-Montero *et al.* reported the variation over an entire window pane is encompassed within an interval of two standard deviations[84].

1.12.2 Laser parameters

There are many factors which could alter the result from the laser. This includes the type of laser and the mode used to analyse the samples.

1.12.2.1 Laser wavelength

Literature on forensic analysis of glass is divided between laser systems with solid state lasers with wavelengths of 213 nm[12, 57, 80, 84, 90] and 266 nm[48, 82]. Excimer lasers based on an ArF mixture with a 193 nm laser are also available but are not readily seen in the literature due to the expense of the instrument. 213 nm lasers have a greater degree of absorbance in transparent materials compared to 266 nm lasers, due to the shorter wavelength. They are reported to give a more stable signal for weakly absorbing samples, such as NIST glass[78]. They also produce a steadier signal more quickly than 266 nm lasers, allowing less data to be disregarded from the analysis[76].

Each type has different output energy, power density and beam profiles. Sub-ppb detection limits are obtainable using a large spot size (100 µm) with a 266 nm Nd: YAG laser. However, ultra trace detection of glass combined with a small spot size is not ideal using 266 nm lasers as small areas are difficult to ablate, causing the surrounding material to be removed. This causes large particles which lower

the precision in the ICP-MS as they are incompletely ionised. This limitation led to the development of 213 nm lasers which have a higher degree of absorbance in transparent materials[76].

Gonzalez *et al.* compared 193, 213 and 266 nm lasers using NIST glasses as the standards. They reported that 193 and 213 nm lasers produced shallow, flat bottom profiles in the crater, but 266 nm produced a deeper crater with more spikes. The different wavelengths ablated different amounts of sample, with the 266 nm laser removing the most sample and having the poorest depth resolution. The 213 nm laser had the best depth resolution for NIST 610 and 612[96].

1.12.2.2 Position in the ablation chamber

Berends-Montero reported no significant difference in results with respect to the position of the fragments in the sample chamber[84].

1.12.2.3 Size and shape of fragments

Trejos and Almirall investigated the effect of fragment size on quantitative analysis due to the heat dissipation and surface-laser interaction and found no significant difference for fragments down to 0.2 x 0.1 mm with a 99 % confidence level[48]. Other research has shown results are similar for various glass sizes and are independent of rough or polished surfaces[87].

Trejos and Almirall reported samples as small as 200 ng have a representative elemental fingerprint of an entire pane[88]. Berends-Montero *et al.* reported no significant difference in results between different sized fragments[84].

1.12.2.4 Drilling vs. scanning

Laser ablation can be performed by scanning (the sample moves under the laser) or drilling (the sample is stationary during analysis). Drilling provides a depth profile[90]. As casework samples are often very small, the method of analysis must be appropriate for sampling small fragments.

Scanning the surface of the sample delivers a steady supply of large particles to the plasma. This has definite matrix effects, lower precision and increased fractionation[80]. In addition, it increases the amount of sample consumed[94].

Drilling is also known as spot ablation. It is reported to provide a more reproducible signal, after the first 10 seconds, than scanning. Smith *et al.* reported increased precision when a spot was used for ablation, due to the steady supply of smaller particles[80]. Spot ablation is frequently reported in the literature with the most common spot sizes being 50, 55 and 60 µm for a 213 nm laser[12, 57, 80, 84, 94]. May reported that a 55 µm spot gave sufficient sensitivity and reproducibility, while using minimal sample[94].

Gonzalez *et al.* used a 213 nm laser to examine the difference between spot and line analyses on rocks using NIST series glass as calibration standards. They reported single spot sampling gave higher accuracy and precision than scanning. They noted this was increased when the first 15 seconds of sampling was eliminated from the data analysis[90]. In a further study they reported a double pulse ablation increased precision. The first pulse moves a mass of particles, after a time delay a second pulse breaks the mass into a fine aerosol for detection. They reported this technique also decreases fractionation[97]. However, double pulse ablation is not required due to the consistency of glass matrices which minimises the problems associated with matrix matching seen with other materials[23].

Bridge *et al.* analysed automotive float glass samples. Each sample was ablated four times, with a raster sequence, in the same area using 40 % power. Each spot was to a depth of 5 µm. The first layer was discarded while the other three were used for analysis. Each layer was compared to the same layer from other samples. It was reported that each layer had slight elemental differences. Each layer was able to discriminate the 23 samples with 100 % accuracy at the 99 % CI. The three layers were also averaged and used for analysis to provide a depth profile able to discriminate all samples at the 99 % confidence interval[65].

Naes *et al.* responded to Bridge *et al.* in 2008 with evidence that compared to a single spot ablation, the rastering technique for ablation is less accurate and

precise and that this results in increased Type I and II errors[57]. A type I error occurs when two samples are said to be different, but actually come from the same population (false exclusion)[98]. A type II error occurs when two samples are said to be the same, but are from different populations (false inclusion)[12].

1.12.2.5 Carrier gas

Carrier gas properties affect the ablation process and efficiency of particle transportation.

Reports in the early 1990s stated that nitrogen as a carrier gas improved signal intensities for high mass elements. Further reports stated nitrogen had reduced effects such as polyatomic interferences. $^{14}N^{14}N^{1}H^{+}$ interferes with $^{29}Si^{+}$, which is used as an internal standard[99].

Horn and Günther studied the effects of He, Ar and Ne as carrier gases for 193 and 266 nm lasers, using the NIST series of glasses. They reported the gas heavily controls particle size distribution for 193nm laser, but not the longer wavelength[100]. More particles deposit next to the crater under an Ar atmosphere compared to He[99, 100]. He gives a larger proportion of smaller particles compared to an Ar atmosphere. Therefore there is a sensitivity gain in the ICP-MS as these particles can be ionised efficiently[100]. Günther and Heinrich noted that the reduced material around the ablation crater may be caused by reduced plasma formation above the crater[101].

Horn and Günther suggest that since He has a higher thermal conductivity than Ar it may allow thermal energy to dissipate away from the ablation site leading to a more rapid end of condensational growth resulting in a greater number of smaller particles[100].

Günther and Heinrich reported a 2-3 fold sensitivity enhancement when He is used as the carrier gas, compared to Ar. Background intensity is decreased across the entire mass range[99].

1.12.2.6 Elements for analysis

^{88}Sr is reported as consistently being the best element for discrimination of glass[57].

Naes *et al.* only used five isotopes for discrimination. ^{49}Ti, ^{85}Rb, ^{88}Sr, ^{90}Zr and ^{137}Ba allowed 99.4 % discrimination of 820 pairs. There were rationalisations for the five indistinguishable pairs[57]. Montero reported Zr, Mn, Ti, Ce, Hf and Pb had the best discrimination power for automotive windows and Zr, Ce, Mn, La, Sr and Hf were the best elements for the manufacturer's survey[89].

The ENFSI best practice manual lists 20 major, minor and trace elements which are able to be quantified using both NIST 612 and FGS 1 and 2[93].

1.12.2.7 Dynamic reaction cell

Polyatomic interferences can greatly hinder detection of some isotopes and prevent accurate determination of their concentration. These can be minimised by correction equations but cannot be eliminated. A dynamic reaction cell (DRC) can be used to stop the formation of polyatomic species and hence eliminate their interference[76].

The collision cell sits in front of the quadrupole. Ions enter the collision cell where a reaction gas, such as H, He or CH_4, is bled into the cell and either converts the interference to a harmless mass or moves the analyte of interest to a new mass free from interference[76].

$^{40}Ar^{16}O^+$, $^{40}Ar^{16}O^1H^+$, and $^{40}Ca^{16}O^+$ interfere with $^{56}Fe^+$ and $^{57}Fe^+$ which limits discriminating power as Fe has been shown to be a useful element for glass analysis[19].

If an element does not have good precision (≤ 10 % RSD) and bias (≤ 10 %), the figures may not be included in analysis which limits Fe as an element for discrimination[19].

Günther *et al*. reported improvement in Fe data by using H as the reactant gas and Ne as the buffer gas. The LOD was enhanced from 5.9 µg g^{-1} to 2.1 µg g^{-1} for $^{57}Fe^{+102}$.

Castro *et al*. reported reduced interferences using DRC mode with CH_4 (0.3 vs. 9.5 µg g^{-1}) allowing lower detection limits and stronger analysis of Fe. While limits of detection are lowered, DRC cannot readily be applied mid-run as the conversion is not fast enough. In addition, it cannot be used for all isotopes as the reaction gas may interfere with other isotopes hindering their detection. Therefore each sample would need to be run twice to acquire DRC and non-DRC analysis[19].

Umpierrez *et al.* used methane as the reaction gas to eliminate interferences on $^{56}Fe^{+}$. The detection limit of $^{56}Fe^{+}$ in DRC mode is substantially lower than in standard mode (0.03 vs. 9.5 µg/g)[103].

1.12.3 Matching criteria

For forensic purposes the criteria used to compare two samples is critical to achieving significant results. This can be defined as the "matching criteria", which depends on both the homogeneity of the samples to be compared and the precision of the method used for detection. Glass has internal homogeneity which makes it good for comparisons. However, the small differences within a glass pane are detected by LA-ICP-MS and can complicate the results. Scheer used three measurements on one fragment of glass to create a database. However, she noted that collecting multiple fragments for measurement is better due to the small differences that LA-ICP-MS can pick up over an entire window pane. Analysis of multiple fragments will allow for better matching of samples[104].

Berends-Montero *et al.* investigated the variation of elemental concentrations within a single float glass pane as the magnitude of variation is related to the matching criteria. This work was carried out for multiple float glass in The Netherlands. They reported that the matching criteria must allow for these small differences within a pane of glass. They also report that there is a fine balance between assigning criteria that are too small and ones that are too large. One

which is too small will raise the probability of a false exclusion, type I error. Whereas if the matching criteria is too large a false inclusion, type II error, may occur[84].

1.12.4 Statistical analysis of glass data

The interpretation of data for forensic purposes is just as important as the recovery and measurement steps. With the wrong analysis, type I or type II errors may occur. This may either free the guilty or convict the innocent. A theoretically sound method is required in order for it to have a valid place within the court system.

Physical data in forensic analysis is often univariate, for example RI. Univariate data can be easily analysed by plots and summary statistics due to its single dimension. Almirall and Trejos state that the arithmetic mean, standard deviation and relative standard deviation are useful for describing the sample sets[25]. Recently forensic analysis has begun to collect multiple measurements for a sample. Each observation can be stored in a data matrix. Dimension reduction methods, such as principal component analysis (PCA), can be used to reduce the dimensionality so that data is more manageable[105].

There are a range of statistical methods found in the literature for the discrimination of glass. Discrimination of samples in forensic interpretation often occurs via a two step process. First, samples are compared to see if they come from a common source. This is the match/non-match step which involves using hypothesis testing. The 3-sigma method or the range overlap method are commonly applied[105].

1.12.4.1 Range overlap, confidence intervals and Student's t-test

Early work used overlapping RI values for statistical analysis. If the control and recovered samples overlapped the samples cannot be distinguished. However, with multi-element analysis, this method is no longer useful[27].

Confidence intervals assess whether the mean value of the recovered sample is within the mean value of the control sample with a plus or minus 2 or 3 standard deviations; if it is they are said to match. The size of the confidence interval depends on how certain an analyser needs to be that it contains the true value[25].

NFI has stated that 9 or more of 10 elements must have ranges that overlap or have values which are within two times a standard deviation measure[23]. Berends-Montero *et al.* used the average of the square of twice the standard deviations, $4s^2$, to differentiate double windows. The two sheets were able to be distinguished[84].

Zurhaar and Mulling stated that all 14 elements must match within a $\pm 3\ \sigma$ range for the sample to be deemed as originating from the same source[68].

BKA evaluated a number of match criteria and reported the best method to be using a standard deviation determined by long-term analysis of a standard reference material. The average of 6 measurements of the sample must concur within four-times the standard deviation[23].

The Student's *t*- test has the advantage that the statement of match or not match can be supported with a probability value[25]. Curran *et al.* suggested that Hotelling's T^2 test, a multivariate equivalent to the Student's *t*- test, may be a better method than the range overlap method[24].

1.12.4.2 Analysis of variance (ANOVA)

A pairwise comparison can be carried out when two or more samples need to be compared. This can be achieved by using analysis of variance (ANOVA). It indicates whether the means differ significantly. However, this is limited as it cannot tell which of the means are significantly different. The Tukey's post hoc test is able to provide this information. Almirall and Trejos state that this test is valuable for estimating the discrimination power of a technique where sets of a large number of comparisons are required[25].

1.12.4.3 Bayesian analysis

The Bayesian approach is where an event is more probable to occur under one of the two (or more) hypotheses. A measure of strength is given by assigning numbers and a set of rules[104].

Almirall and Trejos report the Bayesian approach as popular within the forensic community in the United Kingdom, in European academic institutions and in New Zealand[25].

Scheer reported the use of multivariate likelihood ratios, which is a type of Bayesian analysis. She examined the effect of repeated measurements and reported that the evidence value increases with increased measurements. Therefore there is higher discriminating power between two pieces of glass. Scheer also investigated the effect the size of the database has on likelihood ratios. She reported that as the database increases in size, the variation in the estimation of the natural logarithm of the likelihood ratio and the standard deviation both decrease. However, due to only taking a measurement from one fragment this work does not take into account the within-window variation[104].

A review by Koons reported the use of a full Bayesian analysis with calculation of likelihood ratios as inappropriate for use with multivariate data (elemental concentrations). This is due to unavailability of appropriate databases and the need for large sample sets[23].

1.12.4.4 Multivariate analysis

Multivariate and quantitative approaches have been used for matching glass samples. Becker reported quantitative analysis is better as it allows samples to be compared to other independent techniques such as ICP-OES[15].

Principal component analysis (PCA) is one method available to use as a match criterion for multivariable comparisons. An advantage of PCA is the simple graphic display. However, the theory behind it is complex[25].

Bajic *et al.* used PCA to distinguish between glass samples analysed by LA-ICP-MS. They were able to analyse the data without the need for matrix-matched standards for calibration as they examined the full mass spectrum[25].

Aeschliman *et al.* used PCA to differentiate four glass samples in a blind test using glass supplied by the Illinois State Police Forensic Science Laboratory. They report that PCA is efficient, reproducible and highly selective and has its own quality control. 32 elements were analysed and nine replicates were analysed for each sample. The score plot distinguished 1 and 2 from 3 and 4. A further model was needed to differentiate 1 from 2 and 3 from 4[92].

May used PCA and linear discriminant analysis (LDA) for discrimination of float glass. Samples which were of known time, date and location of manufacture were analysed. 96 % of samples could be discriminated by pairwise comparisons undertaken utilising forward stepwise linear discriminant analysis. The method allowed samples that were manufactured seven hours apart to be distinguished[94].

1.13 Research objectives

- To develop a method that will allow discrimination of automotive glass samples. This will include:
  1) Finding elements which have good precision and accuracy for glass analysis
  2) Determining the validity of NIST 612 and FGS 2 as standards
  3) Finding a robust set of parameters for the LA-ICP-MS by altering gas flows, laser power, spot diameter and ablation time
- Examining the homogeneity of panes of glass.
- Analysing glass relevant to New Zealand. This will be in the form of the 244 samples from ESR.
- Presenting data in a clear format.
- Initiating a database of automotive glass for use in a New Zealand context.
- Examining the possibility of using a database for forensic purposes. This will include:
  1) Categorisation of samples into country of origin

2) Distinguishing samples from other samples in the database

2 Method

2.1 Introduction

Laser ablation inductively coupled plasma (LA-ICP-MS) was the sole analytical technique used during this research for reasons outlined in section 1.10. The main goals of this research were to develop a method which would allow quantitative analysis of automotive glass samples for forensic purposes and to build a database of samples for discrimination.

2.2 Materials and general procedures

2.2.1 Solvents/Liquids

Methanol (Analytical grade) was purchased from Unichrom, Ajax Finechem Pty Ltd. Type 1 water (distilled and deionised) was obtained using a Barnstead system.

2.2.2 Laser ablation inductively coupled mass spectrometer

LA-ICP-MS was performed on a New Wave UP-213 laser ablation system fitted with a Nd:YAG 213 nm laser (New Wave Research, Fremont, California, USA) and was controlled by New Wave Research – Laser Ablation software.

The laser was connected to a PerkinElmer SCIEX ELAN DRC II inductively coupled mass spectrometer with a quadrupole mass spectrometer (PerkinElmerSciex, Concord, Ontario, Canada). The ICP was controlled by ELAN software, version 3.3.

For liquid calibrations the front end of the ICP consisted of a seaspray nebuliser and a baffled cyclonic spray chamber both from Perkin Elmer. A mixing block was used to dilute the sample 1:1 with water.

For solid calibrations and sampling the front end of the ICP-MS was attached to the laser using Tygon tubing which had an internal diameter of 3.1 mm.

2.2.3 Calibration solutions and solids

The ICP-MS was initially calibrated using liquid solutions to confirm its performance. Once verified, the laser system was coupled to the ICP-MS and solid calibrations were performed before starting analysis.

2.2.3.1 Liquid calibration solutions

ELAN DRC Setup/Stability/Masscal 10 ppb solution was used for X-Y calibration, ion lens voltage, auto lens calibration and daily performance.

The dual detector solution was used for dual detector calibration. This was made up by placing 50 mL Ca (1000 ppm), 17 mL Fe (1000 ppm) and 1 mL Merck XXI into a 1 L flask with 2 % nitric acid, and making it up to 1 L. 15 mL of this solution was placed into a Falcon™ tube (50 mL) and made up to 50 mL with type 1 water.

2.2.3.2 Solid calibration materials for LA-ICP-MS

Standard reference material (SRM) NIST 612 (trace elements in glass matrix, 50 $\mu g g^{-1}$), was obtained from the National Institute of Standards and Technology (NIST), Gaithersburg, MD. The certified values used for data analysis (Table 2.1) are from Pearce *et al.*[106].

The float glass standard 2 (FGS 2) was obtained from Dr Stefan Becker, Germany. This was manufactured by SCHOTT Glass, Germany. The values for FGS 2 used for data analysis were obtained from Latkoczy *et al.*[87](Table 2.1).

Table 2.1 Certified and consensus values for NIST 612[106] and FGS 2[87] (ppm)

Element	NIST 612	FGS 2	Element	NIST 612	FGS 2
^{7}Li	41.54	29.00	^{88}Sr	76.15	253.00
^{23}Na	103,719.00	100,500.00	^{90}Zr	35.99	223.00
^{25}Mg	77.44	23,400.00	^{118}Sn	37.96	94.00
^{27}Al	11,164.60	7,400.00	^{121}Sb	38.44	N/A
^{29}Si	335,916.80	341900	^{137}Ba	37.74	199.00
^{39}K	66.26	4,600.00	^{139}La	35.77	23.00
^{42}Ca	85,262.50	59,300.00	^{140}Ce	38.35	25.00
^{49}Ti	48.11	326.00	^{146}Nd	35.24	25.00
^{55}Mn	38.43	221.00	^{178}Hf	34.77	15.00
^{57}Fe	56.33	2,600.00	^{206}Pb	38.96	24.00
^{85}Rb	31.63	35.00			

2.2.4 Glass samples

Te Rapa Parts Ltd kindly donated a Toyota Corolla side window and Novus (Frankton, Hamilton) kindly donated a Holden Commodore (2001) windscreen. A Mitsubishi Cedia (2002) side window was purchased from Mitsi World, Hamilton. These panes were used for the homogeneity tests.

The 244 samples used in this research were supplied by ESR, Auckland and had been obtained from damaged vehicles at Turners Auctions Ltd. They will be referred to as the samples that make up the database. The database consisted of a range of automotive windows (front, side and rear) (Table 2.2), makes (Table 2.3) with a variety of models, country of origin (Table 2.4) and with production years between 2002 – 2006 (Table 2.5). All the samples are assumed to be the original panes from the vehicles. ESR supplied their RI results for each sample. The list of samples can be found in the appendix (section 6.1).

Table 2.2 Origin of glass

Window Type	Number of samples
Left front (LF)	17
Left rear (LR)	4
Left rear quarter (LRQ)	5
Rear Canopy	1
Rear (R)	24
Right Front (RF)	18
Right Rear (RR)	4
Right Rear Quarter (RRQ)	9
Windscreen Total (WS)	162
Windscreen Front (WS_F)	85
Windscreen Back (WS_B)	76

Table 2.3 Make of car

Make	Number of samples
Audi	8
BMW	1
Daihatsu	3
Dodge	2
Ferrari	3
Ford	24
Holden	65
Honda	5
Hyundai	14
Kia	4
Lotus	2
Mazda	12
Mini	2
Mitsubishi	17
Nissan	15
Peugeot	3
Renault	2
Suzuki	4
Toyota	58

Table 2.4 Country of origin

Country of origin	Number of samples
Australia	62
Belgium	6
England	7
France	5
Germany	13
Italy	3
Japan	108
South Korea	20
Spain	1
South Africa	1
Thailand	13
USA	4

Table 2.5 Year of vehicle

Year	Number of samples
2002	49
2003	61
2004	72
2005	25
2006	32
Unknown	5

2.2.5 Data calculation and statistical analysis

Data was imported into time resolved analysis (TRA) software, Gemoc Laser ICP-MS Total Trace Elemental Reduction (GLITTER) (version 4.4.1, Macquarie Limited, Australia) for data analysis. The data was exported from GLITTER in the Comma Separated Values (CSV) format.

Data was entered into Microsoft Excel (2007) on a personal computer then analysed using Excel or uploaded into Minitab or Waikato Environment for Knowledge Analysis (WEKA) for further analysis.

2.3 Optimisation of the system

The analysis of solids by LA-ICP-MS required preliminary calibration using aqueous standards to check the instrument's performance. Once the requirements were met, the instrument was turned off and the front end was connected to the laser. The LA-ICP-MS underwent calibrations using the solids NIST 612 and FGS 2. Analysis of samples did not commence until all requirements were met.

2.3.1 Liquid calibrations

A series of liquid calibrations were run in a specific order to ensure optimum performance of the ICP-MS. All calibrations apart from the Dual Detector Cross Calibration were performed using ELAN DRC Setup/Stability/Masscal 10 ppb Solution. The Dual Detector Cross Calibration was performed using a lab-made calibration solution (Section 2.2.3.1).

2.3.1.1 X-Y calibration of the cones

The sampler cone and the skimmer cone were adjusted in the X and Y directions until maximum counts for In were obtained.

2.3.1.2 Ion lens voltage

The lens voltage was adjusted until maximum counts for In were obtained.

2.3.1.3 Autolens

An autolens calibration was automatically performed by the instrument. The autolens was steadily increased to find the maximum for Mg, In and Pb. A lens voltage versus mass graph was obtained, which should be linear with a positive slope. The calibration was repeated if the line was not correct or if a point sat too far from the line.

2.3.1.4 Dual detector cross calibration

A dual detector cross calibration was automatically performed by the instrument. This ensured the two detectors overlapped. The calibration was repeated if one or more elements only had one data point.

2.3.1.5 Daily performance

The requirements for a successful daily performance calibration are listed in Table 2.6. Net intensity mean values were arbitrarily chosen to monitor the sensitivity of the ICP-MS. The values were chosen according to the reported sensitivity from the manufacturer's specifications and by monitoring the ICP-MS on a long term basis. If the machine failed to meet these criteria, the instrument was recalibrated until they were achieved.

Table 2.6 Expected values for calibration using liquid standard

Element/Parameter	Concentration in Solution	Net intensity mean/Threshold
Mg	10 ppb	> 42000
In	10 ppb	> 200000
Pb	10 ppb	> 100000
Background 220	N/A	< 3 %
% Ba^{++}/Ba	Ba at 10 ppb	< 3 %
% CeO/Ce	Ce at 10 ppb	< 3 %

2.3.2 Solid calibration

The laser was continually fired with the shutter closed, with a 60 µm spot and 60 % power at 10 Hz, for at least 30 minutes to warm it up prior to calibration with solid material. This was to achieve a steady output of the laser; the initial and final laser energies during this warm up were recorded to monitor the day-to-day output.

Once the liquid calibration requirements were achieved, the ICP-MS was connected to the laser and Ar and He were purged through the sample chamber and gas lines to expel oxygen before the plasma was lit.

NIST 612 was used for the initial solid calibration as a generic laboratory check. A line, long enough for 2 minutes of ablation, was set up on the NIST 612. The parameters used were a speed of 5 µm/s, 5 µm depth, 60 % power, 60 µm spot and 10 Hz. The laser was warmed up for 60 seconds at the beginning of the analysis before the shutter was opened and analysis began.

The requirements were approximately 20 000 counts for U and Th and less than 1 % ThO/Th ratio, which is standard procedure in this laboratory. This is able to give instant feedback on the sensitivity of the machine.

A calibration specific to glass was then carried out using FGS 2. The CeO^+/Ce^+ ratio can be calculated as FGS 2 does not contain Gd or Dy so there are no interferences at m/z 156. The doubly charged ions can be determined using Ba^{++}/Ba^+ as Ga is absent from the solid standard.

Mg, Sr and Hf were chosen for detection as they cover the low, medium and high masses. The net intensity mean values serve as a guide to ensure the counts are high enough above the background. Table 2.7 shows the expected values when the machine was calibrated using FGS 2.

Table 2.7 Expected values for calibration using FGS 2

Element/ Parameter	Concentration (ppm)	Net intensity mean/Threshold
Mg	23400	> 200000
Sr	253	> 100000
Hf	34.77	> 500
CeO^+/Ce^+	20	< 3 %
Ba^{++}/Ba^+	200	< 3 %

2.3.3 Laser energy

To ensure the laser was warmed up and working efficiently before analysis the maximum laser energy was checked and tabulated.

A 100 µm spot and 100 % power was selected. The laser was fired with the shutter closed until it reached a steady maximum. This was typically around 2 mJ.

2.4 Sample preparation

The samples from ESR were not washed prior to analysis. Large fragments were placed in thick plastic bags and ground with a mortar and pestle to produce small fragments for analysis. This step was omitted for small fragments.

The windows from Te Rapa Parts, Novus and Mitsi World, used for homogeneity testing, were wiped with methanol then water to remove dirt. The whole of each window was covered in all weather sellotape®. Grids were drawn on the tape with marker pen so each section could be identified by a unique number for testing. The grid was constructed by numbering the individual squares left to right, from the top to the bottom. The side window (which is safety glass) was scored with a glass cutter and hit with a solid object to induce shattering. The windscreen (laminated glass) required each grid segment to be hit in order to collect shattered glass.

Microscope slides were cut to 50 x 25 mm. A 20 x 10 grid, printed on overhead transparency sheets, was stuck to the back of the slide. Strips of double sided tape were placed on the front of the slide to hold the glass fragments in place during ablation. Sample fragments were placed in a petri dish and viewed under an Olympus Limnology dissecting microscope (Japan) for selection. Fragments ranging from 0.5 to 3 mm were selected. Tweezers were used to transfer the samples to the slide. If possible, a flat side of a fragment was mounted facing up. A UV lamp (254 nm) was used to check that the tin-coated side of the glass was not mounted upwards.

For the homogeneity tests, one random fragment from each grid section was mounted onto a slide to test the systematic variation in concentration over the window pane. For the database, four random fragments from each sample were chosen and placed on a slide.

2.5 Instrument analysis

2.5.1 LA-ICP-MS method development

A method was developed to analyse elements in glass fragments to differentiate between fragments. The effect of spot size and diameter on analysis was examined. A Plackett-Burman test was performed to find the most robust set of operating conditions. This involved changing various parameters concurrently. The parameters and their ranges used for the Plackett-Burman experiment are shown in Table 2.8.

In 2009, the European Network of Forensic Science Institutes (ENFSI) released a best practice manual for quantitative analysis of float glass using LA-ICP-MS. The set of isotopes listed in this were, ^{7}Li, ^{23}Na, ^{25}Mg, ^{27}Al, ^{29}Si, ^{39}K, ^{42}Ca, ^{49}Ti, ^{55}Mn, ^{57}Fe, ^{85}Rb, ^{88}Sr, ^{90}Zr, ^{118}Sn, ^{137}Ba, ^{139}La, ^{140}Ce, ^{146}Nd, ^{178}Hf, and ^{208}Pb [93]. These elements were used for analysis throughout method development. ^{206}Pb and ^{207}Pb were also added in order for ^{sum}Pb to be calculated, if needed, according to Berends-Montero[84].

Table 2.8 Parameters for Plackett-Burman experiment

Parameter	Unit	Low Value	High Value
Spot Size	µm	50	60
Laser Power	%	50	90
Repetition Rate	Hz	8	10
Carrier gas (He)	mL/min	0.9	1
Nebuliser gas (Ar)	mL/min	0.6	0.65
Depth	µm	5	7
Time of ablation	s	50	60
Frequency	Hz	8	10

A method that is quick and efficient is beneficial if it is to be used as a routine method in the forensic community. As mentioned in section 1.12.2.7, using DRC would require each sample to be analysed twice. This would add to the time and expense of analysis; therefore it was not used in this research.

2.5.2 Final experimental conditions

These are summarised in Table 2.9 and Table 2.10.

2.5.2.1 Laser conditions

A single spot analysis (50 µm) was used. This allowed a time resolved depth profile to be obtained. Single spot analysis can pick up the tin-coated side of float glass. This is used as a check to prevent the tin side from being ablated. 90 % power was selected. This was equivalent to 0.5 mJ (27 J/cm^2). The same parameters were used for both the samples and standards.

Helium (1 mL/min) was used as the carrier gas. This was controlled using a mass flow controller to ensure there were no fluctuations in the flow. Argon gas (1.2 mL/min) was also added to maintain stable plasma in the ICP-MS. The repetition rate of the laser was 10 Hz. The depth was 5 µm.

Table 2.9 Parameters for Nd:YAG Laser (213 nm)

Parameter	Unit	Value
Ablation mode		Single spot
Spot size	µm	50
Energy output	%	90
Repetition rate	Hz	10
Laser warm up	s	60
Time of ablation	s	60

2.5.2.2 ICP-MS conditions

A RF power of 1350 W was used and a 10 ms dwell time was used for all atomic mass units (AMU). Peak hopping was used as the scan mode. For all analyses, a transient signal of intensity versus time was obtained for each element. This contained a 60 second background (gas blank), during which time the shutter was closed and the laser fired to stabilise it. A 60 second ablation of the sample was obtained followed by 60 seconds of post ablation blank to ensure elements returned to background levels before the next analysis. This was achieved by using 550 readings/replicate.

Table 2.10 Parameters for ICP-MS

Parameter	Unit	Value
He as carrier gas through cell	mL/min	1
Ar as carrier gas after cell	mL/min	0.65
Plasma gas	mL/min	15
Auxiliary gas	mL/min	1.2
Dwell time per AMU	ms	10
RF value	W	1350
Sweeps/ reading	-	1
Readings/ replicate	-	550
Replicates	-	1
Scan Mode	-	Peak hopping

2.5.3 Elements for analysis

^{7}Li, ^{23}Na, ^{25}Mg, ^{27}Al, ^{29}Si, ^{39}K, ^{42}Ca, ^{49}Ti, ^{55}Mn, ^{57}Fe, ^{85}Rb, ^{88}Sr, ^{90}Zr, ^{118}Sn, ^{137}Ba, ^{139}La, ^{140}Ce, ^{146}Nd, ^{178}Hf, ^{206}Pb, ^{207}Pb, ^{207}Pb and ^{208}Pb were used for analysis by LA-ICP-MS for method development and analysis of the database. The suite of elements was reduced to 15 elements which were found to be the best elements for analysis of float glass. The elemental suite was comprised of the following 15 elements: ^{7}Li, ^{25}Mg, ^{27}Al, ^{29}Si, ^{42}Ca, ^{49}Ti, ^{55}Mn, ^{57}Fe, ^{85}Rb, ^{88}Sr, ^{90}Zr, ^{118}Sn, ^{137}Ba, ^{139}La and ^{140}Ce.

In the following discussion and chapters, in order to simplify the text, the specific isotope of interest is omitted for all elements except Pb and the term element will be used to describe the particular isotope of interest, as listed above.

Si, was not used in any statistical analyses as it was set to a fixed value since it was used as the internal standard (see section 2.9). Sb was initially included in the elemental suite but could not be used as it was below detection limits in NIST 612 and is not present in FGS 2.

2.6 Analysis of glass fragments

During ablation of some glass samples Al, Mn and Ti spikes occurred at random intervals. If this occurred, either the spike was cut out of the data when interpreted in GLITTER or, if it was in the middle of the ablation, the sample was re-run. Glass samples that broke were also re-run by moving the spot to a different location on the same fragment.

2.7 Sample sequence

A sample sequence was created which allowed for drift correction every eight ablations. Four fragments from each sample were analysed consecutively to increase the representation for each sample. These four fragments were randomly selected from the sample. A total of eight ablations (two samples) were performed before reanalysing the NIST 612 and FGS 2. The standards were analysed twice

on every odd analysis of standard (1, 3, 5) and only once on every even analysis (2, 4, 6), as shown in Table 2.11.

2.8 Quality control sample

FGS 2 was used as the quality control (QC) sample, which allowed the measured value to be compared to the literature value. Two QC samples were analysed with every run[*]. The first QC sample was analysed at the beginning of the sample sequence after the initial calibration standard, prior to ablation of samples. The second QC sample was analysed after the last sample, just prior to the last calibration standards (Table 2.11). These samples were used to monitor the fluctuation of the instrument inter-day and intra-day and to check that the machine was working correctly.

[*] The end of a run was defined as the opening of the sample chamber.

Table 2.11 An example of a sample sequence

Ablation Number	Sample Analysed	
1	NIST 612	Standard 1
2	NIST 612	Standard 1
3	FGS 2	Standard 2
4	FGS 2	Standard 2
5	QC_date_a	FGS 2
6	Sample 1a	
7	Sample 1b	
8	Sample 1c	
9	Sample 1d	
10	Sample 2a	
11	Sample 2b	
12	Sample 2c	
13	Sample 2d	
14	NIST612	Standard 1
15	FGS 2	Standard 2
16	Sample 3a	
17	Sample 3b	
18	Sample 3c	
19	Sample 3d	
20	Sample 4a	
21	Sample 4b	
22	Sample 4c	
23	Sample 4d	
24	NIST 612	Standard 1
25	NIST 612	Standard 1
26	FGS 2	Standard 2
27	FGS 2	Standard 2
28	Sample 5a	
29	Sample 5b	
30	Sample 5c	
31	Sample 5d	
32	Sample 6a	
33	Sample 6b	
34	Sample 6c	
35	Sample 6d	
36	NIST612	Standard 1
37	FGS 2	Standard 2
38	Sample 7a	
39	Sample 7b	
40	Sample 7c	
41	Sample 7d	
42	Sample 8a	
43	Sample 8b	
44	Sample 8c	
45	Sample 8d	
46	QC_date_b	FGS 2
47	NIST 612	Standard 1
48	NIST 612	Standard 1
49	FGS 2	Standard 2
50	FGS 2	Standard 2

2.9 Statistical data calculation

For data calculation, the intensity versus time measurements from ELAN were imported into the time resolved analysis (TRA) software, GLITTER. GLITTER allows integration intervals to be selected which can eliminate spikes in the signal. This also allowed the first few seconds of ablation to be eliminated from analysis to avoid contamination from the surface of the glass sample. By analysing standards at the beginning and end of a sequence GLITTER can also automatically correct for any instrumental drift.

Isotope concentrations were calculated by standardising counts to the stoichiometric abundance of SiO_2 in glass, which is 72 weight % (336561 ppm). ^{29}Si was used as the internal standard [93].

GLITTER converts the intensity (counts per second) via integration of the time resolved spectra into concentration (ppm). Trace element concentrations are calculated by GLITTER using the following equations:

$$concentration_{ni} = \frac{\left(\frac{cps_{nij}}{abundance_j}\right)}{yield_{ni}} \qquad (2.1)$$

where:

$conc_{ni}$ = the concentration of element **i** in analysis **n**

cps_{nij} = the mean count rate (background-subtracted) of isotope **j** of **i** in analysis **n**

$abundance_j$ = natural abundance of isotope **j**

$yield_{ni}$ = cps per ppm of element **i** in analysis **n**[107]

The yield of element **i** in analysis **n** is determined by:

$$yield_{ni} = yield_{ns} \times Int\left(\frac{yield_{ni}}{yield_{ns}}\right)^{std}$$

where:

$yield_{ns}$ = cps per ppm of the internal standard **s** in analysis **n**

$Int(yield_{ni} / yield_{ns})^{std}$ = the ratio of the yield of element **i** in analysis **n** to the yield of the internal standard **s** in analysis **n**, interpolated over the standard analyses[107]

Minimum detection limits (MDL) were calculated by GLITTER at the 99 % confidence interval using background readings and Poisson counting statistics. The following formula was used:

$$MDL = 2.3 \times \sqrt{2B} \qquad (2.3)$$

where B is the total counts in the background interval[107]

The data was processed twice to give two data sets; one with NIST 612 as the standard and one with FGS 2 as the standard.

All data from GLITTER was saved in the .csv format and placed into Microsoft Excel (2007). Microsoft Excel (2007), Minitab and WEKA were used to analyse the data. The statistical data analysis of the method development and the database were carried out with assistance from Professor Ray Littler of the Statistics Department of the University of Waikato.

3 Method Development

3.1 Sample preparation

Sample preparation methods were investigated and modified to provide a quick, efficient procedure which allowed mounted fragments to be easily viewed while in the ablation chamber and ablated without movement.

3.1.1 Washing samples

The literature is divided between publications where glass samples are washed before analysis and those that are not. Fragments that were reported as washed in the literature were generally not for forensic case work and were therefore a manageable size.

Due to the small size of many case work fragments, it was thought that mounting samples onto a microscope slide before the wash step might eliminate the need for the transfer of fragments between solvents. Samples were mounted using glue, left to dry, then sonicated for 15 minutes immersed in methanol with the intention of further sonication in water. Uhu® glue and Loctite® were tried, but were dissolved by methanol. Further types of glue were not tried due to complications with mounting samples using glue (see section 3.1.2).

Washing samples before mounting was trialled. The samples were placed in plastic vials, covered with sufficient methanol and sonicated for 15 minutes. They were then transferred to new vials and covered with type I water and sonicated for a further 15 minutes. The fragments were transferred onto filter paper using tweezers and left to air dry before mounting.

One complication which may arise from using this washing process is the difficulty in transferring fragments between solvents, as case work fragments are often very small.

After consultation with ESR, it was decided that washing was not necessary as most recovered glass fragments are clean. In addition, control samples are plentiful so can be broken to reveal a clean surface for analysis.

As the washing procedure was omitted from sample preparation, the first 5 - 10 seconds of each sample ablation was eliminated from GLITTER to ensure the results were not influenced by any contamination on the surface of the glass.

3.1.2 Mounting samples

The fragments were placed on to a grid, under view of the microscope, using tweezers. Four fragments from each sample were placed on the slide for analysis.

Samples were initially set in glue and left to dry overnight before analysis. However, this mounting procedure provided some complications; the glue stuck to the tweezers which caused a film of glue to form on the surface of the sample if touched by the tweezers and very small fragments became buried in the glue.

Alternative methods for securing samples onto slides were trialled; double sided tape was found to be the best method to secure samples. It allowed the samples to sit flat on the slide compared with the alternative Blu-Tack™. It was quick and efficient to prepare slides and the samples were held securely in place during ablation. The use of tape would allow samples to be removed if they required further testing. In addition, this allowed transmitted light* to be used.

To indicate if ablation erroneously occurred right through a sample because of cracking or if the laser was positioned off the side of a sample aluminium tape was placed on the slide beneath the double sided tape. This produced a large Al spike in the transient signal which was able to give a visual indication that the sample had not been correctly ablated. However, this prevented light being transmitted through the sample which allows easy viewing and helps to bring the sample into focus for

* Transmitted light is cast from under the slide

ablation. Therefore aluminium tape was removed. Samples which cracked produced two plateaus in the transient signal and were identified this way. Ablations which occurred to the side of a sample were identified by the large standard deviation in replicates (i.e. an outlier in the replicates).

3.2 GLITTER output

GLITTER is able to provide the user with the data in a number of forms, two of which are 'trace element concentrations with minimum detection limit filtered' (reported in ppm) and 'mean raw counts per second – with the background subtracted'. It is important to ensure the correct output is being used for data analysis of the samples.

The concentration output, referred to as the absolute concentration, requires that the exact concentration of the element used as the internal standard is known for both the standards and samples. This output is suited for analysis of samples that have been previously analysed by a different technique to provide this information and samples that are assumed to have a fixed concentration of the element chosen for the internal standard.

The absolute concentration has been used for the comparison of NIST 612 and FGS 2, as their Si content is known, and for analysis of the QC sample, as FGS 2 was used. The ENFSI manual states that quantification of float glass is based on the assumption that the ^{29}Si concentration is 72 wt % SiO_2 (336561 ppm silicon)[93] in float glass. Using this assumption, the absolute concentration is the best estimate of the data. This approach has been used throughout the literature and is the approach that has been used in this research to analyse the data. Compositional data (for example, PCA and LDA) does not need to rely on this assumption as it compares the relative proportions of elements.

The formula that GLITTER applies to the raw data to give the concentration of each sample was shown in section 2.9. For their reasons, the term 'yield' is used. However, to the non-mathematical mind this equation is somewhat confusing. Therefore in this research it will be explained in an easier manner. The general formula discussed here is equivalent to that used by GLITTER, with the 'F factor' used in this research being the equivalent of 1/'yield ratio' in the GLITTER manual.

The formula in equation 3.1 is used to report the concentration of each sample. The intensity[*], I, of the sample (denoted by superscript Sa) is converted to concentration[†], C, by multiplying the intensity ratio of element x over the internal standard (IS) in the sample by a factor, which will arbitrarily be called 'F factor'. The F factor (portion in brackets) is interpolated from the standard reference material (denoted by superscript R); it is a ratio of the concentration ratio of element x over the IS divided by the intensity ratio of element x over the IS. For more information refer to the GLITTER manual[107] or the report by Lee[108].

$$\frac{C_x^{Sa}}{C_{IS}^{Sa}} = \frac{I_x^{Sa}}{I_{IS}^{Sa}} * \left(\frac{\frac{C_x^R}{C_{IS}^R}}{\frac{I_x^R}{I_{IS}^R}} \right) \qquad (3.1)$$

The type of interpolation that is used to derive the yield ratios for the unknown elements can be changed in GLITTER to best suit the data. There are four yield ratio interpolation options; average yield, linear fit, quadratic fit and cubic fit. Quadratic and cubic fit are only used if there is atypical instrument drift. When the drift in the instrument is assumed to be normal, the GLITTER manual recommends using 'linear fit' across all standard analyses as the yield ratio interpolation[107].

[*] Intensity is measured in counts per second (cps)
[†] Concentration is measured in ppm

GLITTER uses interpolation to correct instrumental drift. The method developed during this research ensured that standards were run after 8 ablations to allow for sufficient data for drift correction (see section 2.7).

A short run of 30 ablations was analysed to examine the extent of the instrument drift and the ability of 'linear fit' to correct this. Figure 3.1 shows the Sr/Si cps ratio for the standard and the QC samples (both are FGS). Over time the Sr/Si cps increased due to instrumental drift. If 'average yield' was set as the yield ratio interpolation option, an average Sr/Si cps value would be used in the F factor. This value would be used for all samples in the entire run and would cause the value to be overestimated for the samples at the beginning of the run and underestimated at the end of the run. The 'linear fit' option adjusts the value used for Sr/Si cps throughout the run, which will give a more accurate concentration for each sample. Figure 3.2 shows the value of the F factor that was applied across the run. As the Sr/Si cps increased, the F factor decreased to compensate for this.

The results show the importance of standards being analysed throughout the course of the day. The results also show the importance of the standards being measured correctly; if a standard is measured with an abnormally high or low value, the linear fit will be skewed and the wrong F value will be applied to the samples.

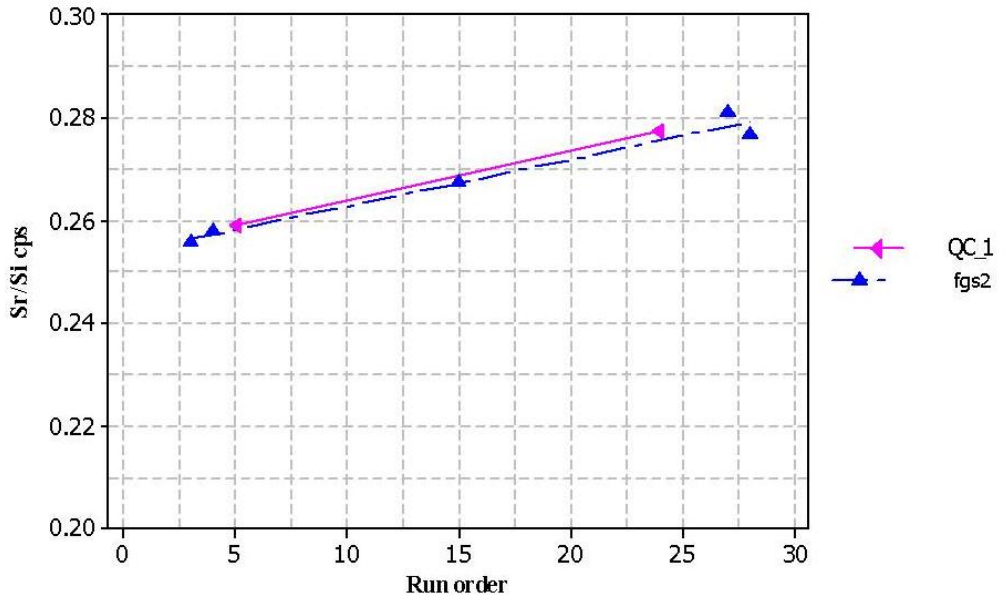

Figure 3.1 Sr/Si cps vs. run order. Over time the Sr/Si cps increased due to instrumental drift.

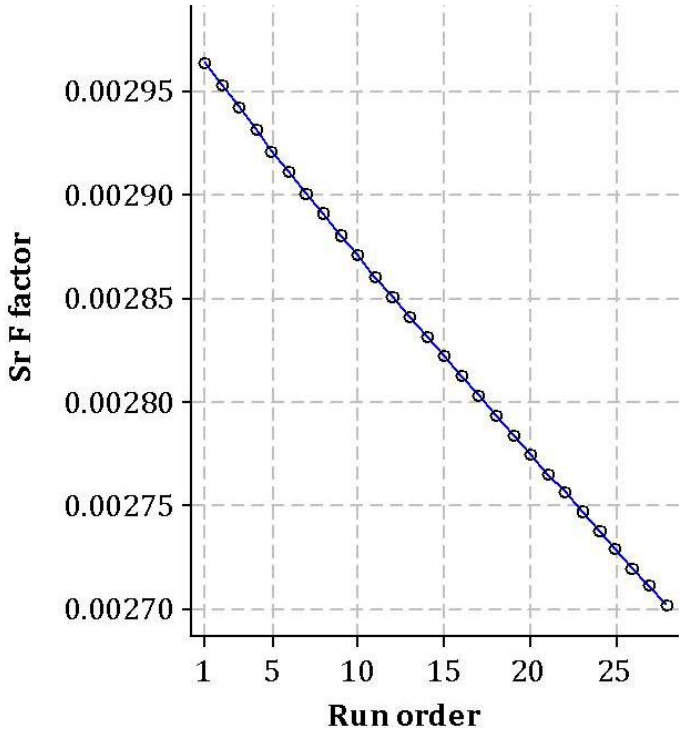

Figure 3.2 F factor for Sr. The F factor used to calculate the concentration of each sample decreased over time due to the increase in the Sr/Si cps.

3.3 LA-ICP-MS parameters development

A LA-ICP-MS method was developed that would provide a robust quantitative analysis of automotive float glass. The optimal ablation and acquisition parameters were obtained by finding the best signal response, high ion counts, low precision and high accuracy. NIST 612 and FGS 2 were compared as standards for calibration. The best choice of elements was also investigated.

LA-ICP-MS has multiple parameters that can be varied to optimise the ablation of glass. This includes gas flows (plasma gas, carrier gas and make up gas), dwell time, acquisition time and acquisition mode. There is limited literature on LA-ICP-MS methods for discrimination of automotive glass. ENFSI have written a Best Practice Manual for forensic examination of glass which is approved by the European Paint Group (EPG). It states that a single spot analysis with a dwell time of 10 ms should be used for a 50 Hz power supply. The repetition rate should be 10 Hz. Also He should be used as the carrier gas, with additional Ar[93].

Fixed values for many ICP parameters, such as gas flows, are not typically stated in the literature as optimum parameters are specific to an individual instrument and may vary on a day-to-day basis. Therefore instead of reporting specific fixed values in the literature, a calibration procedure is usually set up to ensure maximum sensitivity and stability of the analyte signals, while minimising ratios of oxides and doubly charged species. For analysis of float glass ENFSI have published a calibration procedure[93].

For this research the optimum nebuliser gas flow was checked every day before analysis to find the highest counts of U and Th and less than 1 % ThO/Th ratio, as per standard laboratory procedure. This gave instant feedback on the performance of the machine. FGS 2 was then analysed to confirm the machine was set up for the analysis of glass.

It was decided that the values for dwell time and repetition rate stated by the ENFSI Best Practice Manual would be used for this research as they are a standard guide.

The gas parameters were investigated using a ruggedness test (refer to section 3.4.1). Laser power and spot size were the two remaining parameters which needed to be considered for designing the method for quantitative analysis of glass.

3.3.1 Laser power

For samples to be analysed in GLITTER, a flat transient signal is required. The longer and flatter this signal is, the better the data produced. The power of the laser affects the outcome of the transient signal due to the amount of material which is removed during ablation.

In preliminary experiments, glass fragments and NIST 612[*] were ablated with a combination of powers and spot diameters. The parameters were altered to find the best combination and to see if the variation made a difference to the results.
40 % power was very weak and was not able to effectively ablate the samples or standard. Therefore 50 % power was deemed the lowest practical power. NIST 612 was analysed in triplicate with a 60 µm spot with laser power from 50 % to 100 % (in increments of 10 %). The calibration spots were analysed with a 60 µm spot and 90 % power regardless of the sample parameters. 90 % power gave the lowest minimum detection limit (99 % confidence) for all elements, and the highest mean counts for all elements except ^{49}Ti as reported by GLITTER[†]. However, these results may have been bias due to analysis of the standard at the same parameters. To eliminate this possibility the experiment was repeated using the same parameters for both the standard and the samples. 9 of the 17 elements had the best agreement using 80 % power. 7 of the 17 elements had the closest agreement to the certified NIST values (Pearce) using 90 % power and had the lowest 1 σ error for 14 of the elements. In addition, all elements analysed had the lowest minimum detection limit and maximum counts for 90 % power.

Many journal articles and the ENFSI manual do not mention the energy density of the laser used during ablation. Those that do are divided between 3, 12 and 27 J/cm^2. 50 %

[*] FGS 2 had not arrived at this point in the research.
[†] Ti was later found to be below detection limits

and 90 % power were trialled as they match the two extremes of laser power reported in the literature (Table 3.1). The test was carried out for both a 50 µm and 60 µm spot (see section 3.3.2 for explanation of diameter choice).

Table 3.1 Laser power converted to J/cm^2 and mJ

Power (%)	J/cm^2	mJ
50	3-6	0.07-0.10
90	20-30	0.40-0.55

Initially, NIST 612 was trialled using a 50 µm spot; with both power settings a flat transient signal that could be analysed by GLITTER was produced. However, when FGS 2 was ablated using 50 % power, a sloping signal was produced which GLITTER could not interpret efficiently (Figure 3.3). 90 % power gave a strong flat transient signal (Figure 3.4). The same observations were made using a 60 µm spot.

After the standards were trialled, ablation of glass samples was examined. Glass samples ablated using a 60 µm spot and 50 % power also did not produce a long flat transient signal suitable for GLITTER. When the power was increased to 90 % the signal had a long flat area, as for the standards. This was able to be easily interpreted by GLITTER.

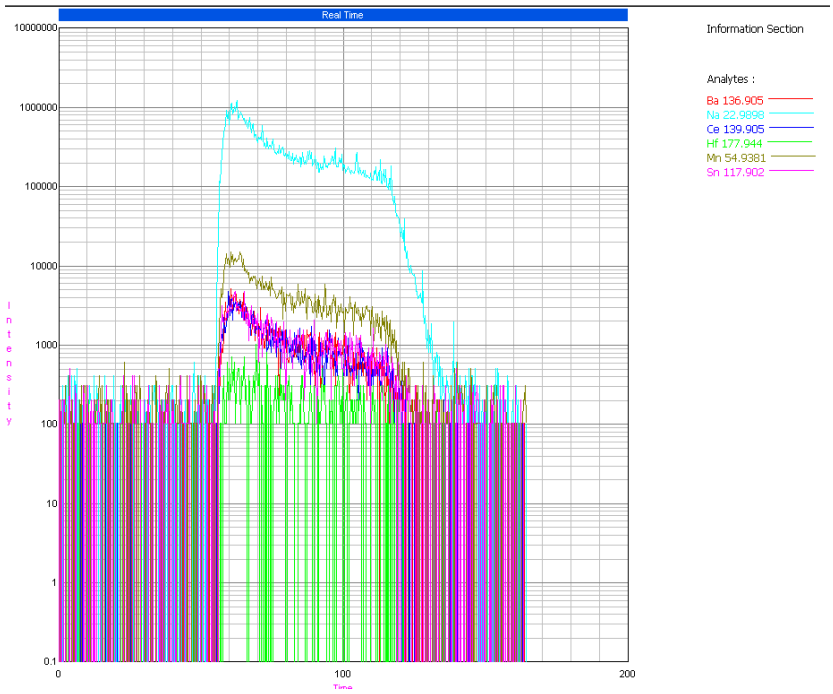

Figure 3.3 Transient signal for FGS 2 with a 50 µm spot and 50 % power. The sloping line is not suitable for processing data in GLITTER.

Figure 3.4 Transient signal for FGS 2 with a 50 µm spot and 90 % power. The flat signal is suitable for processing data in GLITTER.

Scanning electron microscopy (SEM) pictures were taken of the two spot sizes at 50 % and 90 % power. Material in the centre of the ablation crater appears to have melted when 50 % power was used or the material may have been re-deposited inside the crater (Figure 3.5 and Figure 3.6). When the power was increased to 90 % the crater was clean (Figure 3.7 and Figure 3.8). The 60 µm spot at 50 % power has a plume deposited above the crater (Figure 3.9) which the other combinations of parameters did not show. This may be due to heavier particles which have fallen out of the carrier gas as it is transported to the exit of the sample chamber.

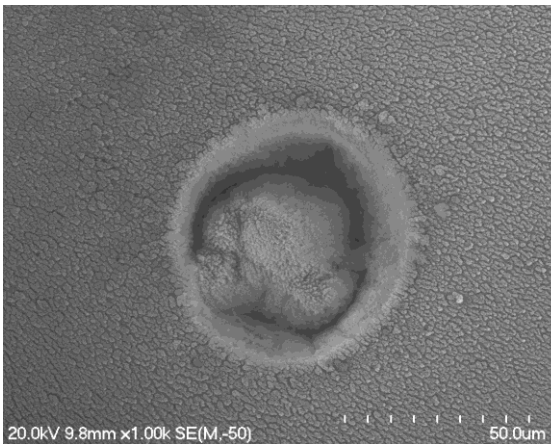

Figure 3.5 Analysis of float glass using a 50 µm spot with 50 % power. The middle of the crater has melted glass present.

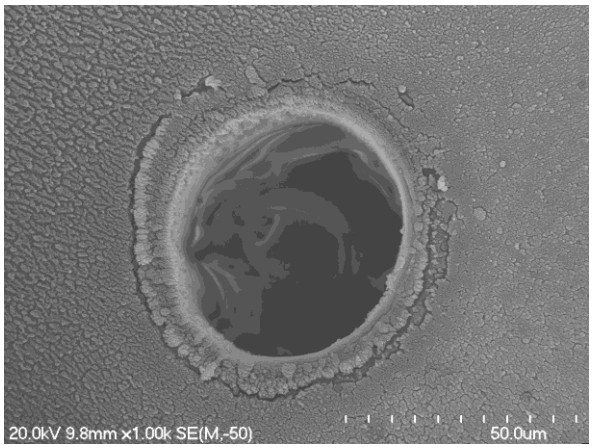

Figure 3.7 Analysis of float glass using a 50 µm spot with 90 % power. The middle of the crater is clean.

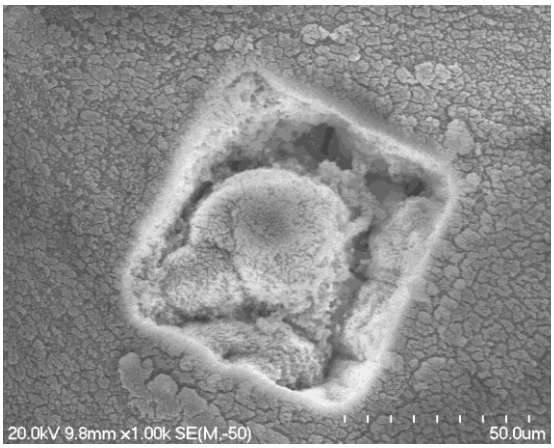

Figure 3.6 Analysis of float glass using a 60 µm spot with 50 % power. The middle of the crater has melted glass present.

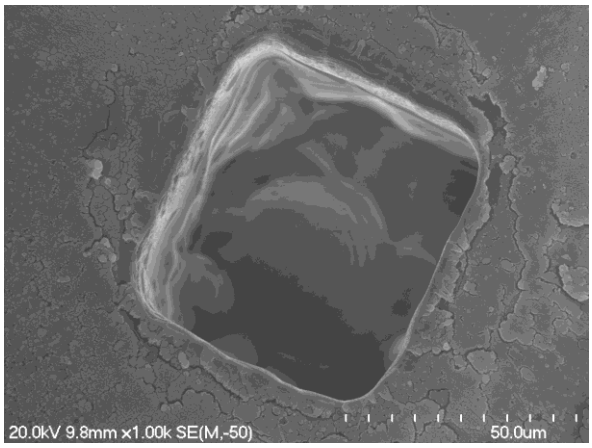

Figure 3.8 Analysis of float glass using a 60 µm spot with 90 % power. The middle of the crater is clean.

Figure 3.9 Plume from 60 µm spot with 50 % power (right), which is not observed for the 60 µm spot at 90 % power (left).

3.3.1.1 Choice of power

90 % power (24 – 27 J/cm^2) was chosen as it produces a flat transient signal which can be interpreted in GLITTER. It gives high counts and is a common value found in the literature. The SEM photographs confirm that 90 % power ablates the sample and does not melt it. Therefore a clean ablation crater is formed.

3.3.2 Spot diameter

The choice of spot size is a compromise between stability during ablation and sensitivity. A spot diameter large enough to achieve high sensitivity of the low level elements is required. However, if the diameter is too large the sample may shatter. Spot diameters in the literature are divided between 50, 55, 60 and 100 µm. The ENFSI Best Practice Manual recommends a spot diameter of 50-80 µm. Although some journal articles report use of a 100 µm spot with a 213 nm laser, this large

diameter is best suited to a 266 nm laser. Therefore it was not considered as an option for this research. A study was conducted to see if altering the spot size changed the measured concentrations, since a range of values were suggested by the ENFSI manual.

The power was held at 90 % (24-27 J/cm^2); FGS 2 was ablated 12 times using 50 µm and 60 µm spots. They were chosen as they are frequently found in the literature and adhere to the ENFSI manual. A 55 µm spot was not available on the laser machine used in this research.

A t-test was performed to see if there was a significant difference between the two diameters. The t-test showed significant differences for K and Sn. K had a high background on the instrument and the concentration of K in the standard was barely above this background noise; therefore K will not be discussed (see section 3.4).

Table 3.2 gives a summary of the data. The upper and lower confidence limits (UCL, LCL) show the maximum and minimum which is acceptable for the mean difference of the spot sizes, before a significant difference is seen. If there is no difference between the measurements for the two spot sizes the UCL and UCL will include zero. The UCL and LCL for Sn do not encompass zero which means a significant difference in measurements between the two spot sizes was found. However, the difference between the measurements for the two spot sizes (2.22 ppm) only just exceeds the UCL for mean differences (2.08 ppm). Therefore it is acceptable to say there is no difference between the measurements when using a 50 µm or 60 µm spot diameter for any element. This is also found in the ruggedness test (see section 3.4.1).

Table 3.2 Comparison of 50 µm and 60 µm spot with 90 % power[‡]

Element	^{7}Li	^{23}Na	^{25}Mg	^{27}Al	^{39}K	^{42}Ca	^{49}Ti	^{55}Mn	^{57}Fe	^{85}Rb	^{88}Sr
Overall Mean, ppm	28.59	100480.93	23378.65	7445.96	4610.18	59522.58	328.00	221.44	2595.86	35.11	253.89
Estimated mean difference	-0.93	1689.07	201.11	91.42	86.53	825.41	5.00	1.71	-18.22	0.23	1.69
Estimated % bias	-3.51	0.73	0.38	0.24	1.04	0.59	0.28	0.28	-0.78	0.12	0.12
UCL for mean difference	0.16	1907.93	222.99	146.84	77.13	947.59	8.13	2.16	4.17	0.37	2.76
LCL for mean difference	-2.17	-437.73	-43.77	-110.85	18.80	-244.36	-6.26	-0.90	-44.77	-0.29	-2.15

Element	^{90}Zr	^{118}Sn	^{137}Ba	^{139}La	^{140}Ce	^{146}Nd	^{178}Hf	^{206}Pb	^{207}Pb	^{208}Pb
Overall Mean, ppm	224.91	93.80	199.18	17.98	22.85	25.25	14.96	24.12	24.37	24.11
Estimated mean difference	6.18	2.22	0.28	0.265	0.2	1.055	-0.33	0.485	1.165	1.22
Estimated % bias	1.03	1.26	-0.43	0.45	0.16	1.87	-2.60	0.82	2.18	2.61
UCL for mean difference	7.74	2.08	2.29	0.37	0.33	1.17	0.12	0.58	1.26	1.18
LCL for mean difference	-3.12	0.28	-4.02	-0.21	-0.26	-0.23	-0.90	-0.19	-0.19	0.08

[‡] The table is based on 50 µm - 60 µm data. Therefore if there is a significant difference, a higher measurement is recorded for the 50 µm spot diameter.

Even though there was no significant difference between measurements for the two crater sizes, the 50 µm spot is round while the 60 µm spot is square[*]. Glass could be seen coming off the sample when a 60 µm spot with 90 % power was used. These particles originated from the ablation crater and also the area immediately surrounding the crater. These large fragments will not ionise completely in the plasma which will reduce precision. Another complication was that one of the nine samples analysed cracked; this was shown by two plateaus in the transient signal.

A 50 µm spot was tested to see if it could reduce the shattering of particles from around the ablation pit due to its shape. Shattering occurred on a few fragments while using the smaller spot size, but at a lower frequency than for a 60 µm spot. Shattering appeared to be unpredictable and unavoidable on some areas of samples. These samples were run again with the ablation spot in a different position on the sample, which overcame the problem as the samples did not shatter again. The reduced spot size gave a visibly cleaner crater, with none of the surrounding area removed for the majority of samples tested. In addition, large particles of glass were not ejected by the sample.

3.3.2.1 Choice of spot size

A 50 µm spot was chosen for analysis of the database as it provided a more efficient ablation and reduced the number of shattered fragments. It decreased the large particles entering the ICP-MS and also provided a long flat transient peak for analysis in GLITTER. The SEM image confirmed that a clean crater was produced when used with 90 % power. In addition the 50 µm spot is round, which is consistent with other spot sizes.

3.3.3 Background levels between subsequent ablations

Trace element analysis requires background levels to be kept as low as possible. A wait time between samples is necessary as some elements, such as Na, did not

[*] New Wave produce a square 60 µm spot as this was requested by biologists. All other spot sizes on the laser are round.

immediately revert to background level. The minimum wait time was examined to maximise the number of samples that could be run. The time chosen is a compromise between time efficiency and the need for low background levels.

Initially, after each analysis the system was purged with He (1 minute and 30 seconds) followed by Ar (1 minute and 30 seconds) to flush out any residue. The purge time was shortened to 1 minute for each gas, with no noticeable increase in background, while complete removal of the Ar purge gave no increase in the background signal between consecutive ablations. The reading/replicate was increased to record 1 minute of signal after ablation; this allowed background levels to be monitored to ensure they dropped before the next analysis was performed. This 1 minute He purge was sufficient to allow all elements to return to their former background level.

If the background appeared to be increasing, the system was purged with He (5 minutes) then Ar (5 minutes), to wash out any residual elements.

3.4 Minimum detection limits (MDL) and limits of quantification (LOQ)

The LA-ICP-MS system used during this research is also used by Earth Scientists and Biologists. A diverse range of samples are ablated, including otolith and zircons. Therefore some days of analysis may have higher background levels due to the samples ablated the previous day. In addition there may be memory effects[*] of some elements. However, it should be noted that memory effects are significantly reduced in LA-ICP-MS compared to ICP-MS.

It was noted that the minimum detection limit (MDL) will change over time, but an estimate was obtained by taking the MDL levels from a range of days (94 values) and averaging the values.

[*] Memory effects occur when elements stick to the tubing and enter the plasma at a later date, thus elevating the concentration level of this element for another sample.

The MDL for each element was found by firing the laser with the shutter closed for 60 seconds prior to analysis. The MDL was calculated by GLITTER at the 99 % confidence level. This is determined by Poisson counting statistics using the following equation:

$$MDL = 2.3 * \sqrt{(2B)} \quad (3.2)$$

where B is the total counts in the background interval.

The limits of quantification (LOQ) were calculated as ten times the MDL[109]. Table 3.3 shows the MDL, LOQ and the concentration of standards NIST 612 and FGS 2 for each element.

The LOQ for K and Ti (57.59 and 52.12 ppm respectively) in this research are very close to the concentrations in NIST 612 (63.56 ppm and 50.92). The concentration reported by Pearce[106] for Ti has been suggested as being incorrectly reported. Gao *et al.* states the concentration as 44 ppm[110]; this is lower than the concentration reported by Pearce and is below the limit of detection. Therefore the reported concentrations may not be correct for K and Ti when NIST 612 is used as the standard. In contrast, FGS 2 has a much higher concentration of these elements, so will be useful for their detection. The LOQ for Fe is higher than the concentration in NIST 612 (88.12 compared to 56.38 ppm). Therefore the background reading is too high and a reading for Fe cannot be obtained. In contrast, FGS 2 has a very high concentration of Fe so can be detected in glass. All other elements have a sufficient margin between the LOQ and the concentration in the standard. Therefore they were analysed further to assess if they are good elements for determination of glass.

From this point K, Ti and Fe were removed from all analyses performed when the data was calibrated using NIST 612, but were included for analyses using FGS 2 as the calibration standard.

Table 3.3 MDL and LOQ for all elements and the literature values of NIST 612 and FGS 2. Values in bold in the standards columns are very close to or below LOQ

Element	MDL, ppm	LOQ, ppm	NIST 612, ppm	FGS 2, ppm
^{7}Li	0.58	5.85	40.8	28.09
^{23}Na	1.44	14.42	104786.87	100848.48
^{25}Mg	2.19	21.95	80.12	23423.45
^{27}Al	1.57	15.67	11223.67	7454.96
^{39}K	5.76	57.59	**63.56**	4634.16
^{42}Ca	99.00	990.04	86146.29	59698.39
^{49}Ti	5.21	52.12	**50.95**	328.47
^{55}Mn	0.21	2.11	38.8	221.76
^{57}Fe	8.81	88.12	**56.38**	2585.71
^{85}Rb	0.11	1.09	31.71	35.13
^{88}Sr	0.03	0.29	77.06	254.04
^{90}Zr	0.04	0.45	36.03	226.06
^{118}Sn	0.32	3.24	37.62	94.40
^{137}Ba	0.18	1.83	38.08	198.75
^{139}La	0.02	0.23	35.9	18.02
^{140}Ce	0.02	0.21	38.8	22.87
^{146}Nd	0.10	1.01	35.56	25.49
^{178}Hf	0.06	0.63	35.2	14.77
^{206}Pb	0.15	1.53	39.49	24.22
^{207}Pb	0.18	1.82	39.67	24.64
^{208}Pb	0.09	0.90	39.55	24.42

3.4.1 Ruggedness test

For results in the database to be reliable the instrument must not have fluctuations in measurements caused by slight changes in parameters. A ruggedness test was carried out to see if small changes in parameters had an effect on the analysis at the 95 % confidence level. The test was carried out using FGS 2 to determine the significance of the effect on each element when the chosen parameters are varied.

For this research a Plackett-Burman design was generated in Minitab. It contained 8 parameters, each with a high and low value (Table 3.4). The levels set were designed

so that differences were only slight. This allowed the ruggedness test to have less unimportant interactions compared to the main interactions. The experiment was carried out on two separate days to allow for possible day-to-day variation. The run sequence can be seen in appendix 6.2. The parameters were concurrently changed and the significance of the alteration of each parameter was assessed. Each run was comprised of one ablation spot.

Table 3.4 Parameters for Plackett-Burman experiment

Parameter	Unit	Low Value	High Value
Spot Size	µm	50	60
Laser Power	%	50	90
Repetition Rate	Hz	8	10
Carrier Gas (He)	mL/min	0.9	1
Nebuliser Gas (Ar)	mL/min	0.6	0.65
Depth	µm	5	7
Time of ablation	s	50	60
Frequency	Hz	8	10

The Plackett-Burman design was analysed in Minitab using a 95 % CI. A normal plot of the standardised effects was produced for each element. Parameters which are classed as having unimportant effects are smaller and are centred around zero. Parameters which have an important effect on the result are larger and do not sit near the line; these are labelled as significant. However, some parameters which are labelled as significant do not lie very far from the line (classed as marginal concern) while others lie very far from the line (classed as critical). The p value of each parameter was assessed for each element; they were categorised into parameters which had only a marginal effect (p values from 0.03 – 0.05) and those which had a critical effect (p value < 0.03). Table 3.5 gives an overview for each element; columns with a ‘C’ or ‘M’ show elements which showed a significant effect for the given parameter according to the Plackett-Burman test; those with ‘C’ are parameters which have a very significant effect and are classed as critical; parameters labelled with ‘M’ are only of marginal concern.

Table 3.5 Significant effects for the Plackett-Burman test. Parameters labelled 'C' have a critical concern when the parameter is altered between the high and low value; parameters labelled as 'M' only have a marginal effect when the parameter is altered

Element	Spot Diameter (um)	Laser Power (%)	Carrier Gas -He (mL/min)	Neb Gas, Ar (mL/min)	Frequency (Hz)	Ablation time (s)	Depth (um)	Repetition Rate (Hz)
^{7}Li								
^{23}Na	M	C						
^{25}Mg		C	C	C				
^{27}Al		C	M	C				
^{42}Ca		C		C				
^{55}Mn		C	C	C				
^{85}Rb		M						
^{88}Sr		C						
^{90}Zr		C		M				
^{118}Sn								
^{137}Ba		C	M	M				
^{139}La		C	M	C				
^{140}Ce		C						
^{146}Nd		C	C	M				
^{178}Hf		C		M				
^{206}Pb		C			M			
^{207}Pb		C						
^{208}Pb		C						

Figure 3.10 shows the normal plot for Zr. It illustrates the above explanation; laser power sits far from the line ($p = 0$) and has an important effect on the measurement values but nebuliser gas sits relatively close to the line ($p = 0.032$) so has a smaller effect on the data. Therefore the influence of changing the nebuliser gas flow from 0.60 to 0.65 mL/min makes a slight difference to the results. The normal plot of the standardised effects is, as the name suggests, standardised. Therefore the extent of influence one parameter has cannot easily be compared to another parameter.

A main effects plot shows the absolute values, allowing the scale of the parameters to be compared. The main effect plot for Zr (Figure 3.11) shows the absolute difference in the mean for all 7 parameters. The difference between 50 % and 90 % power is

very large, as shown by the large difference in the mean. The change in nebuliser gas from 0.60 to 0.65 mL/min has a change in mean which is not much larger than that of the parameters which are classed as not significant. The main effects plots for each element can be found on the electronic media in appendix 6.3; the normal plot of the standardised effects for each element can be found on the electronic media in appendix 6.4.

A reduction in power from 90 % to 50 % had the most significant effect on the results, critically affecting 18 of the 22 elements and marginally affecting one. The effect of altering laser power was also noted in section 3.3.1. This confirms that it is necessary for one laser power to be assigned for use in the method.

As discussed in section 3.3, standard practice is to use a calibration procedure to ensure the instrument is performing before testing samples. This generally involves altering the nebuliser flow to get maximum counts. However, the Plackett-Burman test showed alteration of the nebuliser gas from 0.60 – 0.65 mL/min has a critical effect on six elements and a marginal effect on five elements. This parameter has the second most prominent effect on elements. Investigation of the best gas flow over the period of three months showed 0.65 mL/min gave the best results during the calibration sequence; it had high sensitivity and a low ThO/Th ratio. In addition, it also gave sufficient counts when FGS 2 was calibrated. Therefore the nebuliser gas flow was set to 0.65 mL/min for all analyses. The gas flow was still tested as part of the daily calibration to verify 0.65 mL/min was still performing better than other gas flows.

The carrier gas (He) had a critical effect on four elements and a marginal effect on three elements when the flow was changed from 0.9 to 1 mL/min. A flow of 1 mL/min was chosen as in combination with the 0.65 mL/min flow of nebuliser gas it gave acceptable sensitivity.

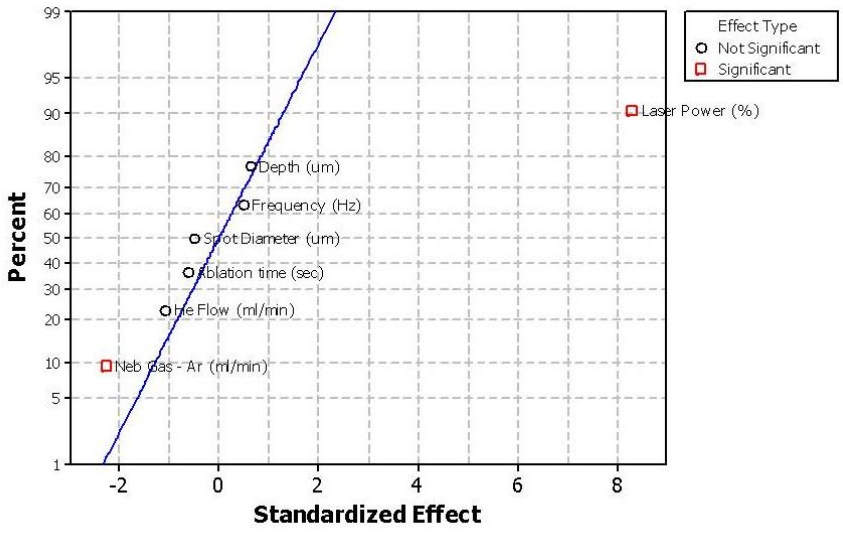

Figure 3.10 Normal plot of the standardised effects for Zr. If there is no significant effect the parameters will be close to the line. Changes in laser power and nebuliser gas are classed as having a significant effect on the measurement of Zr. However, nebuliser gas (p = 0.032) lies relatively close to the line, so is only of small concern compared to laser power (p = 0) which lies very far from the line and has a significant effect on the measurement result.

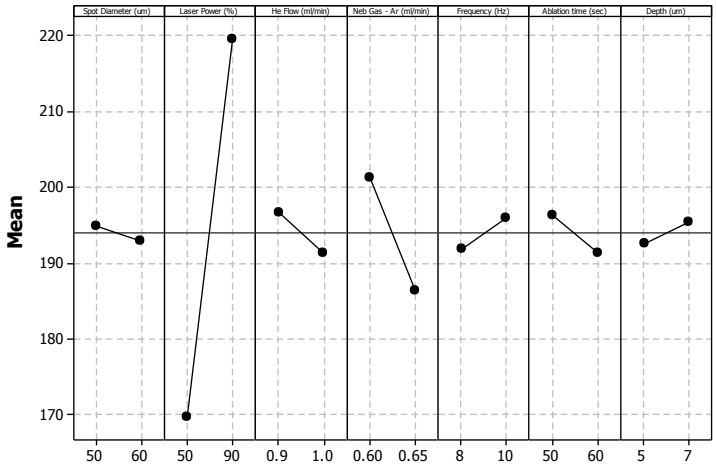

Figure 3.11 Main effects plot for Zr. If the two extreme values are far from the horizontal line, for each parameter, they have a larger affect on the element. The main effects plot is a relative scale. Laser power has a large difference in mean for the high and low parameters, compared to nebuliser gas which has a change that is not much larger than for parameters which do not have a significant effect.

Spot diameter only affected Na, however, this was only marginal ($p = 0.035$). The t-test (section 3.3.2) also showed no difference in measurements when the spot diameter was changed. Therefore a 50 µm or 60 µm spot can be used without any significant variation in the results. However, for reasons noted in section 0 a 50 µm spot was chosen.

Altering the frequency affected only ^{206}Pb, but this was marginal ($p = 0.034$). The repetition rate and depth of ablation did not affect any of the elements. The ablation time did not have an effect on any element. Therefore for a small fragment the ablation time can be reduced without any effect on the data; this will prevent small samples shattering. An additional bonus is it that it allows spikes to be removed from the beginning or end of an analysis, in GLITTER, without the data being altered.

Berends-Montero *et al.* previously used a Plackett-Burman design of 8 experiments to evaluate effects of frequency, energy, spot diameter, nebuliser flow and three dummy parameters to test the ruggedness of the instrument[84]. They reported there was no significant difference for most elements and in general most variation was no larger than for replicate samples. However, Zn was affected by changes in the parameters studied.

3.4.2 Final choice of parameters for glass analysis

The final parameters are summarised in Table 3.6. These parameters provided the best overall transient signal. Any samples which shattered were repeated. This was carried out by moving the ablation site to a new area on the glass sample.

Table 3.6 Final parameters for method

Parameter	Unit	Value
Spot Size	µm	50
Laser Power	%	90
Repetition Rate	Hz	10
He flow	mL/min	1
Ar flow	mL/min	0.65
Laser Warm up	sec	60
Time of ablation	sec	60
Frequency	Hz	10
Depth	µm	5

Multiple publications by Trejos and Almirall[48, 82, 88], as well as a publication from Montero[12] use a 50 µm spot. However, it should be noted that they both use a 266 nm laser. Bridge *et.al.* use a 50 µm spot with a 213 nm laser[65]. The small spot size allowed for replicate ablations to occur on one sample and lessened the size of particles chipping off the sample during ablation.

Naes *et al.*[57] and Smith *et al.*[80] report the laser energy as 27.2 J/cm^2, which concurs with this research. Montero[95], Bridge *et al.*[65] and Trejos *et al*[82]. report lower laser energies (3.8 -12 J/cm^2).

The flow rate for He as the carrier gas (1 mL/min) is slightly higher than that reported in the literature (0.75 – 0.95 mL/min)[12, 48, 57, 80, 82, 88, 95]. However, 1 mL/min was chosen as this gives the best results for the individual instrument with the Ar flow rate (0.65 mL/min). The Ar carrier gas (0.65 mL/min) is lower than the flow reported in the literature (0.90 – 1 mL/min).

A 60 second ablation time was chosen to maximise the flat transient signal and allow the first 5 – 10 seconds of ablation to be eliminated instead of washing samples. The ablation time differs to ENFSI who use 50 seconds, but it is in line with some papers in the literature.

A value of 10 Hz was chosen for the frequency and repetition rate, in accordance with the ENFSI manual. This is also consistent with the bulk of the literature. 5 µm was

chosen for depth to be consistent with the bulk of the literature as it is not mentioned in the ENFSI manual.

3.5 Variation between replicates and days

The extent of day to day variation is of interest as casework samples may be analysed on a different day to control samples in the database. Normalisation of the variation between days would allow samples analysed on different days to be compared and still show a match if there is one. Trejos *et al.* suggested that the variation appears to be systematic. They stated that by taking a ratio of two elements this variation can be eliminated[82]. This approach is not necessary when using GLITTER as the software eliminates the instrumental drift. Moreover the concentration output from GLITTER is a ratio of each element to Si (see section 3.2). Therefore the concentration data from GLITTER is suitable for analysis without further alteration.

The capability of GLITTER and the reliability of the data were examined. For this experiment NIST 612 was analysed four times a day for eight days, as both the sample and standard. A fully nested ANOVA was performed to examine the variation between replicates on a given day and the between day variation. The contribution of each source of variation is shown as a percentage in Table 3.7.

Most variation comes from the four replicates; this ranges from 51.84 (Na) to 89.32 % (Mg). Li and ^{206}Pb have slightly more variation between days (52.17 and 51 % respectively). Hf, ^{207}Pb, ^{208}Pb have > 56 % variation between days.

The data shows that the output from GLITTER is stable over time which will allow samples analysed on different days to be compared.

Table 3.7 Variation between days and replicates of NIST 612

Element	^{7}Li	^{23}Na	^{25}Mg	^{27}Al	^{42}Ca	^{55}Mn	^{85}Rb	^{88}Sr	^{90}Zr
Variation between days, %	52.17	48.16	10.68	23.56	39.79	44.86	11.64	34.73	40.46
Variation between replicates, %	47.83	51.84	89.32	76.44	60.21	55.14	88.36	65.27	59.54

Element	^{118}Sn	^{137}Ba	^{139}La	^{140}Ce	^{146}Nd	^{178}Hf	^{206}Pb	^{207}Pb	^{208}Pb
Variation between days, %	30.54	41.29	16.41	19.86	20.86	58.59	51	56.95	62.52
Variation between replicates, %	69.46	58.71	83.59	80.14	79.14	41.41	49	43.05	37.48

3.6 Long term stability and quality control

Trace element work deals with very small values. It is important that the data output from the machine does not vary too widely so the reported value has a small error associated with it. Section 3.5 shows that variation between days is not larger than between replicates of samples analysed on the same day. To ensure the instrument was stable over the course of this work every run of database samples had two quality control (QC) samples analysed in the same sequence; the QC standard was analysed prior to any samples being ablated, and at the end of the sample set. FGS 2 was used as the QC standard.

Na was found to have very large sample ranges for days two and four which exceeded the upper control limit. This was most likely from the nature of the samples that had been run in the days prior to glass analysis. The Na had not sufficiently washed out of the tubing. Examination of the sum of all elements of database samples showed samples on these days had much larger means than any other day. Therefore all samples analysed on days two and four were repeated. When the sum of all elements was recalculated, the re-analysed samples had a sum which was in line with all other samples from the database.

Figure 3.12 shows the QC chart for Ba. It shows that samples analysed on day 23 were below the lower control limit. This was also seen for most other elements. The concentration of samples ablated on this day may not be representative. Therefore these samples were re-analysed. The samples on the other days were between the upper and lower control limits. The QC charts can be found in appendix 6.5 for NIST 612 as the calibration standard and appendix 6.6 for FGS 2 as the calibration standard on the electronic media.

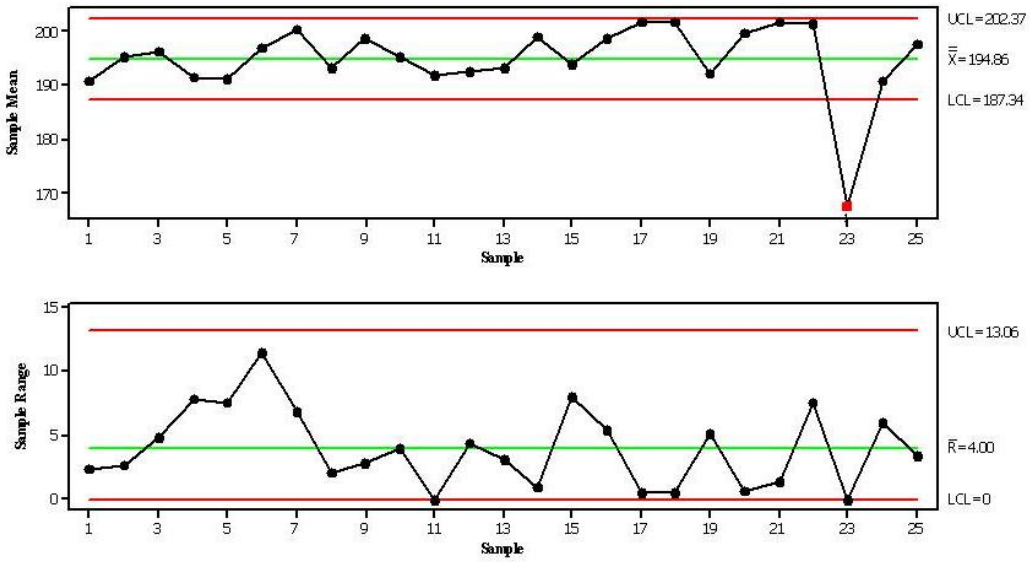

Figure 3.12 Quality control chart for Ba. Samples ablated on day 23 were below the lower control limit; hence they were re-analysed.

3.7 Validity of standards (matrix matched standards)

Literature on inter-laboratory tests report that a protocol for LA-ICP-MS optimisation is fundamental for providing comparable data[87]. However, as some parameters vary widely between laboratories, it is important to have a matrix-matched standard in order for the results to be comparable.

NIST 612 is an established standard and is commonly used as the SRM in the literature for calibration of glass. NIST 612 is used instead of NIST 610 as it has a

lower concentration of elements (40 vs. 400 mg/kg) which are more in line with the levels in glass. Even so, it does not closely resemble float glass and some elements are reported to be inhomogeneous. Literature states that it may not be the best calibration standard for glass, but until recently there has been no other option available.

FGS 2 is a new calibration standard in the forensic community. It was manufactured to closely resemble float glass. The first published results for the consensus values of FGS 2 were available in 2005 by Latkoczy *et al.*[87]. However, at the time Latkoczy *et al.* stated that further characterisation was needed before it can be used as a SRM. In 2009, ENFSI published a manual which approved the use of FGS 2 as a tuning standard and a calibration standard for forensic float glass LA-ICP-MS analysis[93]. At the time of publishing there were limited articles using FGS 2 as a tuning standard or SRM for float glass analysis with LA-ICP-MS.

This section of research has investigated the feasibility of using FGS 2 as a SRM. It has been compared to NIST 612 to examine if it is a viable and/or superior standard.

The accuracy and precision of all elements for both standards were determined. NIST 612 and FGS 2 were analysed by the sample experimental procedure as used on the glass samples.

Major and minor elements (Na, Mg, Al, K, Ca, Ti and Fe) were assessed using only the relative thresholds (% bias and % RSD) due to their large concentrations which will always exceed the 3 ppm limit for both accuracy and precision. Trace elements were assessed using both relative and absolute (bias, ppm, standard deviation (σ), ppm) values. Accuracy was calculated using the absolute (bias, ppm) and relative (% bias) values and defined as the closeness of the experimental values to an accepted reference value. The precision of a measurement was calculated as the absolute (σ) and relative (% RSD) values and defined as the scatter of data about the expected value. Standard deviation represents the total variation. In other case work, day-to-

day variation would not be a problem as replicates of case work samples and control samples are usually analysed on the same day, using the same calibration. However, for a database the case work samples will be analysed at a later date compared to the database samples. In addition, new samples will be added to the database. Therefore the measure of standard deviation in this research would be an accurate assessment of precision as the samples were acquired over many days with different calibrations.

Initially, accuracy was defined as elements with |bias| ≤ 5 ppm and/or |% bias| ≤ 10 % and precision was defined as RSD ≤ 10 % and/or σ ≤ 3 ppm. These threshold values were chosen as they have been reported in the literature for LA-ICP-MS methods for forensic glass analysis[69, 84]. However, it was decided that |% bias| and RSD would be reduced to ≤ 5 % as forensic work requires very accurate analysis.

The following analyses were carried out using the initial suite of elements which were closely inspected before being included in the final method.

3.7.1 NIST 612

Data collected over two months was averaged to evaluate the accuracy and precision of NIST 612. Averages and standard deviations for the reference values were obtained from Pearce *et. al*[106]. The summary statistics are shown in Table 3.9. The values shown in bold are below the threshold values.

A t-test was carried out at the 5 % and 1 % confidence levels to see if the experimental values were significantly different from those reported by Pearce. No trace elements had a significant difference; only Na and Ca had significantly different values to the reference values at both confidence levels.

All elements, were below the threshold for % bias, which ranged from -3.46 (Mg) to 1.79 % (Li). All trace elements met the absolute threshold; which ranged from -0.77 (Li) to 0.91 ppm (Sr).

The concentrations reported by Pearce[106] for Mg and Hf have been suggested as being incorrectly reported; Gao *et al.* states the concentrations as 64 and 35 ppm respectively[110]. The bias of Hf is decreased from -1.24 % to -0.57 %, but it is not significant as it already meets the threshold. The bias of Mg increases from -3.46 % to 19.58 % using the values from Gao, which pushes it over the threshold.

The relative precision of Mg, (5.12 %), ^{207}Pb (5.78 %) and Li (7.54 %) did not meet the < 5 % requirement; however, Mg and ^{207}Pb were only marginally outside the cut off value. The % RSD for all other elements ranged from 1.55 (Al) to 4.64 % (^{208}Pb). For the trace elements only Li did not meet the < 3 ppm requirement for standard deviation (3.07 ppm). The standard deviation for the other trace elements ranged from 0.76 (Rb) to 2.29 ppb (^{207}Pb).

Figure 3.13 is a scatter plot for the margin of error (as a percentage of the mean) vs. the average for each element. The margin of error was calculated as two standard deviations. Most elements sit well below the 5 % error. Only Li, Na, Mg, Ca and Al are above this.

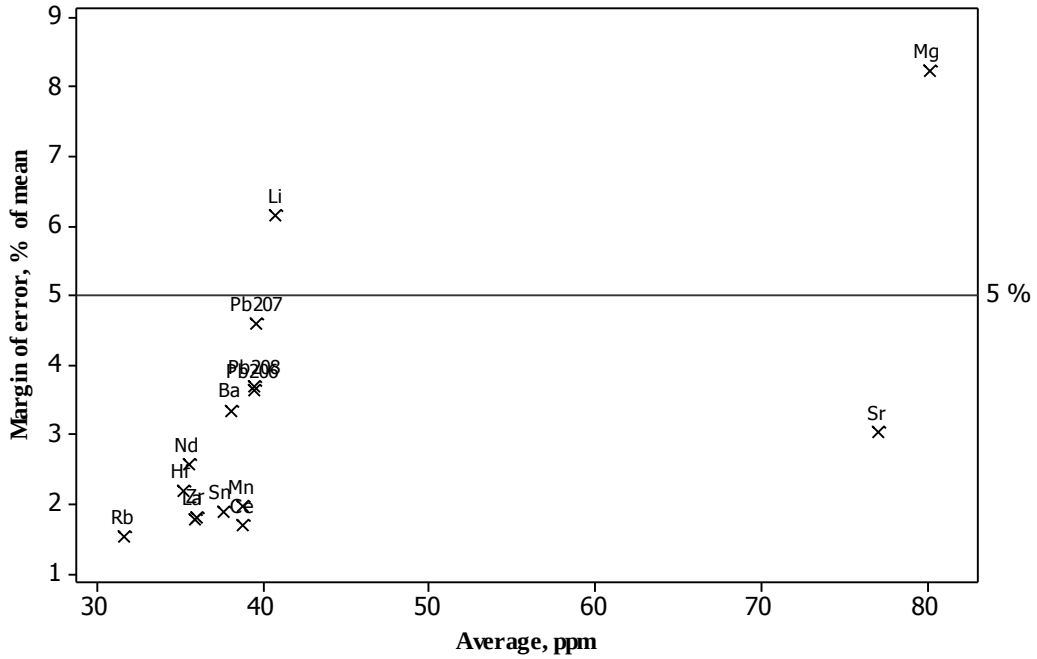

Figure 3.13 Element vs. margin of error, excluding Na, Ca and Al.

Precision and accuracy data can be combined into four levels to assess how good they are; quadrant 1 represents elements which have a small bias and good precision; quadrant 2 has large bias but good precision; quadrant 3 has small bias and poor precision; quadrant 4 has large bias and poor precision. Both relative and absolute values are used to place trace elements in a quadrant; however, due to matrix elements having large concentrations the use of absolute values is not a good measure of precision as it will always exceed 3 ppm. Therefore the matrix elements are only assigned a quadrant by looking at their relative values. These have an * in the table.

The best elements for detection are those found in quadrant 1; Major and minor elements Na, Al and Ca which meet the requirements for the relative data and the trace elements Mn, Rb, Sr, Zr, Sn, Be, Ce, Nd, Hf, ^{206}Pb, and ^{208}Pb which meet both relative and absolute criteria. These elements have both good precision and accuracy (Table 3.8) and are the best elements to use for discrimination. No elements are in quadrant 2. Li, Mg, and ^{207}Pb are in quadrant 3. Mg slightly exceeds the arbitrary cut off value for both standard deviation (4.11 ppm) and % RSD (5.12 %). ^{207}Pb only slightly exceeds the % RSD requirement (5.78 %). Therefore they have been included in further assessment. However, Li exceeds % RSD by 7.54 %. This gives reason to exclude it from analysis.

Table 3.8 Quadrant table for NIST 612 (50 µm, 90 %). Elements in quadrant 1 have high precision and accuracy and will be the best elements for discrimination. Elements with a * are major or minor elements which have only been assigned using relative values. All trace elements have been assigned to a quadrant using both relative and absolute values.

	Accuracy	
Precision	Relative Bias < 5 % AND |bias| < 5 ppm	Relative Bias ≥ 5 % OR |bias| ≥ 5 ppm
RSD < 5 % AND σ < 3 ppm	*Quadrant 1* Na*, Al*, Ca*, Mn, Rb, Sr, Zr, Sn, Ba, La, Ce, Nd, Hf, ^{206}Pb, ^{208}Pb	*Quadrant 2*
RSD ≥ 5 % OR σ ≥ 3 ppm	*Quadrant 3* Li, Mg*, ^{207}Pb	*Quadrant 4*

Table 3.9 Accuracy and precision for NIST 612 (n = 32, 50 µm, 90 %). The values in bold are below the threshold value (|bias| ≤ 5 ppm,|% bias| ≤ 5 % RSD ≤ 5 % and s ≤ 3 ppm). Major and minor elements are denoted with an * and are not included in absolute threshold considerations

Element	Average, ppm	σ, ppm	RSD, %	Bias, %	Bias, ppm
^{7}Li	40.8	3.07	7.54	**1.79**	**-0.74**
^{23}Na*	104786.9	2171.26	**2.07**	**-1.03**	1067.87
^{25}Mg*	80.12	4.11	5.12	**-3.46**	**2.68**
^{27}Al*	11223.67	174.43	**1.55**	**-0.53**	59.07
^{42}Ca*	86146.29	1745.42	**2.03**	**-1.04**	883.79
^{55}Mn	38.8	**0.98**	**2.53**	**-0.97**	**0.37**
^{85}Rb	31.71	**0.76**	**2.39**	**-0.24**	**0.08**
^{88}Sr	77.06	**1.51**	**1.96**	**-1.19**	**0.91**
^{90}Zr	36.03	**0.9**	**2.48**	**-0.1**	**0.04**
^{118}Sn	37.62	**0.94**	**2.51**	**0.9**	**-0.34**
^{137}Ba	38.08	**1.67**	**4.39**	**-0.9**	**0.34**
^{139}La	35.9	**0.89**	**2.49**	**-0.38**	**0.13**
^{140}Ce	38.8	**0.84**	**2.16**	**-1.18**	**0.45**
^{146}Nd	35.56	**1.28**	**3.61**	**-0.9**	**0.32**
^{178}Hf	35.2	**1.09**	**3.09**	**-1.24**	**0.43**
^{206}Pb	39.49	**1.81**	**4.57**	**-1.35**	**0.53**
^{207}Pb	39.67	**2.29**	5.78	**-1.82**	**0.71**
^{208}Pb	39.55	**1.84**	**4.64**	**-1.52**	**0.59**

Table 3.10 Accuracy and precision for FGS 2 (n = 32, 50 µm, 90 %). Values in bold are below the threshold value. Elements with an * are not included in absolute threshold considerations

Element	Average	σ, ppm	RSD, %	Bias, %	Bias, ppm
^{7}Li	28.11	**1.62**	5.77	**3.06**	**-0.89**
^{23}Na*	99841.41	8922.10	8.94	**0.66**	-658.59
^{25}Mg*	23182.09	436.87	**1.88**	**0.93**	-217.91
^{27}Al*	7339.59	169.21	**2.31**	**0.82**	-60.41
^{39}K*	4601.54	369.01	8.02	**-0.03**	**1.54**
^{42}Ca*	58282.53	1763.54	**3.03**	**1.72**	-1017.47
^{49}Ti*	324.10	9.55	**2.95**	**0.58**	**-1.90**
^{55}Mn	218.90	4.56	**2.08**	**0.95**	**-2.10**
^{57}Fe*	2564.78	47.40	**1.85**	**1.35**	-35.22
^{85}Rb	34.66	**0.69**	**1.99**	**0.97**	**-0.34**
^{88}Sr	250.84	4.91	**1.96**	**0.85**	**-2.16**
^{90}Zr	221.16	6.80	**3.07**	**0.83**	**-1.84**
^{118}Sn	93.14	**1.92**	**2.06**	**0.91**	**-0.86**
^{137}Ba	196.33	4.80	**2.44**	**1.34**	**-2.67**
^{139}La	17.75	**0.45**	**2.54**	**1.40**	**-0.25**
^{140}Ce	22.65	**0.48**	**2.13**	**1.53**	**-0.35**
^{146}Nd	24.92	**0.94**	**3.75**	**0.31**	**-0.08**
^{178}Hf	14.81	**0.55**	**3.68**	**1.27**	**-0.19**
^{206}Pb	23.69	**0.91**	**3.83**	**1.31**	**-0.32**
^{207}Pb	24.22	**1.03**	**4.24**	**-0.94**	**0.22**
^{208}Pb	23.92	**0.85**	**3.54**	**0.35**	**-0.08**

3.7.2 FGS 2

FGS 2 was kindly donated for use in this project by Stefan Becker (BKA, Germany) part way through the method development stage of the research. FGS 2 is a relatively new standard and is not widely used as it is not available for purchase. Therefore accuracy and precision were calculated and compared to NIST 612. 12 analyses were done on the same day; the remaining 20 analyses were obtained later from QC data. The consensus values for FGS 2 with a ± 1 σ were obtained from Latkoczy *et al*[87].

A t-test showed no elements had statistically detectable biases from the literature values ($p = 0.05$ and 0.01).

The summary statistics for accuracy and precision are shown in Table 3.10. The values in bold are the accepted values as they fall below the threshold values.

All elements were below the 5 % bias limit; the values ranged from -0.94 (^{207}Pb) to 3.06 % (Li). All trace elements meet the 5 ppm requirement for accuracy; these range from -2.67 (Ba) to 0.22 ppm (^{207}Pb).

For relative precision, Li (5.77 %), K (8.02 %) and Na (8.94 %) did not meet the < 5 % requirement. The % RSD for all other elements ranged from 1.85 (Fe) to 4.24 % (^{207}Pb). Trace elements Mn (4.56 ppm), Ba (4.8 ppm), Sr (4.91 ppm) and Zr (6.8 ppm) did not meet the absolute threshold of < 3 ppm. The other trace elements had a standard deviation of 0.45 (La) to 1.92 ppm (Sn).

Figure 3.14 shows the margin of error (as a percentage of the mean) vs. the trace elements. All major elements except Ti had a margin of error greater than 100 % and are not shown on the graph.

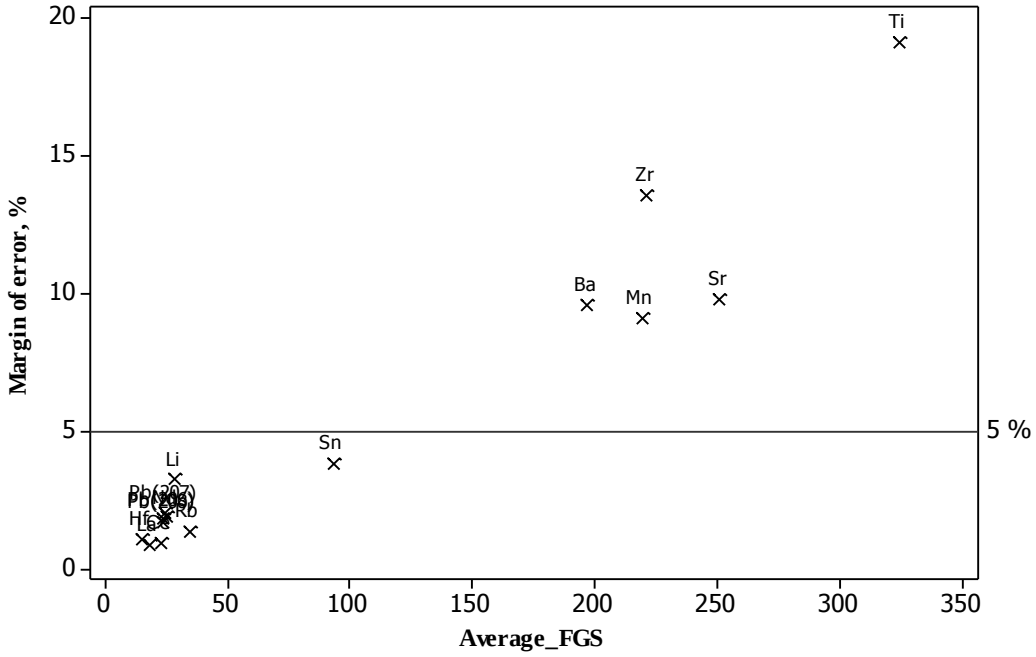

Figure 3.14 Margin of error for elements using FGS 2 as calibrating standard, excludes Na, Ca, Mg, Al, K and Fe.

Table 3.11 combines the precision and accuracy data together into four levels to assess the quality of each element. As for analysis of NIST 612, quadrant 1 represents elements which have a small bias and good precision; quadrant 2 has large bias but good precision; quadrant 3 has small bias and low precision; quadrant 4 has large bias and low precision. Both relative and absolute values have been used to place trace elements in a quadrant; however, due to matrix elements having large concentrations the use of absolute values is not a good measure of precision as it will always exceed 3 ppm. Therefore the matrix elements are only assigned a quadrant by looking at their relative values. These have an * in the table.

The best elements for detection are those found in quadrant 1. The major and minor elements Mg, Al, Ca, Ti and Fe which meet the requirements for the relative values and the trace elements Rb, Sn, La, Ce, Nd, Hf, ^{206}Pb, ^{207}Pb and ^{208}Pb which meet all of the four accuracy and precision thresholds. These elements have the most promise for being highly discriminating elements.

Li is in quadrant 3, but is only just above the threshold for % RSD (5.77 %), therefore it may still be a useful element. Na and K have % RSDs > 8 %, therefore they may not be good elements to include*. Mn, Sr and Ba only slightly exceed the 3 ppm cut off (4.56, 4.91 and 4.80 ppm respectively). Zr is over double the cut off value (6.80 ppm). However, these elements have higher concentrations than in NIST 612 (around 200 ppm compared to approximately 40 ppm).

Table 3.11 Quadrant table for FGS 2 (50 um, 90 %). Elements in quadrant 2 have high precision and accuracy and will be the best elements for discrimination

	Accuracy	
Precision	Relative Bias < 5 % AND |bias| < 5 ppm	Relative Bias ≥ 5 % OR |bias| ≥ 5 ppm
RSD < 5 % AND σ < 3 ppm	*Quadrant 1* Mg*, Al*, Ca*, Ti*, Fe*, Rb, Sn, La, Ce, Nd, Hf, ^{206}Pb, ^{207}Pb, ^{208}Pb	*Quadrant 2*
RSD ≥ 5 % OR σ ≥ 3 ppm	*Quadrant 3* Li, Na*, K*, Mn, Sr, Zr, Ba	*Quadrant 4*

3.7.3 Comparison of NIST 612 and FGS 2

At the 5 % threshold level for % RSD and % bias, 10 of the elements in quadrant 1 are the same for both standards: Al*,Ca*, Rb, Sn, La, Ce, Nd, Hf ^{206}Pb and ^{208}Pb.

Figure 3.15 shows the deviation of the value from the certified value for both standards. Most elements have a positive bias for FGS 2, compared to NIST for which they show a negative bias. All of the elements have less than 5 % bias. Figure 3.16 compares the % RSD for both standards. Most elements are below 5 %.

* K was later found to have a correlation with Rb (see section 4.2.2). Therefore it is not an issue that it is removed

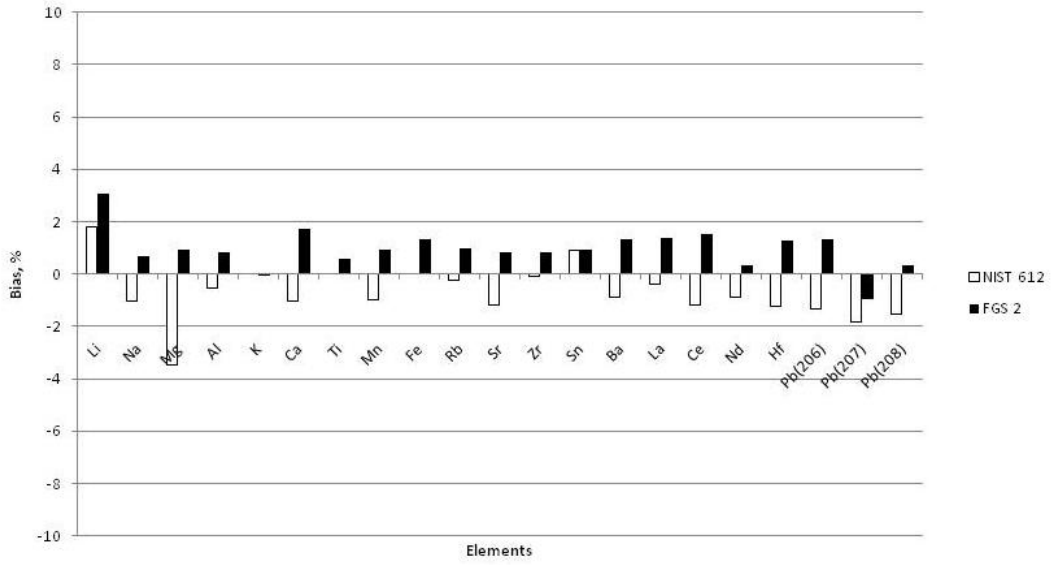

Figure 3.15 Comparison of % bias for NIST 612 and FGS 2 with the literature values. All elements are below 5 %.

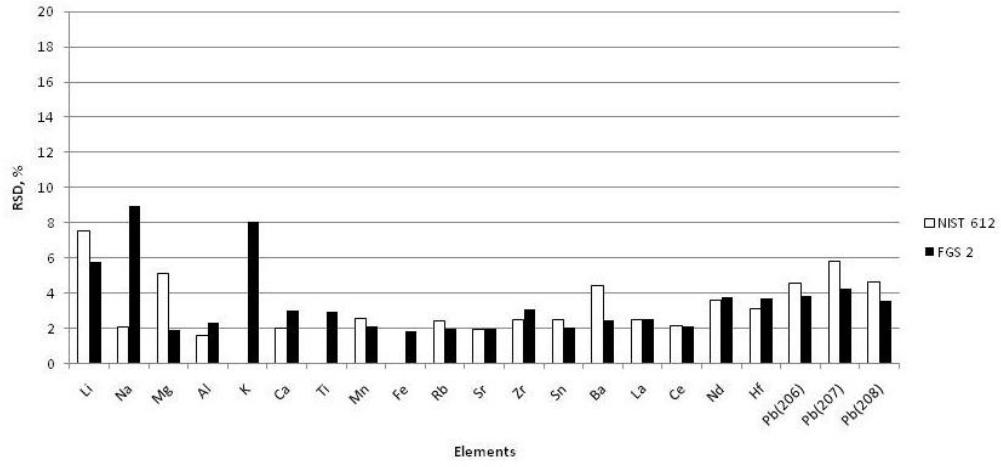

Figure 3.16 Comparison of % RSD for NIST 612 and FGS 2. Most elements are below 5 %.

3.8 Representative samples

FGS 2 was used as a surrogate sample to compare the bias in the calibration of the two standards. Real glass samples were also analysed using both standards.

3.8.1 Accuracy and precision of representative sample (FGS 2)

The standard used for calibration may alter the concentration output of the samples. It is beneficial to determine if the data from the LA-ICP-MS is reading the concentration accurately or whether there is a bias in the measurement.

NIST 1831 has been used in the literature as a surrogate sample and calibration standard[19, 57, 84]. However, this was not available for this research. Therefore FGS 2, which is a good representation of float glass, was used as the surrogate for this research. The experimental values were able to be compared to the literature values. The effect each standard had on the concentration was examined. This illustrates the variation of concentration which will occur in real samples.

NIST 612 and FGS 2 were both used as the calibration standard. Results for NIST 612 are shown in Table 3.12; the results for FGS 2 are given in Table 3.13. The threshold values for the accuracy and precision are the same as those used in section 3.6. The values in bold are below the threshold. A t-test was carried out ($p = 0.05$ and 0.01) to see if the measured values of elements in FGS 2 are significantly different to the consensus values in the literature[87]. When NIST 612 was used as the standard only Al was detected to have a significantly detectable bias ($p = 0.05, 0.01$). When FGS 2 was used as the standard no elements were detected as having significantly different values.

The results show that using FGS 2 as the calibrating standard for float glass produced concentrations more in line with the literature values for some elements; especially for Li, Mg, Al, Rb and La (Figure 3.17). In addition, it is also able to detect K, Ti and Fe. These results show that FGS 2 can be a viable standard for the analysis of glass fragments. However, this may be due to FGS 2 being the representative sample. Section 3.8.2 compares the measured values of real glass samples when the two standards are used.

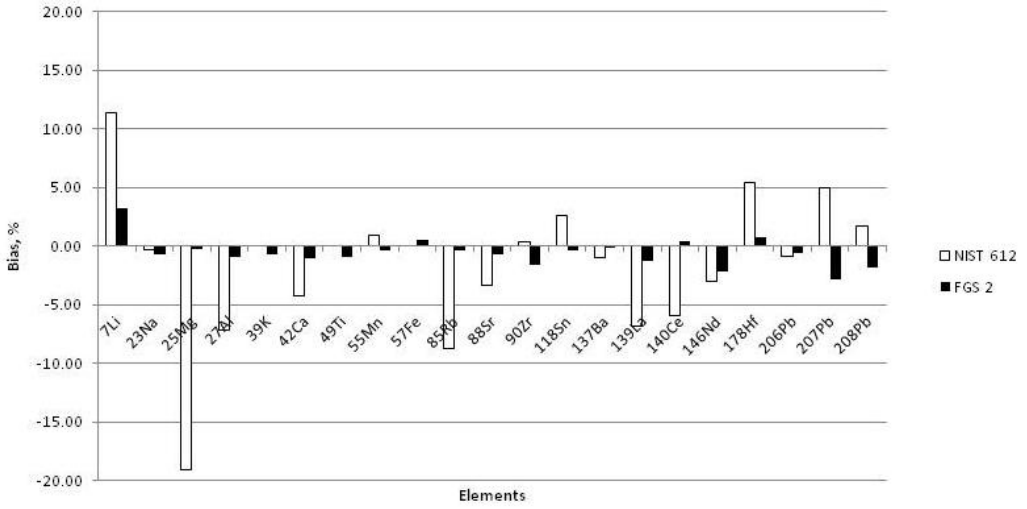

Figure 3.17 Comparison of the bias of measured values of FGS 2 with the literature values when NIST 612 and FGS 2 are used as standards.

Table 3.12 Accuracy and precision of FGS 2 using NIST 612 as the calibration standard (n =10) (50µm, 90 %). The values in bold are below the threshold

Element	Average, ppm	σ, ppm	% RSD	% bias	Bias, ppm
^{7}Li	25.72	**1.25**	**4.86**	11.30	**-3.28**
^{23}Na	100846.53	1106.57	**1.10**	**-0.34**	346.53
^{25}Mg	27855.47	552.20	**1.98**	-19.04	4455.47
^{27}Al	7932.82	113.02	**1.42**	-7.20	532.82
^{42}Ca	61834.17	897.82	**1.45**	**-4.27**	2534.17
^{55}Mn	218.88	**1.95**	**0.89**	**0.96**	**-2.12**
^{85}Rb	38.05	**0.44**	**1.16**	-8.71	**3.05**
^{88}Sr	261.51	**2.80**	**1.07**	**-3.36**	8.51
^{90}Zr	222.24	4.29	**1.93**	**0.34**	**-0.76**
^{118}Sn	91.58	**0.97**	**1.05**	**2.57**	**-2.42**
^{137}Ba	200.94	**0.88**	**0.44**	**-0.97**	**1.94**
^{139}La	19.24	**0.31**	**1.60**	-6.87	**1.24**
^{140}Ce	24.38	**1.54**	**6.30**	-5.98	**1.38**
^{146}Nd	25.76	**0.88**	**3.40**	**-3.04**	**0.76**
^{178}Hf	14.20	**0.48**	**3.42**	5.36	**-0.80**
^{206}Pb	24.20	**0.39**	**1.61**	**-0.83**	**0.20**
^{207}Pb	22.82	**0.75**	**3.27**	**4.94**	**-1.19**
^{208}Pb	23.58	**0.39**	**1.64**	**1.75**	**-0.42**

Table 3.13 Accuracy and precision of FGS 2 using FGS 2 as the calibration standard (n =12) (50 µm, 90 %). The values in bold are below the threshold

Element	Average, ppm	σ, ppm	% RSD	% bias	Bias, ppm
^{7}Li	28.08	**0.83**	**2.95**	**3.17**	**-0.92**
^{23}Na	101156.83	1719.80	**1.70**	**-0.65**	656.83
^{25}Mg	23468.01	209.72	**0.89**	**-0.29**	68.01
^{27}Al	7472.30	154.85	**2.07**	**-0.98**	72.29
^{39}K	4633.99	37.36	**0.81**	**-0.74**	33.99
^{42}Ca	59889.53	810.38	**1.35**	**-0.99**	589.53
^{49}Ti	329.19	10.56	**3.21**	**-0.98**	3.19
^{55}Mn	221.91	**2.14**	**0.96**	**-0.41**	**0.91**
^{57}Fe	2587.56	27.80	**1.07**	**0.48**	-12.44
^{85}Rb	35.15	**0.46**	**1.31**	**-0.42**	**0.15**
^{88}Sr	254.91	3.65	**1.43**	**-0.76**	**1.91**
^{90}Zr	226.57	6.91	**3.05**	**-1.60**	3.57
^{118}Sn	94.35	**0.88**	**0.94**	**-0.37**	**0.35**
^{137}Ba	199.23	4.51	**2.26**	**-0.12**	**0.23**
^{139}La	18.23	**0.51**	**2.79**	**-1.25**	**0.23**
^{140}Ce	22.90	**0.40**	**1.73**	**0.45**	**-0.10**
^{146}Nd	25.53	**0.68**	**2.68**	**-2.13**	**0.53**
^{178}Hf	14.88	**0.60**	**4.01**	**0.77**	**-0.12**
^{206}Pb	24.15	**0.53**	**2.18**	**-0.63**	**0.15**
^{207}Pb	24.67	**1.04**	**4.23**	**-2.79**	**0.67**
^{208}Pb	24.43	**0.84**	**3.45**	**-1.80**	**0.43**

3.8.2 Comparison of standards using real glass samples

The difference in the measurements* with each standard was divided by the average of the two measurements and plotted against the sample in a scatter plot to examine the difference in reported concentrations.

The Holden windscreen was used as a sample to compare the difference in measurement between the two standards. Figure 3.18 shows the percentage difference in reported values. The elements which exceed 5 % are the same elements found when NIST 612 is used as the calibration standard to report the values of FGS 2 (section 3.8.1). NIST 612 reports Mg with a value 18.5 % higher than FGS 2. NIST 612 reports Al, Rb, La, Ce and Nd between 5 and 8 % higher. FGS 2 reports Li values 7.7 % higher than NIST 612 does. Data from the Mitsubishi side window also showed the same trend.

All database samples (including replicates) were averaged, and this value was used to examine the measurement difference between the two standards across all samples. Most elements had less than 5 % difference between the two standards (Figure 3.19). Al, Rb and La were about 7 % higher when using NIST 612 and Ce was 5.3 % higher. Li had a 10 % higher measurement when FGS 2 was used as the calibration standard. However, this set of data does not have a large difference in the Mg values. There is no obviously apparent reason for this.

* The values are calculated using NIST 612 measurements minus FGS 2 measurements.

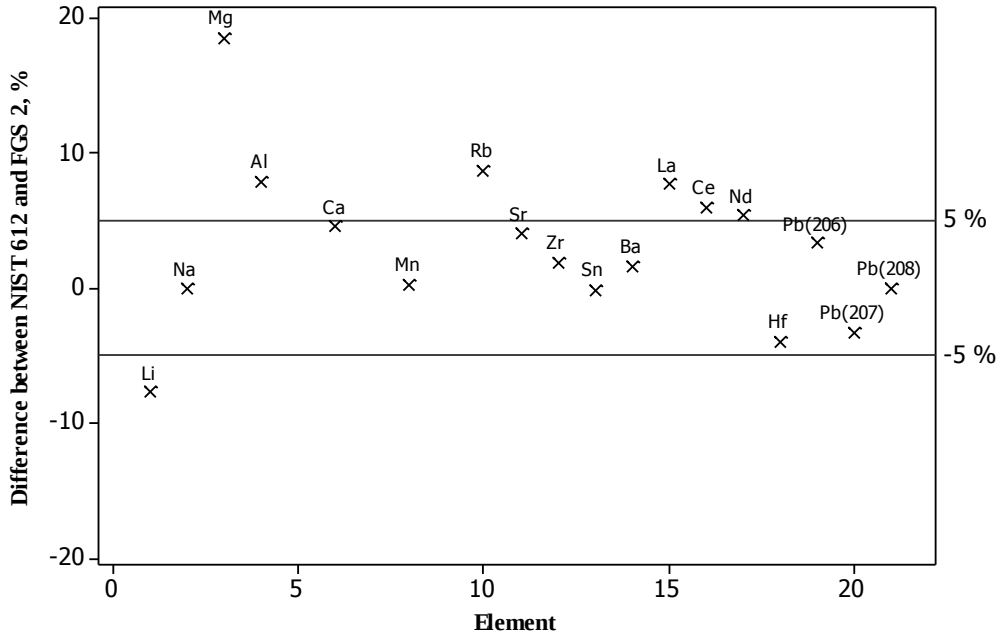

Figure 3.18 Difference between measurement values for the Holden windscreen using NIST 612 and FGS 2 as the standards.

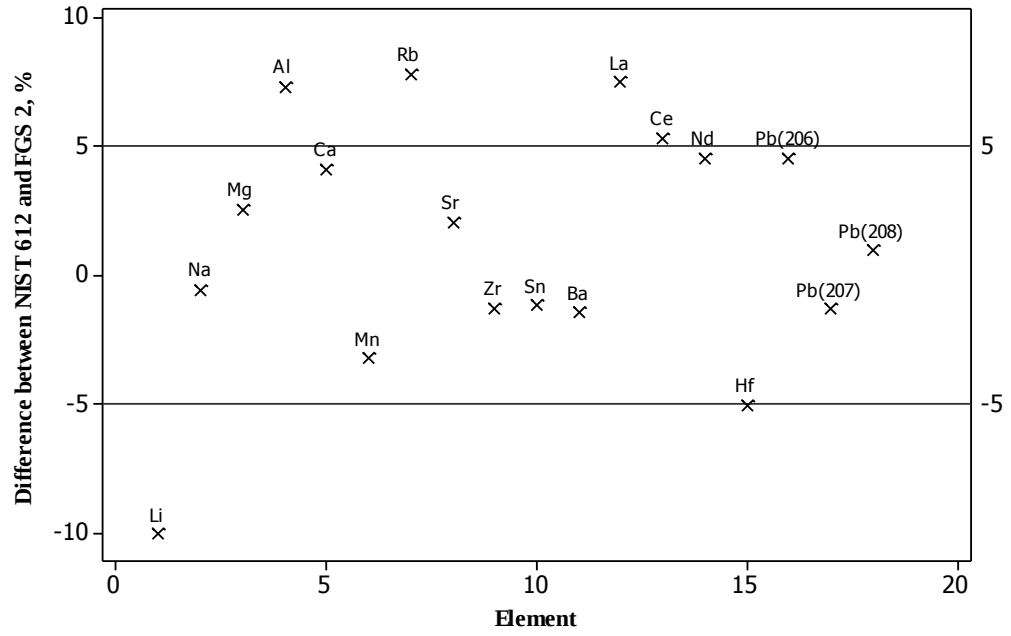

Figure 3.19 Difference between measurement values for all database samples using NIST 612 and FGS 2 as standards.

3.9 Inter-laboratory comparision

An inter-laboratory study is usually the final stage for validating a method. However due to very few LA-ICP-MS systems in New Zealand, an inter-laboratory study could not be conducted until the end of the research once the database had been analysed. This section has been placed at this point in the thesis as it belongs with the method development.

The Centre for Forensic Science (CFS), University of Western Australia kindly agreed to take part in a comparison study. The CFS uses a 213 nm Nd:YAG New Wave laser coupled to an Agilent ICP-MS. The method validated in this research was used to analyse four samples and the raw data files were processed in GLITTER to produce the concentration data. These samples will be identified as 'CFS', while the samples analysed in the bulk of this research will be identified as University of Waikato (UoW).

CFS tuned the instrument using NIST 612 before analysis of the samples. Fluence of the samples was approximately 0.7 mJ (30 J/cm^2). This is similar to the fluence of samples analysed during this research. Na was above the detection limits for the first two standards ablated which caused incorrect calibration of the samples. Therefore Na will be excluded from the discussion. In addition, Zr was missed from analysis, so could not be compared.

The two QC samples (FGS) analysed by CFS were averaged and the bias with the literature and UoW were calculated. 5 % was the threshold chosen for the % bias of elements with the literature values (see section 3.7). All elements, except ^{208}Pb (-6.93 %) have less than 5 % bias between the two laboratories and only Al, Sr and ^{208}Pb marginally exceeded this (5.11, 5.30 and -5.40 % respectively) when compared to the literature values.

Table 3.14 Bias of FGS values from CFS with UoW and literature values

Element	Bias between laboratories, %	Bias with literature, %
^{7}Li	-1.86	-1.00
^{25}Mg	1.75	3.21
^{27}Al	3.70	5.11
^{39}K	-2.92	-2.51
^{42}Ca	0.36	2.32
^{49}Ti	2.07	3.58
^{55}Mn	0.10	1.33
^{57}Fe	1.09	2.22
^{85}Rb	-0.85	0.36
^{88}Sr	4.13	5.30
^{118}Sn	-0.48	1.33
^{137}Ba	2.76	4.26
^{139}La	2.11	3.83
^{140}Ce	-0.33	1.30
^{146}Nd	3.18	4.80
^{178}Hf	3.70	4.73
^{206}Pb	-3.66	-1.50
^{207}Pb	-1.87	-1.77
^{208}Pb	-6.93	-5.40

Four glass samples from the database were analysed on both instruments; details of these samples are listed in Table 3.15. The four replicates were averaged for analysis. The bias between the two laboratories for each sample was calculated. The results are displayed in a column graph (Figure 3.20) and Table 3.16. As stated in section 3.7, the bias is a measure of accuracy. Most elements had less than 10 % bias in this study. However, the accuracy for the samples is not as good when compared to the results for the standard, which had less than 5 % bias. A round-robin study in the literature reported a typical bias of 10 % between laboratories[87]. This is an acceptable bias for the measurement of real samples.

Li and Sn had a bias larger than 10 % for all four samples. Li was reported by CFS as having a lower concentration than UoW values, while Sn was reported by CFS as having a higher concentration. In addition, two samples had a bias larger than 10 % for K, Fe, Rb and ^{208}Pb.

Table 3.15 Details of the four samples compared in the inter-laboratory test

Sample	Make	Model	Year	Country	RI
50 WS_F	Holden	Commodore Wagon	2004	Australia	1.52352
92 LF	Ford	Courier	2002	Thailand	1.51942
112 WS_B	Hyundai	Elantra	2003	South Korea	1.52006
153 WS_F	Toyota	Hiace	2006	Japan	1.52012

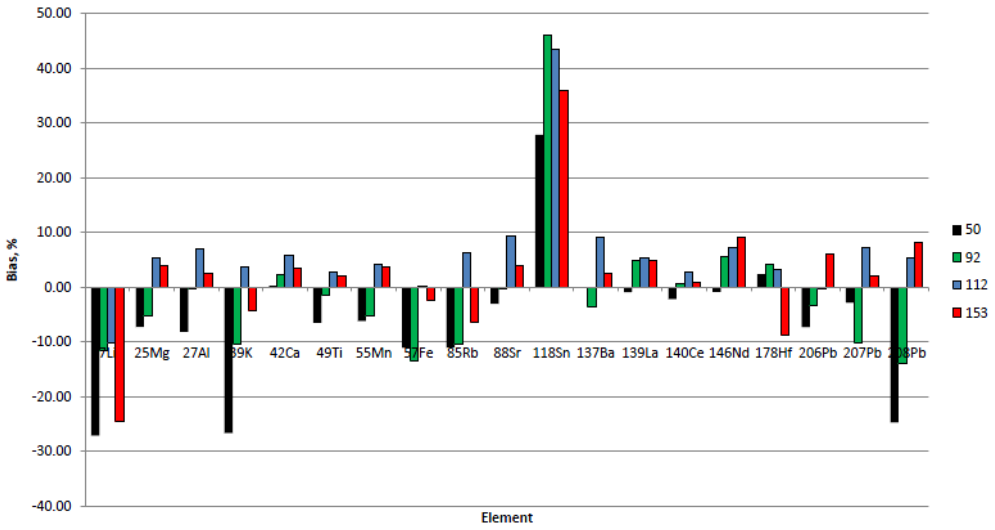

Figure 3.20 Bias of the four samples between the two laboratories. Most elements have less than 10 % bias. Sn has the most bias between the two laboratories.

Table 3.16 Bias of the four samples between the two laboratories. Values in bold text are below 10 % bias

	Bias of sample 50, %	**Bias of sample 92, %**	**Bias of sample 112, %**	**Bias of sample 153, %**
^{7}Li	-27.15	-11.65	-10.25	-24.59
^{25}Mg	**-7.28**	**-5.26**	**5.31**	**3.84**
^{27}Al	**-8.13**	**-0.29**	**7.11**	**2.63**
^{39}K	-26.64	-10.35	**3.70**	**-4.38**
^{42}Ca	**0.27**	**2.40**	**5.81**	**3.56**
^{49}Ti	**-6.49**	**-1.39**	**2.68**	**2.00**
^{55}Mn	**-6.19**	**-5.19**	**4.27**	**3.71**
^{57}Fe	-11.09	-13.45	**0.20**	**-2.34**
^{85}Rb	-11.02	-10.43	**6.23**	**-6.46**
^{88}Sr	**-2.97**	**-0.22**	**9.28**	**3.90**
^{118}Sn	27.83	46.07	43.46	36.02
^{137}Ba	**0.00**	**-3.53**	**9.11**	**2.59**
^{139}La	**-0.92**	**4.84**	**5.35**	**4.79**
^{140}Ce	**-2.22**	**0.63**	**2.66**	**0.99**
^{146}Nd	**-0.81**	**5.66**	**7.20**	**9.09**
^{178}Hf	**2.41**	**4.28**	**3.26**	**-8.82**
^{206}Pb	**-7.29**	**-3.33**	**-0.34**	**6.08**
^{207}Pb	**-2.83**	-10.10	**7.33**	**2.16**
^{208}Pb	-24.68	-13.87	**5.24**	**8.24**

As stated in section 3.7, precision is defined as the scatter of data about an expected value; relative precision is calculated using % RSD. Table 3.17 shows the % RSD of each element for the two laboratories. Most elements had a RSD less than 5 % for both laboratories. However, sample 112 analysed by CFS had larger measurement deviation for most elements; only K and Ce were below the threshold. 8/19 elements were between 5 and 10 %, while 9/19 elements had a % RSD larger than 10 %. Most Pb isotopes measured by UoW gave RSDs larger than 10 % (up to 25.14 %) compared to CFS which has smaller values. Nd, Hf

and the Pb isotopes were the main elements to show large deviations over all the samples for both laboratories. However, this was more prominent for UoW measurements.

Table 3.17 Relative standard deviation for all elements for both laboratories

	50		92		112		153	
	UoW	**CFS**	**UoW**	**CFS**	**UoW**	**CFS**	**UoW**	**CFS**
^{7}Li	6.37	2.23	6.11	2.50	9.80	7.82	12.79	5.18
^{25}Mg	1.92	3.72	2.06	2.60	1.66	11.58	1.19	2.12
^{27}Al	2.04	3.93	1.10	3.91	1.39	13.52	1.00	1.91
^{39}K	9.18	5.49	1.18	3.41	0.58	4.60	0.62	2.20
^{42}Ca	1.52	3.81	2.08	2.68	1.77	7.17	1.41	2.42
^{49}Ti	1.91	1.99	0.60	3.01	2.48	8.53	3.23	1.72
^{55}Mn	2.64	1.71	1.23	1.98	2.05	8.69	1.97	1.34
^{57}Fe	0.20	0.82	2.38	0.98	5.46	10.45	1.51	1.03
^{85}Rb	6.60	3.94	1.00	2.79	2.32	6.65	1.32	2.07
^{88}Sr	1.86	2.80	2.20	2.64	2.43	12.31	1.16	2.77
^{118}Sn	3.60	3.77	4.87	2.69	5.88	13.29	3.08	4.64
^{137}Ba	4.90	4.09	3.10	2.17	3.24	12.31	2.58	2.19
^{139}La	2.10	4.06	1.99	3.92	2.33	10.03	5.61	3.09
^{140}Ce	1.04	1.18	1.41	3.45	6.19	4.26	1.55	2.33
^{146}Nd	9.81	4.35	8.44	3.72	6.31	10.75	12.52	1.36
^{178}Hf	14.63	6.60	9.89	6.29	6.99	13.32	10.90	5.22
^{206}Pb	17.54	6.49	15.26	13.50	14.50	8.80	23.62	4.00
^{207}Pb	25.14	12.72	11.02	5.61	12.13	6.42	10.92	5.34
^{208}Pb	15.31	4.89	5.92	6.24	5.50	6.64	1.51	5.32

The inter-laboratory results show that the validated method is robust, not only day-to-day on the UoW instrument, but also between laboratories for the calibration standard and samples. Analysis of Li and Sn are the most problematic elements to compare between laboratories. All other elements have a bias < 10 %. Overall, the precision of most elements is acceptable and in most cases is less than

5 %. However, Nd, Hf and the Pb isotopes have the most deviation for both laboratories.

3.10 Decision on which calibration standard to use for analysis of glass samples

The preceding sections have shown that FGS 2 is a viable standard for calibration of float glass samples. It has good accuracy and precision. It is superior to NIST 612 for some elements; it calibrates Mg with a lower bias than NIST 612. In addition, it is able to detect Ti and Fe as they have concentrations in the standard which are sufficiently above the background level. Therefore the analysis of the database will be carried out using samples calibrated using FGS 2.

4 Analysis of database samples

As mentioned in chapter 2, the database is comprised of 244 samples from ESR which have been previously measured by RI. All the glass is assumed to be from the original pane in the car. The RI gives univariate data which has limited discriminating ability; in addition, there has been a decrease in the spread of RI measurements. Therefore it is no longer an ideal stand alone discriminating technique.

The second part of this research examines the use of LA-ICP-MS to categorise and differentiate the ESR database samples. The intra- and inter-homogeneity of glass was examined to ensure small fragments were representative of an entire pane. Principal component analysis (PCA) is a statistical data reduction technique that was used to examine natural splitting in the data. It is a way to display the data graphically for interpretation. Waikato environment for knowledge analysis (Weka), data mining software and linear discriminant analysis (LDA) were compared in their ability to categorise samples into country of origin. PCA and range overlap were used in an attempt to discriminate fragments. The range overlap method was then combined with RI in a three step process for further discrimination.

4.1 Refractive index

During casework analysis, the RI for recovered and control fragments are compared. Recovered fragments that have RI values which are close[*] are assumed to have originated from one source. The group of recovered fragments is compared to the control glass using a t-test to determine if they can be differentiated. If this provides a 'match', a portion of the recovered and control glasses are annealed and their RI is measured again. The difference, delta RI, is calculated. If both the recovered and control samples are from either tempered or non-tempered glass then they are deemed to match.

[*] Samples from the same source generally lie within ~±0.0005 RI

Tempered glass and laminated glass are forms of secondary modification. Therefore the two types cannot be separated by elemental composition as they were manufactured in the same way. Delta RI is useful for categorising samples into tempered and non-tempered groups (delta RI > ~125 $x10^{-5}$ and < ~125 $x10^{-5}$ respectively). Figure 4.1 shows the separation of tempered and non-tempered glass in the database.

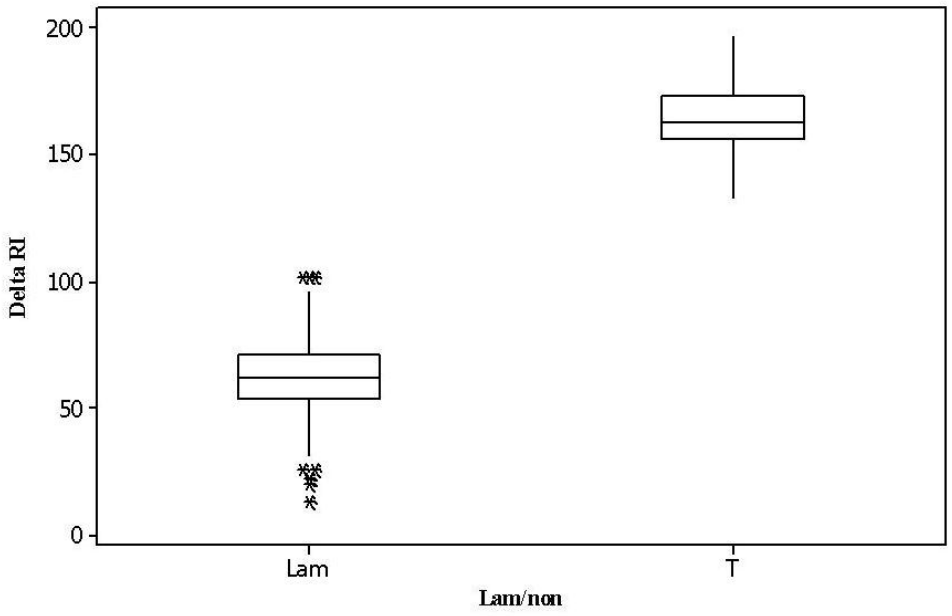

Figure 4.1 Box plot of delta RI vs. laminated and tempered glass for database sample. Delta RI can categorise the two types of glass. If delta RI is > ~125x10^{-5} it is tempered glass; if it < ~125x10^{-5} it is non-tempered glass.

For the 244 samples, RI ranges from 1.5175 to 1.5424, which is a spread of only 0.0249. Figure 4.2 shows the samples ranked in ascending RI value. The error bars are set at ± 0.0005. The samples with overlapping error bars are indistinguishable from each other. The graph shows that most of the samples are unable to be distinguished by RI alone; there are small groups of samples at both ends that can be discriminated from the bulk of the samples, but not from each other.

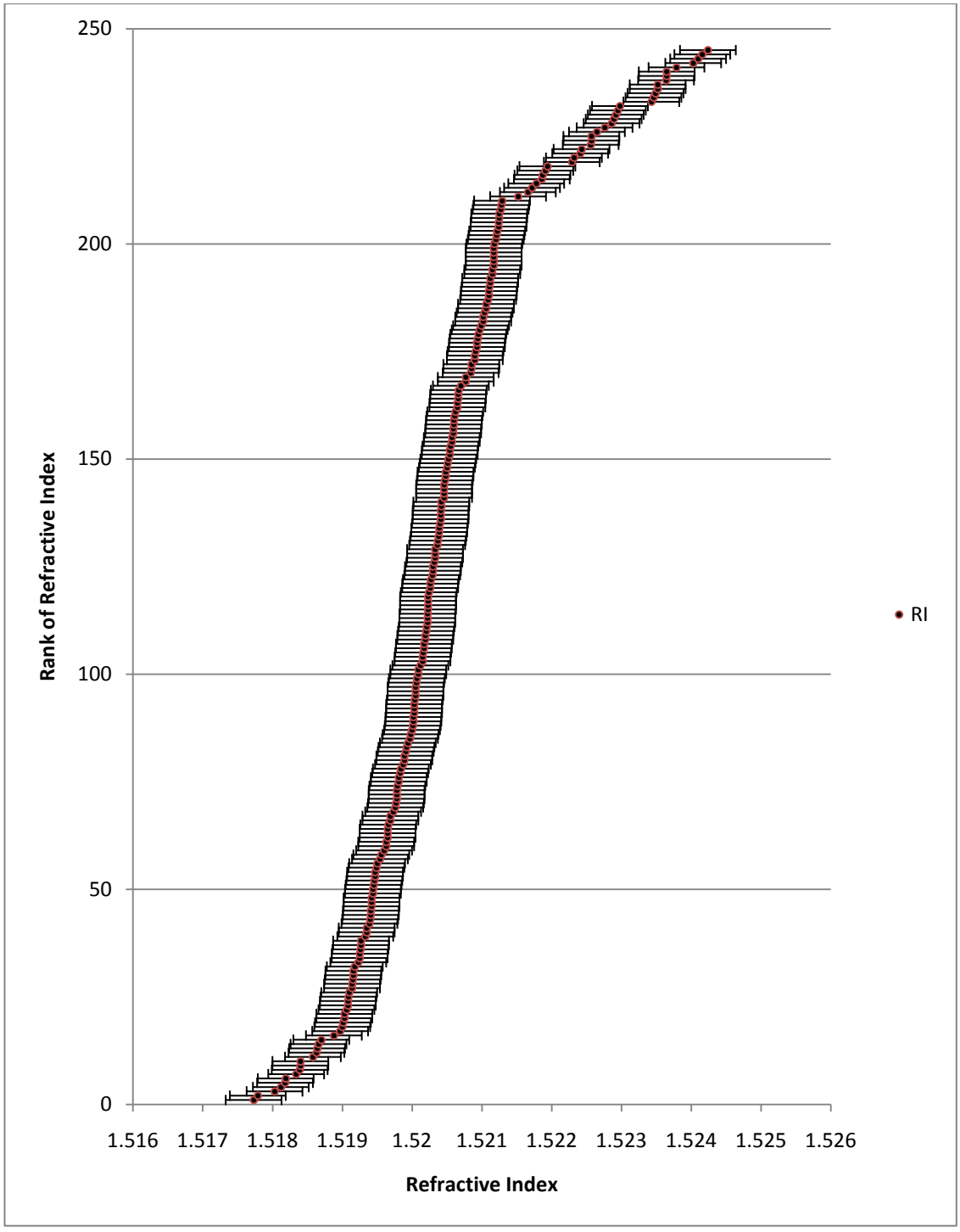

Figure 4.2 Rank of the 244 database samples by increasing RI value. Error bars are set at ± 0.0005. Samples with overlapping error bars are indistinguishable. No samples can be distinguished from all other samples using RI.

4.2 Refinement of method validation using database samples

All database samples were ablated using the method that was verified in chapter three. The quality of the data was examined before being used. This included evaluating the elemental suite for elements below detection limits and elements which had correlations, and investigating the effect of analysing samples on different days.

4.2.1 Values below zero and minimum detection limits

The suite of elements used for analysis of the database was further considered once all analyses had been completed. The intention was to remove any elements that were predominantly below detection limits during construction of the database. However, this was not necessary as no elements were consistently below the limit of detection (LOD). There were only three occasions where one of the four replicates for ^{208}Pb was below the LOD.

4.2.2 Correlation of elements

A matrix plot of all elements was used to examine whether there were any correlations between elements. K and Rb, Zr and Hf, La and Nd and the three Pb isotopes are correlated. La and Ce have been noted to have a natural correlation. However, no correlation is seen in the database. This may be due to Ce_2O_3 being added as a decolourising agent during glass manufacture[26]. Figure 4.3 shows a matrix plot of the elements of interest. Only one element from each correlated set was required for analysis of PCA; however, all elements were examined in the homogeneity test before removal of one of the correlated elements from each set.

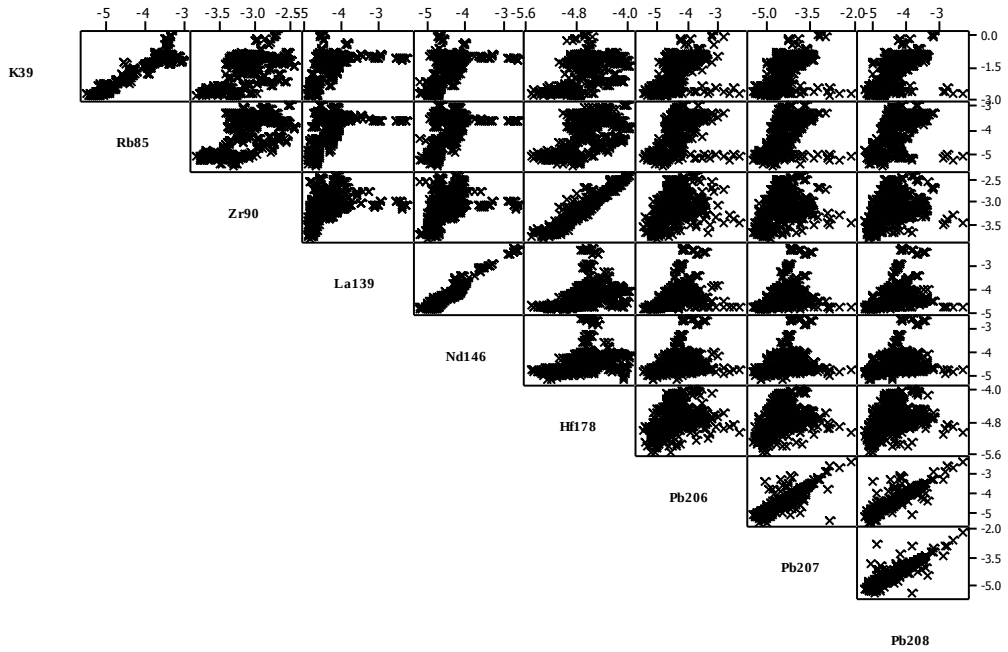

Figure 4.3 Matrix plot of elements that have correlations. K and Rb, La and Nd, Zr and Hf and the three Pb isotopes are correlated.

4.2.3 Analysis of replicates on different days

A small number of samples had the replicates analysed on different days for various reasons (e.g. repeated shattering of sample, sample missing from grid or missed from analysis). Replicates of samples ablated on the same day were compared to replicates of samples ablated on different days. The residual value for each element was examined as this shows the variation about the mean. The results showed that the scatter of residual value of the sets of replicates that were analysed on different days was no larger than that for samples analysed on the same day for any of the elements. Figure 4.4 shows the results for Sr, which is representative of the other elements. Therefore replicates of samples can be analysed on separate days if necessary. These results show that the method will allow control and recovered samples to be analysed on different days and still show a match if there is one (see sections 4.10.1.1 and 4.10.2.2).

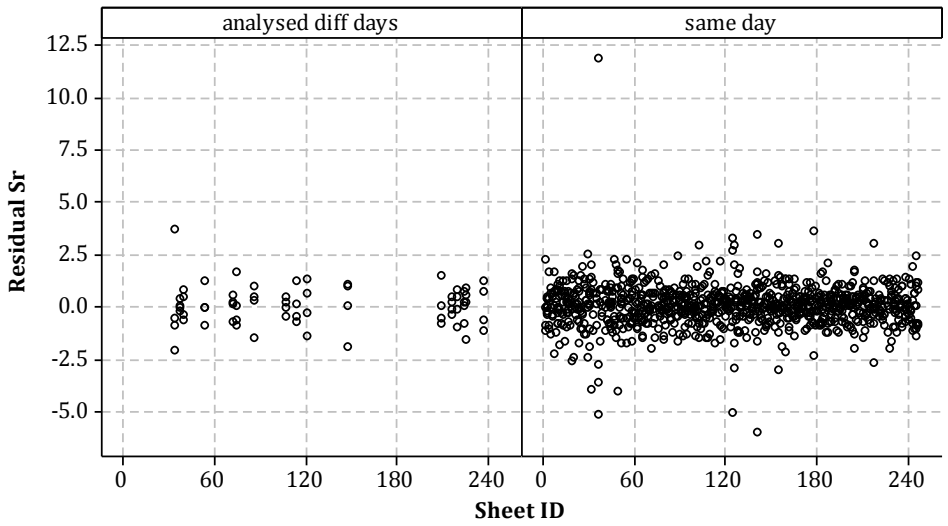

Figure 4.4 Scatter plot of residual Sr vs. sheet ID. Replicates of samples on the left were analysed on different days; replicates of samples on the right were analysed on the same day. There is no difference in the scatter of residual Sr between the two groups.

4.3 Normalisation of the database

Statistical methods which examine elements individually, such as ANOVA, can use the data in their natural form; this is referred to as raw data[*]. However, to use multivariate analysis, such as PCA (see section 4.7 for explanation of PCA) and LDA (see section 4.8.1), the raw data must be normalised so that samples can be compared to each other. PCA and LDA must be transformed in different ways.

PCA requires centred log-ratio (clr) transformation. This is calculated by taking the logarithm of the ratio of each element to the geometric mean of the variables:

$$clr(x) = \left[ln\left(\frac{x_1}{g(x)}\right), ln\left(\frac{x_2}{g(x)}\right), \ldots, ln\left(\frac{x_p}{g(x)}\right)\right] \qquad (4.1)$$

where the geometric mean is calculated by

$$g(x) = \left(\prod_{i=1}^{p} x_1\right)^{\frac{1}{p}} \qquad (4.2)$$

This data is referred to as clr transformed data.

[*] This is the concentration output (measured in ppm) from GLITTER

LDA data requires the data to be transformed by additive log-ratio (alr); this takes the natural logarithm of each component over the *p*th component:

$$alr(x) = \left[ln\left(\frac{x_1}{x_p}\right), ln\left(\frac{x_2}{x_p}\right), \dots, ln\left(\frac{x_{p-1}}{x_p}\right)\right] \quad (4.3)$$

where

$$x = \left(x_1, x_2, \dots, x_p\right)^T \quad (4.4)$$

alr requires the log of each element to be divided by a common denominator. This denominator needs to be a stable element for all samples. As Si is used as the internal standard in GLITTER, another element was required; this element needs to have a low measurement error for the samples. Ca has been reported as an alternative internal standard to Si due to its stability in glass[87] and was one of the least variable elements for the database samples. Therefore the log of each element was divided by Ca to give a normalised value; this is referred to as alr transformed data.

4.4 Homogeneity of glass panes

4.4.1 Intra-pane variation

This section of research examined the homogeneity of glass panes to prove that analysis of small automotive fragments from a crime scene, often less than 1 mm, will be representative of an entire pane. This is critical in order to form a database. The spatial variation of elements over a pane can give a reliable estimate of the chance that two samples originating from the same pane will not match due to the large variation. Trejos and Almirall reported that there is no spatial heterogeneity in glass[88].

The homogeneity of glass fragments can be visually observed in the time-resolved signal; the flat nature of the signal for each element indicates that it is not varying. Lee defines a homogeneous section as all elements having parallel time-resolved signals[108]. All analyses that were run throughout the entire research project only

used data where all elements had parallel time-resolved signals[*]. However, it is necessary to know if the fragment is representative of the rest of the pane.

Early in the research a left rear side window of a 1990 Toyota Corolla hatchback was tested[†]. The window was divided into 12 sections (four columns and three rows approximately 15 x 15 cm), covered in tape then smashed. Four random fragments from each section were prepared and analysed. The fragments were analysed with a 60 µm spot diameter[‡] and 90 % power. NIST 612 was used as the calibration standard[§]. Square nine had one replicate, square eight had two replicates and square 11 had three replicates; the remaining squares had four replicates.

The % RSDs were below 5 % for all elements except Li (9.32 %), Nd (5.18 %), Hf (5.88 %), and all three Pb isotopes (5.69, 5.56 and 11.31 % respectively).

A nested analysis of variance (ANOVA) test was carried out to examine the variation between squares of the pane compared to the variation between the four replicates (Table 4.1). 17 of the 19 elements had more variation between replicates. This ranged from 75.1 (Al) to 100 % (Hf and Li). Greater variation between the replicates may occur for two reasons; either the replicates are very variable or the spatial variation within the pane is very small. The variation due to heterogeneity in the sample was only greater for Mg and Sn (71.0 and 51.5 % respectively). These elements may have a large spatial variation over the pane.

[*] Signal that had a spike from an individual element were eliminated
[†] This glass is prior to the year range examined in the database
[‡] This portion of research was carried out before a 50 µm spot diameter was decided upon.
[§] FGS 2 had not arrived. Therefore K, Ti and Fe could not be examined.

Table 4.1 One way ANOVA – Variation between squares in replicates in the Toyota Corolla side window

Element	% variation between squares	% variation between replicates
^{7}Li	0.0	100.0
^{23}Na	20.8	79.2
^{25}Mg	71.0	29.0
^{27}Al	25.0	75.1
^{42}Ca	15.0	85.1
^{55}Mn	6.85	93.2
^{85}Rb	25.8	74.2
^{88}Sr	0.0	100.0
^{90}Zr	3.1	96.9
^{118}Sn	51.5	48.5
^{137}Ba	11.3	88.7
^{139}La	3.79	96.2
^{140}Ce	15.4	84.7
^{146}Nd	14.0	86.0.
^{178}Hf	0.0	100.0
^{206}Pb	12.8	87.1
^{207}Pb	21.3	78.7
^{208}Pb	13.4	86.6

Table 4.2 P values for ANOVA tests for Toyota Corolla side window. Values in bold do not show a significant difference between squares

Element	Column	Row
^{7}Li	**0.155**	**0.356**
23Na	**0.731**	0.049
^{25}Mg	**0.855**	**0.115**
^{27}Al	**0.688**	0.03
^{42}Ca	**0.383**	**0.114**
^{55}Mn	**0.247**	**0.922**
^{85}Rb	**0.816**	**0.184**
^{88}Sr	**0.948**	0.022
^{90}Zr	**0.925**	0.043
^{118}Sn	**0.406**	**0.211**
^{137}Ba	**0.794**	0.031
^{139}La	**0.822**	0.022
^{140}Ce	**0.364**	**0.352**
^{146}Nd	**0.757**	0.021
^{178}Hf	**0.205**	**0.787**
^{206}Pb	**0.648**	**0.678**
^{207}Pb	**0.684**	**0.625**
^{208}Pb	**0.3**	**0.501**

The within-pane spatial variation was examined to find if analysis of fragments from different areas of a pane would have an effect on matching the samples. ANOVA tests were used to mimic situations where two casework samples are compared that have originated from different locations on the same pane. If there is spatial variation within the pane the two samples may be mistaken as originating from two different panes.

A one way ANOVA was carried out on the data at the 5 % level for the side window across the rows and down the columns (Table 4.2). If the P value is > 0.05 there are no significant differences between any of the means. The values

shown in bold type are not significantly different. Down the columns no elements had a significant difference. However, across the rows Na, Al, Sr, Zr, Ba, La and Nd showed a significant difference. Therefore these elements may show heterogeneity or the significant difference may be influenced from a slightly higher or lower reading for one square.

An ANOVA test is limited as it can only indicate whether the squares are different; it is unable to identify which of the squares are significantly different or show if there is a spatial trend. Analysis of the response surface regression recognises the spatial relationship between rows and columns in the panes. There are five parameters, which allow more degrees of freedom than would be possible in an ANOVA. Surface and contour plots were created for each element to see the elemental distribution over the entire pane. It has been noted that contour and surface plots may not be the most sophisticated technique to use to observe changes over the pane, but they allow the change in concentration over the pane to be easily visualised.

A contour plot is used to show the two-dimensional view of the spatial relationship in the pane. The x and y axes show the column and row of the pane respectively. The third variable, concentration, is represented by shaded regions on the plot; the darker the colour, the higher the concentration. Figure 4.5 shows a contour plot for Sr for the side window. The middle of the window has less Sr than the top and the bottom. However, when the scale is considered this is only over 1.5 ppm. Therefore it is necessary to define the acceptable variation over a pane which occurs from both spatial variations in the pane and measurement error. This value will differ for each element (see section 4.4.2 for analysis).

A surface plot shows the same information as the contour plot, but it is displayed in three-dimensions with the concentration on the y axis. Figure 4.6 shows a surface plot for the distribution of Sr over the side window. The contour and surface plots for all elements for the Toyota Corolla side window can be found in the appendices on the electronic media (Appendices 6.7 and 6.8).

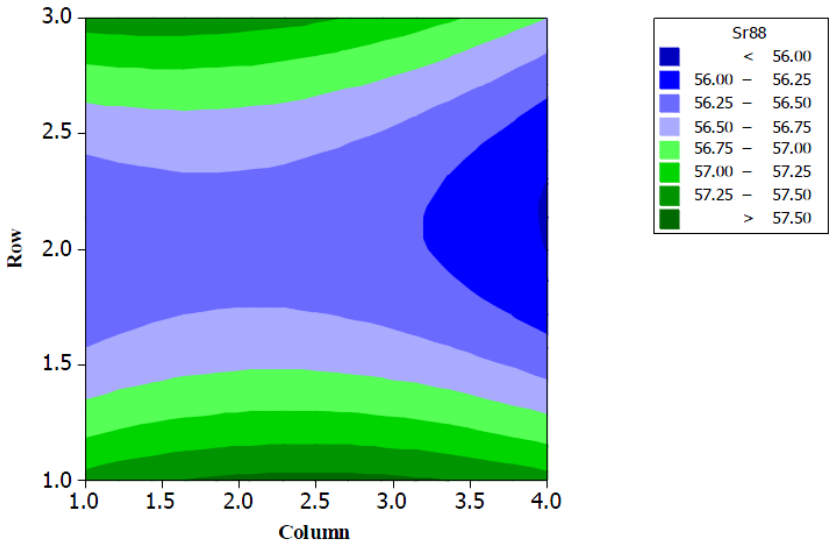

Figure 4.5 Contour plot of Sr for the Toyota Corolla side window. There is a small spatial trend over the window with the top and bottom having higher Sr than the middle of the pane.

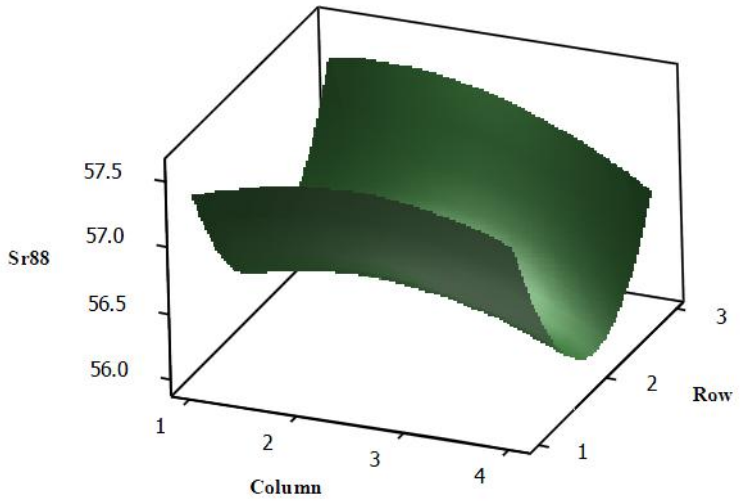

Figure 4.6 Surface plot for Sr in the Toyota Corolla window. The higher Sr in the top and bottom of the window is easily visible.

Further into the research both tempered and laminated panes were analysed. A 2001 Holden Commodore windscreen and a 2002 Mitsubishi Cedia side window (which left the factory on 1 March 2002) were obtained. The windscreen was divided into a grid; due to the taper of the windscreen the top row had 12 columns while the remaining four rows had 13 columns. This gave 76 pieces of

approximately 13 x 10 cm. The side window was divided into six columns and four rows. Each segment had one random piece of glass sampled from it.

The % RSD was over 5 % for Li, Al, Ti, Mn, Rb, Ba, La, Ce, Hf and all three Pb isotopes in the windscreen and Li, Nd, Hf and all three Pb isotopes in the side window.

A one way analysis of variance (ANOVA) was carried out on the data at the 5 % level for both the rows and columns of the windows (Table 4.3). A P value > 0.05 shows that there are no significant differences between any of the squares. The values shown in bold type are not significantly different. Across the windscreen, only Ce was significantly different. 10 of the 21 elements had a significant difference going down the pane. For the side window, all elements were homogeneous going down the pane of glass. All elements, except Na, Ca, Ti and Ba, are homogeneous across the columns of the side window.

As mentioned for the analysis of the Toyota pane, an ANOVA test is limited as it can only indicate whether the squares are different; it is unable to identify which of the squares are significantly different or show if there is a spatial trend. Therefore contour and surface plots were created. Figure 4.7 shows a contour plot for Sr for the side window. All contour and surface plots can be found in the appendices (Appendices 6.9, 6.10, 6.11 and 6.12).

Table 4.3 P values for ANOVA tests for Holden and Mitsubishi windows. Values in bold do not show a significant difference between squares

Element	Holden Row	Holden Column	Mitsubishi Row	Mitsubishi Column
^{7}Li	**0.369**	**0.839**	**0.820**	**0.561**
^{23}Na	0.000	**0.996**	**0.870**	0.014
^{25}Mg	0.000	**0.902**	**0.583**	**0.560**
^{39}K	0.059	**0.309**	**0.641**	0.026
^{27}Al	0.041	**0.091**	**0.491**	**0.139**
^{42}Ca	0.000	**0.086**	**0.594**	0.045
^{49}Ti	0.044	**0.585**	**0.808**	0.044
^{55}Mn	**0.064**	**0.740**	**0.168**	**0.325**
^{57}Fe	0.000	**0.996**	**0.897**	**0.962**
^{85}Rb	0.031	**0.445**	**0.986**	**0.091**
^{88}Sr	0.001	**0.600**	**0.583**	**0.091**
^{90}Zr	**0.958**	**0.125**	**0.775**	**0.066**
^{118}Sn	0.000	**0.459**	**0.671**	**0.731**
^{137}Ba	**0.977**	**0.363**	**0.966**	0.010
^{139}La	**0.100**	**0.857**	**0.576**	**0.399**
^{140}Ce	**0.892**	0.001	**1.000**	**0.524**
^{146}Nd	0.033	**0.549**	**0.666**	**0.282**
^{178}Hf	**0.824**	**0.325**	**0.386**	**0.705**
^{206}Pb	**0.390**	**0.490**	**0.707**	**0.772**
^{207}Pb	**0.393**	**0.500**	**0.496**	**0.532**
^{208}Pb	**0.056**	**0.567**	**0.856**	**0.873**

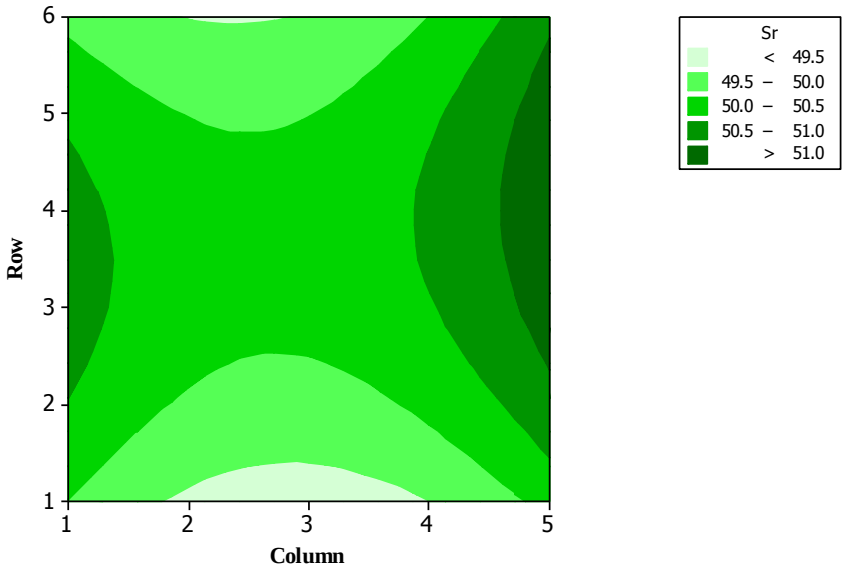

Figure 4.7 Contour plot of Sr for the Mitsubishi Cedia side window.

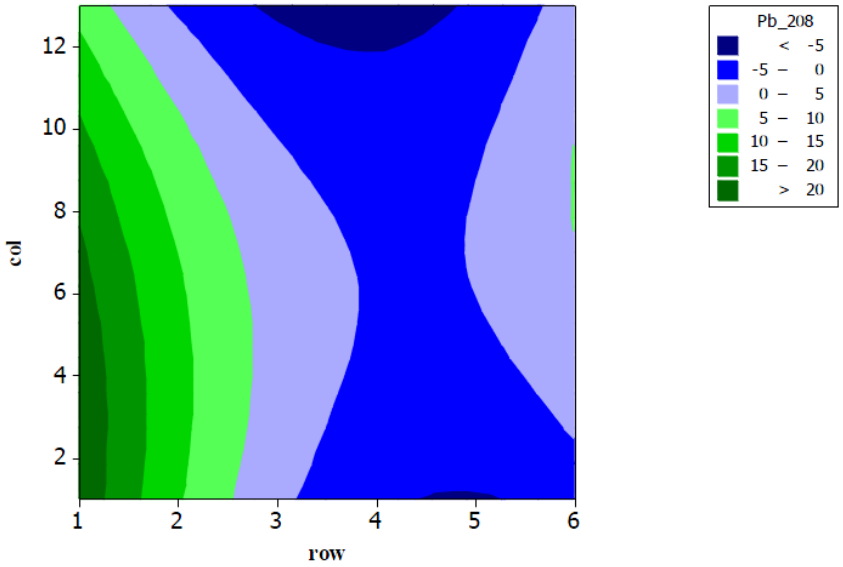

Figure 4.8 Contour plot for ^{208}Pb in the Holden Commodore windscreen. There is a large systematic change in concentration across the windscreen.

The Holden Commodore windscreen had noticeable Pb outliers. Pieces 44 and 70 had large outliers for ^{206}Pb (2.08 and 143.81 ppm respectively). Piece 41 had a ^{207}Pb concentration lower than the detection limit and piece 70 had a very high reading (119.16 ppm). ^{208}Pb pieces 21, 70 and 74 had high concentrations (2.23, 98.51 and 132.73 ppm respectively). In addition, Pb also had a larger systematic change across the windscreen than the other elements. Figure 4.8 shows the

systematic change of ^{208}Pb across the windscreen. The bottom left hand corner has the highest concentration. The same effect was seen in ^{207}Pb and to a lesser extent in ^{206}Pb. There is no obviously apparent reason for this spatial variation of Pb isotopes.

The ANOVA test showed that Ce had a significant difference in the windscreen. However, the contour plot did not show a large variation across the pane. The significant difference was influenced by a slightly higher value in one corner.

4.4.2 Inter-pane variation

If the variation within a pane is larger than that found between all panes then glass samples will not be efficiently distinguished from other samples in the database.

The following equation can be used to work out the variation between panes:

$$\sigma^2_{database} = \sigma^2_b + (\sigma^2_w/4) \quad (4.5)$$

where: b = variation between panes
w = variation within a pane

σ^2_w is divided by 4 to take into account that each sample in the database is an average of four analyses.

$\sigma^2_{database}$ is known from the analysis of the entire database and σ^2_w can be estimated from the four replicates of each sample in the database. Therefore σ^2_b can be calculated using equation 4.5.

Instead of using equation 4.5, a nested ANOVA can be used to work out $\sigma^2_w$and σ^2_b to find the influence of each value. The samples were tested for normal distribution and were found to behave normally. Therefore assuming normality, if there is 25 % variation in replicates for a specific element, only 32 % of samples would be distinguishable using only that element. If there is 2 % variation in replicates for a specific element, 78 % of samples could be distinguished and if there was 0.5 % variation in replicates 89 % of samples could be distinguished.

The raw data from the database was used to carry out a nested ANOVA for each element individually to examine how much variation occurs due to the samples and due to the replicates. The results are shown in Table 4.4. Most elements have less than 5 % variation in the replicates which arises from measurement error. Na, Mg, Ca and the three Pb isotopes had the highest variation in replicates (24.36, 10.13, 8.98, 87.91, 94.33 and 89.03 % respectively). Therefore these elements may affect the ability to distinguish samples.

Table 4.4 Variation in sample and replicates

Element	Variation in Sample, %	Variation in replicates, %
Li	96.24	3.76
Na	75.64	24.36
Mg	89.87	10.13
Al	99.94	0.06
K	98.66	1.34
Ca	91.02	8.98
Ti	99.94	0.06
Mn	99.61	0.39
Fe	95.24	4.76
Rb	99.89	0.11
Sr	99.42	0.58
Zr	99.73	0.27
Sn	97.52	2.48
Ba	99.75	0.25
La	99.95	0.05
Ce	99.81	0.19
Nd	99.91	0.09
Hf	97.85	2.15
^{206}Pb	12.09	87.91
^{207}Pb	5.67	94.33
^{208}Pb	10.95	89.03

A PCA analysis (see section 4.7 for explanation on PCA) of all elements (only one from each correlated set was required, see section 4.2.2) was carried out using the clr transformed data. The scores for the first 4 principal components were obtained and a nested ANOVA was carried out with each score against samples and replicates. The variation in replicates is slightly elevated for scores 2 – 4. This is most likely caused by the large variation in Na and Pb replicates. Therefore

they were removed and the test was repeated which showed a decrease in variation for replicates (Table 4.5). The PCA analysis was repeated without Mg and Ca; however, this did not make a significant difference to the variation in samples. Both elements were retained in the elemental suite. Mg is an important element to retain because 90.5 % of its variation arises between samples which will help with discrimination (see section 4.6 for further explanation).

Table 4.5 Variation in sample and replicates excluding Na and Pb

Score	Variation in Sample, %	Variation in replicates, %
1	99.91	0.09
2	99.80	0.20
3	99.67	0.33
4	99.11	0.89

It should be noted that the trends seen in the intra-pane study could have occurred only in the panes tested and not be a representative study of automotive float glass. To establish if this is so, the pooled standard deviation of the database was compared to the standard deviation of the three panes analysed for the intra-homogeneity study (see section 4.4.1) to see if the three panes were reflective of the entire database. The results are shown in Table 4.6.

Table 4.6 Standard deviation of the database and the three windows analysed during the homogeneity test

Element	Database	Toyota*	Holden	Mitsubishi
^{7}Li	0.90	1.24	1.11	0.96
^{23}Na	2277.72	3971.42	3672.26	2170.71
^{25}Mg	10589.45	851.65	508.89	320.44
^{27}Al	96.82	168.15	8.73	55.85
^{39}K	549.33	-	16.45	114.97
^{42}Ca	1137.37	805.92	1489.52	1059.07
^{49}Ti	10.76	-	6.63	16.58
^{55}Mn	2.83	1.90	2.57	2.29
^{57}Fe	394.53	-	98.03	108.67
^{85}Rb	0.34	0.34	0.08	0.33
^{88}Sr	1.29	0.84	1.09	0.95
^{90}Zr	2.17	0.67	0.57	1.16
^{118}Sn	1.22	0.55	1.15	0.87
^{137}Ba	3.14	2.84	0.46	3.38
^{139}La	0.80	0.14	0.07	0.3
^{140}Ce	92.66	1.29	1.85	16.02
^{146}Nd	0.52	0.26	0.17	0.43
^{178}Hf	0.16	0.08	0.09	0.14
^{206}Pb	14.44	0.30	16.43	0.33
^{207}Pb	18.88	0.27	13.7	0.42
^{208}Pb	13.48	0.59	18.75	0.23

Most elements have a similar standard deviation in the database and in the three panes. Therefore these standard deviations are likely to be representative of other panes. Moreover, these values can be used to work out the ± error for matching two samples of glass to ensure samples which originate from the same pane are found to match. Each element has its own deviation.

Mg has a larger standard deviation in the database than in the individual panes used in the homogeneity test. As Mg does not have a large spatial variation, this large standard deviation may be influenced by MgO addition as a stabiliser during glass manufacture. K also has a larger standard deviation in the database. This may be influenced by spatial heterogeneity or due to the RSD (see section 3.7.2)

* The Toyota pan was analysed using NIST 612 as the standard. Therefore K, Ti and Fe could not be analysed.

The Fe standard deviation is also larger in the database. Fe does not appear to have spatial heterogeneity, which would contribute to a larger standard deviation in the database. Iron oxides are closely monitored during the manufacturing process. However, the tolerance level in an industrial sense differs radically from tolerance in an analytical sense. To produce transparent glass iron oxides must be less than 0.1 wt %. However, this tolerance level will still give rise to variation that can be measured by LA-ICP-MS. Therefore the reason for the larger standard deviation in the database for Fe is unknown.

Ce had a significant difference going across the Holden Commodore windscreen. However the contour plot showed there was minimal spatial variation. Ce is also found to have a much larger standard deviation in the database compared to the entire panes that were analysed. This may be due to addition of Ce_2O_3 as a decolourising agent during some glass manufacture which would increase the concentration range in the database.

Pb isotopes have a much larger standard deviation in the database than in the Toyota and Mitsubishi side windows, but are similar to that found in the Holden windscreen. Therefore the trend seen in the windscreen may also occur in other panes. Due to this, Pb is not a good element for analysis as its large variation in a single pane may prevent accurate discrimination when two samples are compared.

4.4.3 Conclusion on inter- and intra- homogeneity

This section of research has shown that most elements analysed are homogenous in laminated and tempered glass. Therefore small fragments can be considered as representative of an entire pane. The standard deviation found in the homogeneity tests and in the database are good estimates of the variation found within a pane. This can be used to work out the ± error range which will allow samples originating from a single pane to have a match, and those that originate from two different panes to be distinguished.

Pb isotopes have been shown to have a spatial variation across a pane of glass. This was seen in both the inter-homogeneity study of the Holden windscreen and

the intra-homogeneity study of the entire database. Therefore Pb should be used for automotive float glass analysis only with caution or it should be removed from analyses due to its variable nature.

Mg, Fe and Ce had large standard deviations in the database. However, this did not occur from spatial heterogeneity in a pane. Therefore their variation is beneficial as there is a large spread within the database that will increase the discriminating ability. The large standard deviation arising in K data may affect the quality of the data as it appears this is arising from spatial heterogeneity and a large relative standard deviation (see section 4.5 for recommendation on K).

4.5 Final decision on elements

Na has a large RSD (8.94 %) in measurements which caused a high percentage of variation to come from replicates. Therefore it was removed from further analyses.

As previously mentioned, only one element from a correlated pair is required for analysis. K and Rb are correlated; K was removed as it has a high RSD (8.02 %) compared to Rb and showed spatial variation in the homogeneity test. Nd and Hf were also removed due to correlations with La and Zr respectively.

Pb isotopes had a large standard deviation in the database and were also not homogeneous in the windscreen which was tested. In addition the inter-pane variation test showed that it had less variation in the database compared to variation in replicates. Therefore it was removed from analyses.

The final suite of elements used for analysis of glass samples in the database was: ^{7}Li, ^{25}Mg, ^{27}Al, ^{29}Si*, ^{42}Ca†, ^{49}Ti, ^{55}Mn, ^{57}Fe, ^{85}Rb, ^{88}Sr, ^{90}Zr, ^{118}Sn, ^{137}Ba, ^{139}La and ^{140}Ce.

* ^{29}Si was used as the internal standard so was not used for analysis.
† ^{42}Ca was used for alr transformation for LDA analysis.

4.6 Elemental variation within the database

The raw data was used to carry out an ANOVA test for each element to assess where most of the variation in the database occurred. Initially make, model, individual pane (sample) and replicate were used as the variables. However, when the transformed data was used to carry out PCA and the samples were grouped into makes many of the makes did not group together. This led to an investigation of each car's country of origin as it was likely samples would be influenced by the raw materials used in manufacture. This was carried out by searching the registration plate on www.carjam.co.nz[*]. This revealed that not all cars of the same make are produced in the same country. For example, most Toyotas are manufactured in Japan; however, the Toyota Camry is manufactured in Australia. Moreover, not all cars of the same model are produced in the same country. For example, sample 64 is a 2003 Holden Barina from Spain and sample 148 is a 2006 Holden Barina from South Korea. Table 4.7 shows a selection of the vehicles which do not fit the usual expectations of country of origin.

A second ANOVA test, which included country of origin, was carried out. The variables were: country, make, model, individual pane (sample) and replicate. Samples with unknown country of origin were removed from the analysis. This revealed that country of origin is a better means of differentiating the samples than make of car. This is because of the influence of trace elements in raw materials differing in certain areas of the world. However, it was noted that the country of origin for a vehicle does not always match the country of origin of the glass (see section 4.7.3).

[*] CarJam provides an assortment of information on a vehicle by entering its registration number.

Table 4.7 Examples of makes and models of cars which do not fit the expected countries of origin

Make	Model	Country of Origin
Toyota	Camry	Australia
Holden	Rodeo	Thailand
Nissan	Pulsar	England
Ford	Courier	Thailand
Ford	Transit	England
Ford	Fiesta	Belgium
Ford	Mondeo	Belgium
Ford	Territory	Thailand
Ford	Focus	Germany
Mazda	Bounty	Thailand
Holden	Barina	South Korea
Holden	Barina	Spain

The results of the ANOVA test are shown in Table 4.8. Al and Ba have the most variation between countries (67.19 and 52.18 % respectively). All elements show low or no variation for make of car. There is more variation between models than makes; however, all elements have less than 25 % variation due to the model of a car, except for Ca (32.87 %).

La and Mg have the highest variation between samples (91.84 and 90.50 % respectively). One possible explanation for the large variation of Mg could be because it is added as a stabiliser during glass manufacture. Sr and Ce have the next highest variation between samples (71.99 and 73.17 % respectively). It is thought the large variation of Ce is due to addition of Ce_2O_3 as a decolourising agent during glass manufacture. These results are in contrast to reports of Sr being the most discriminating element[57].

Most elements had more than 45 % variation arising between samples, which will allow samples to be discriminated. Almost all elements had less than 0.5 % variation between replicates; the elements that have higher variation have been shown to have no influence on the data (see section 4.4.2).

Table 4.8 Source of variation between database samples, with respect to country, make, model, sample and replicate

Element	Country, %	Make, %	Model, %	Sample, %	Replicate, %
Li	10.52	2.33	17.08	66.53	3.64
Mg	1.42	0	0	90.50	8.08
Al	67.19	0	22.31	10.45	0.05
Ca	17.68	0	32.87	41.21	8.23
Ti	4.82	0	19.17	75.95	0.05
Mn	31.65	0	25.04	42.94	0.37
Fe	2.75	4.63	0	88.11	4.51
Rb	37.99	16.77	15.89	29.25	0.10
Sr	19.52	0	8.14	71.99	0.55
Zr	13.98	26.06	6.16	53.54	0.26
Sn	28.13	0.50	17.04	51.98	2.35
Ba	52.18	6.13	19.07	22.21	0.23
La	0	7.64	0.47	91.84	0.05
Ce	4.56	0	22.09	73.17	0.18

4.7 Unsupervised learning (PCA)

PCA was used to examine the distribution of samples. PCA is a type of unsupervised learning; the user is not required to input sample grouping, instead PCA is used to expose natural groupings in the data. PCA reduces the dimensionality of the dataset. Therefore all elements should be considered in the model. However, this often does not give the best discrimination and analyte selection is commonly used to find elements which aid in discrimination between the groups.

Each component of PCA explains a percentage of variation. The number of components reported are the number which are required to explain all variation within the dataset. Principal components (PC) are orthogonal to each other; there is no correlation between information in different principal components. In addition they are extracted in decreasing order of importance. That is, the first

principal component has the most information. Score plots are obtained when two PC are plotted against each other to show the arrangement of the data in a small number of dimensions.

Each element is given a value; those with a large component have more influence than other elements. This is visually displayed in a loading plot; the longer the line, the more influence the element has.

Spain, South Africa, Belgium, England, France, USA and Italy had less than 10 samples analysed in the database. Therefore, they were unable to be used for categorisation of country, but were left in the PCA analysis for completeness. The clr transformed data was used for PCA analysis.

4.7.1 Consideration of all variables

A 14 element model (Li, Mg, Ca, Al, Ti, Mn, Fe, Rb, Sr, Zr, Sn, Ba, La and Ce) was used. 13 principal components were required to explain all of the variation in the database (Table 4.9 and Figure 4.9).

The score plot (Figure 4.10) shows the first two principal components. The numbers in parentheses on each axis are the percentage of the variance captured by that PC. Over half of the variation is described by the first two PC (63.6 %); therefore it is expected that this score plot is a fair representation of the dataset.

The PC values reveal that Al, Rb and Ba made a large negative contribution to the first PC; Ca, Li, Mg, Fe, Sr and Sn made a large positive contribution to the first PC. Ti and La made a large positive contribution to the second PC and Al and Rb made a large negative contribution to the second PC. This is displayed in the loading plot (Figure 4.11).

Table 4.9 Contribution of each PC and the overall percentage of samples that can be discriminated in the full database (14 element model)

Number of PC	Individual contribution, %	Total, %
1	48.9	48.9
2	14.7	63.6
3	12.5	76.1
4	7.9	84
5	3.6	87.5
6	3.3	90.8
7	2.8	93.7
8	1.7	95.3
9	1.5	96.9
10	1.3	98.1
11	0.9	99
12	0.6	99.6
13	0.4	100

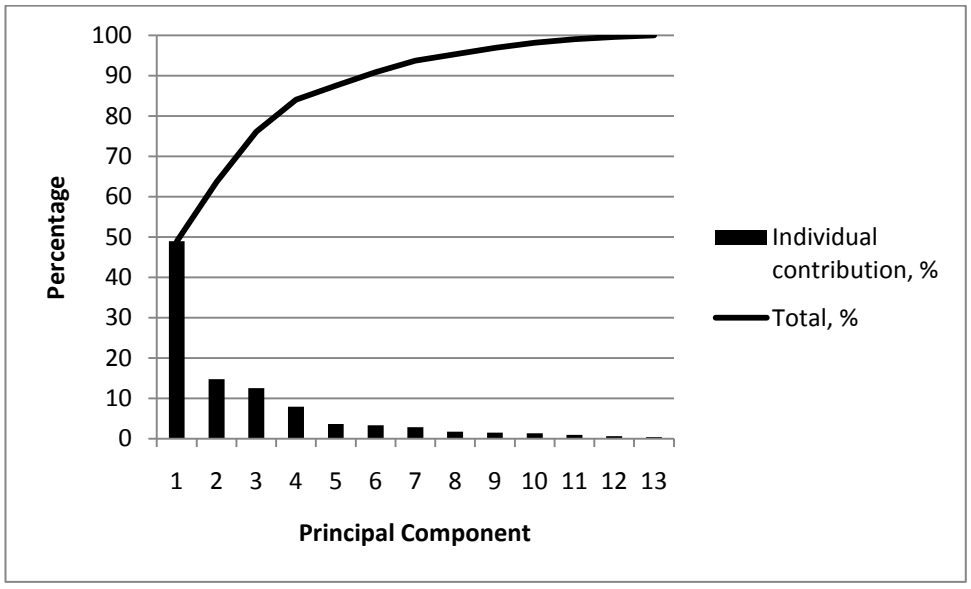

Figure 4.9 Contribution of each principal component and the accumulative discrimination. PC 1 is able to account for almost half of the variance in all the samples (14 element model).

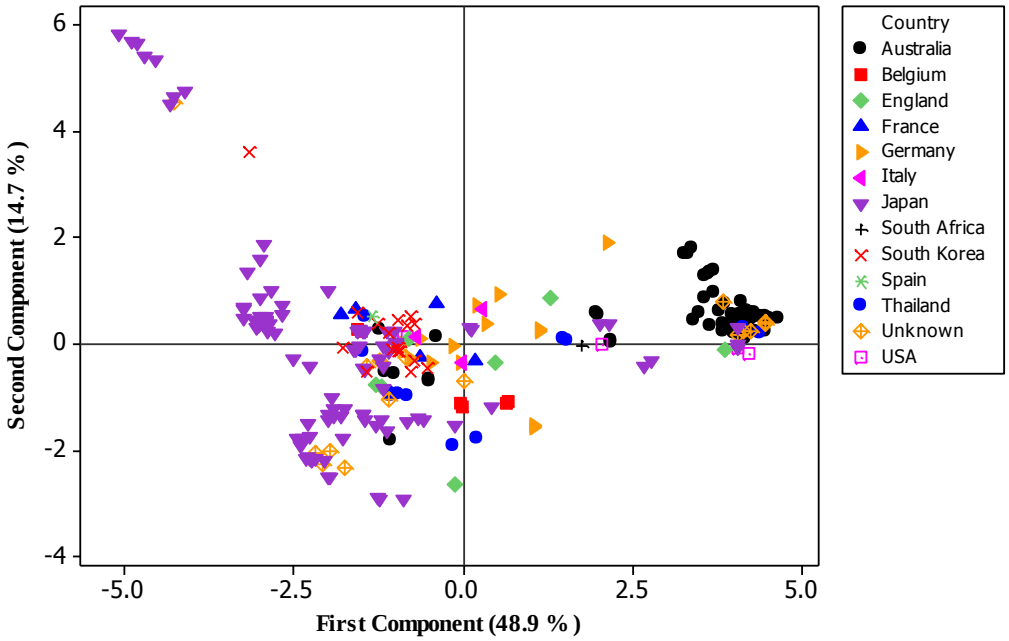

Figure 4.10 Score plot with samples categorised into country of origin (14 element model). 63.6 % of data is explained in the first two principal components. Samples from Australia sit predominantly on the right hand side and samples from Japan are predominantly on the left hand side. South Korean samples are clustered in the middle of the score plot.

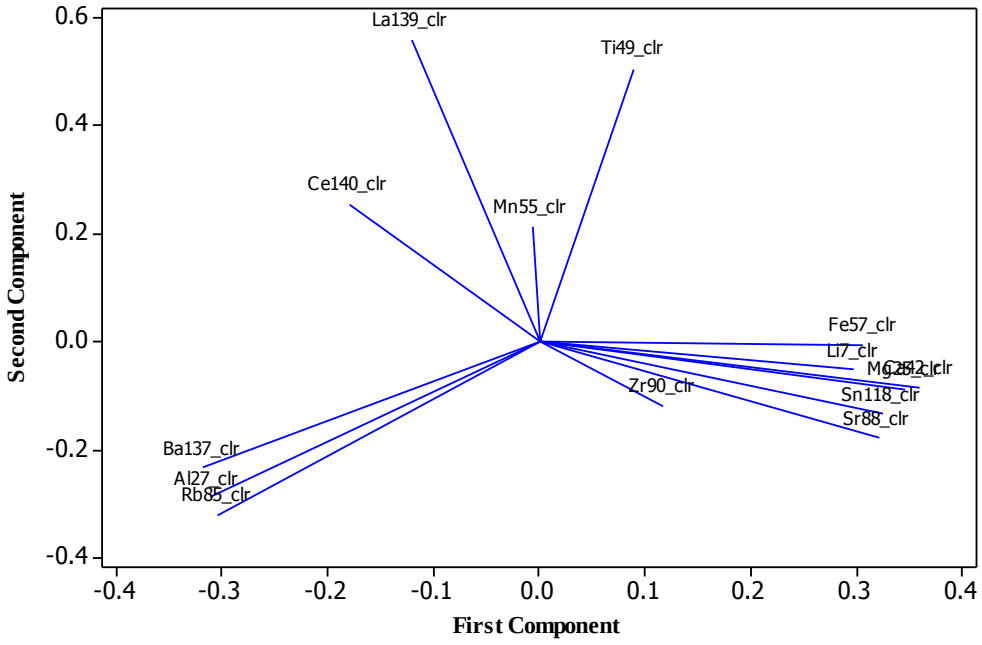

Figure 4.11 Loading plot (14 element model) Al, Rb and Ba make a large negative contribution to the first component. Ti and La make a large positive contribution to the second component.

Most samples from each country are grouped with other samples from the same country on the score plot. Samples from Japan are predominately on the left hand side, samples from Australia are clustered on the right hand side and samples from South Korea are situated in the middle of the score plot. The samples that do not belong in the correct country are discussed in section 4.7.3.

Figure 4.12 is a box plot of score 1, with samples categorised by country; samples with less than 10 samples analysed for a country were grouped together and labelled as 'other' as the limited number does not allow a good representation of their placement on the score plot. Australian glass has good discrimination using only PC 1. The Thailand samples that overlap with Australia are explained by the exportation of glass from Australia to Thailand; moreover, the outliers for Australia can be explained by importation of glass from Thailand* (see section 4.7.3 for further discussion). At least 50 % of glass from Japan can be distinguished from other countries using only PC 1. Japan and Thailand have a large spread of data compared to the other countries.

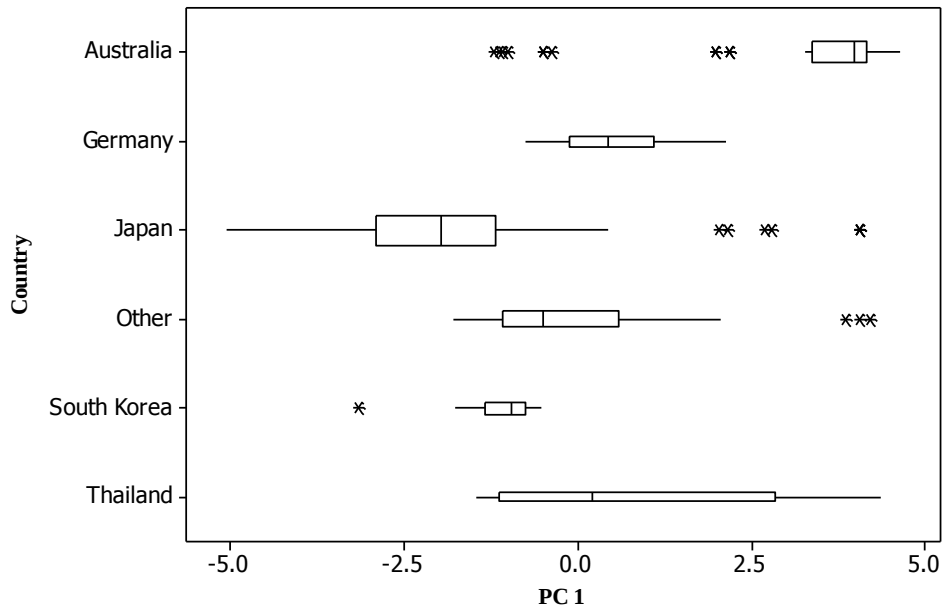

Figure 4.12 Box plot of score 1 separated into countries of origin. The box widths are proportional to the number of samples. Samples labelled as 'other' are a grouping of those which have less than 10 samples analysed for a country.

* Australia and Thailand have a free trade agreement

4.7.2 Semi-automated selection of elements

To increase the discrimination of PCA, the ANOVA (see section 4.6) was used to select elements which have the most variation between countries. Al, Mn, Rb and Ba had more than 30 % variation and were chosen for analysis. This had a large improvement in the results; the first two PC can account for 90.5 % of variation in the dataset (Figure 4.13). 100 % of the variation was defined in four PC (Table 4.10 and Figure 4.14). However the spread of South Korean samples has increased.

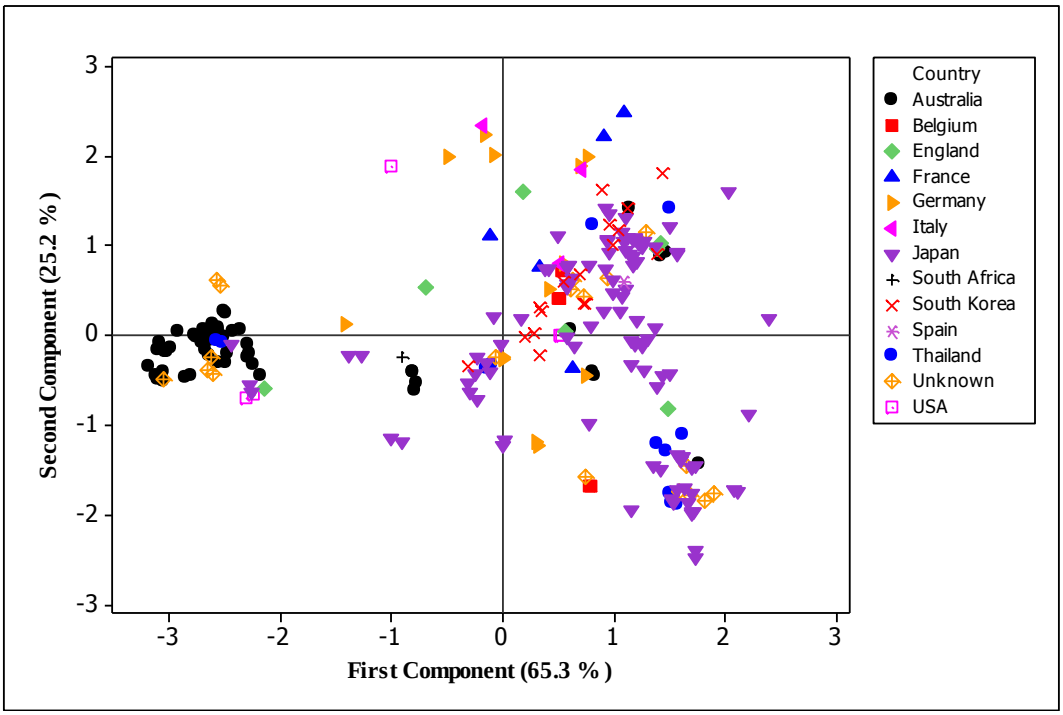

Figure 4.13 Score plot of database (4 element model). 90.5 % of data is explained in the first two principal components.

Table 4.10 Individual and total contribution of principal components (4 element model)

Number of PC	Individual contribution, %	Total, %
1	65.3	65.3
2	25.2	90.5
3	6.8	97.3
4	2.7	100

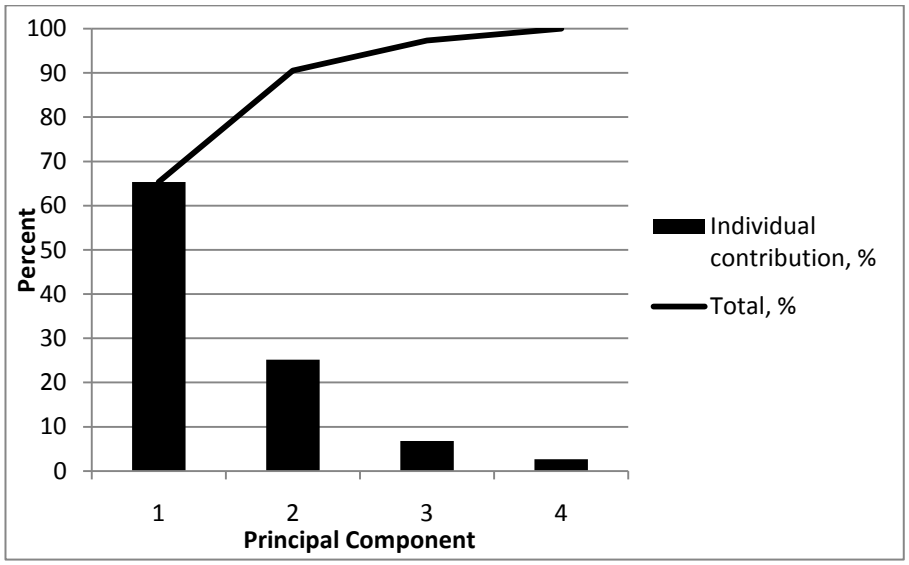

Figure 4.14 Contribution of each principal component and the accumulative discrimination (4 element model). The first two PCs can account for 90.5 % of the variance in all the samples.

4.7.3 Discussion of categorisation of samples

Categorisation of samples into country of origin may be of benefit to New Zealand as it does not manufacture any of its own cars or glass. Therefore there are a wide range of imported vehicles. However, the following discussion shows why this should be approached with caution.

Most Australian samples are located on the right hand side of the score plot when using the 14 element model and have a very small spread of data compared to other countries. This is due to the source of materials for the manufacture of the glass; the Viridian glass plant in Geelong, Australia is Australia's main source of automotive glass. The Viridian site at Dandenong manufactures the float glass before sending it to Geelong for processing to produce automotive windows. Viridian provides glass for Holden, Ford, Chrysler, Nissan, Mitsubishi and Toyota. Therefore the elemental composition of glass will be very similar for the large range of vehicles that come from Australia.

There are a few samples that are not of Australian origin which also sit in the Australian area (Table 4.11). There are two possible reasons for this; the first

reason is that the panes are not the original panes of the windscreen. It is highly likely that New Zealand imports their replacement glass from Australia. The second reason may be due to Australia exporting glass to other countries for use in vehicles. Throughout the 1980s and 1990s, glass was exported from Viridian to Mercedes Benz in Germany, Toyota in Japan and Seat in Spain. They currently supply glass for the Toyota Camry/Aurion and Ford Territory ranges. Australia and Thailand have a free trade agreement; therefore glass for the Ford Territory would have been imported to Thailand from Australia.

Table 4.11 Samples placed in the Australian region which are not of Australian origin

Sample	Make	Model	Year	Type of Glass	Country of Origin
35	Lotus	Elise	2004	Windscreen	England
42	Mazda	626	2003	Windscreen	Japan
139	Toyota	Hilux	2004	Windscreen	Japan
161	Ford	Territory	2005	Windscreen	Thailand
171	Ford	Explorer	2004	Windscreen	USA

There are seven samples of Australian origin which do not sit in the region with the other Australian samples (Table 4.12). Their placement may be explained by imported glass being used. Viridian no longer supplies glass for the AU Falcon and VE Commodore[*] due to tariff reductions. The glass is now imported from Thailand due to the free trade agreement with Australia.

Table 4.12 Samples from Australia which do not sit in the Australian region

Sample	Make	Model	Year	Type of Glass
2	Holden	Calais	2003	Windscreen
97	Ford	Falcon	2003	Left Front
98	Ford	Falcon	2005	Windscreen
67	Holden	Commodore	2005	Windscreen

The 14 element model clearly shows the separation of Japanese samples on the left hand side of the score plot. The bulk of the samples sit together. However, all

[*] Holden Calais is part of the Commodore range

three Toyota Hilux samples sit away from the bulk to the right of this group. This is close to the Australian samples. Nine Japanese samples sit to the left and above the main bulk of Japanese samples; this group includes Toyota Echo, Toyota Rav 4, Honda CRV and Mitsubishi Colt samples. The reason for this split may be due to the plant the glass has come from. However, there is no readily available reason for the location of these samples.

The results show that categorisation of samples into country of origin should be approached with caution. However, it may be a useful tool to help police narrow their search. For example, analysis of glass collected from the scene of a hit-and-run may allow police to ask the public if they saw suspicious activity from a limited range of vehicles.

4.8 Supervised learning

Section 4.6 addressed the possibility of the police using classification of glass to help narrow their search. This section explores the strength of categorising samples into country of origin.

Supervised learning methods require the user to input the group classifications so that the technique can generate a model from them to correctly assign samples into a group. This model can then be used to classify new samples into a group. This is also known as data mining. Linear discriminant analysis (LDA) was performed with Minitab using the alr transformed data. Waikato environment for knowledge analysis (Weka) software was used for multiclass classifier-classification by regression - Gaussian processes, J4.8, SMO and Naive Bayes algorithms on the raw data. Weka uses the term ‘instances’ to describe individual samples and ‘attributes’ to describe features of the samples. Therefore the elements are termed attributes.

The percentage of correct assignments is evaluated to assess the strength of the model. To increase a model’s strength a 10-fold cross validation is used to test the data. This divides the data into ten parts and uses nine parts for training, and the last tenth for testing. Weka performs this ten times, holding back a different tenth

each time for testing, giving an averaged error rate. Therefore it allows the maximum amount of data to be used for training and can still generate a realistic error estimate.

Countries that were not correctly placed into their country of origin (see section 4.7.3) were included in the analyses. Therefore the ability of the methods was slightly hindered.

Countries with less than 10 samples (Spain, South Africa, Belgium, England, France, USA and Italy) were excluded from analyses. Also, samples which could not have their country of origin traced were excluded; these samples were reserved for the test set (see section 4.8.6).

4.8.1 Linear discriminant analysis (LDA)

LDA was initially performed for individual elements to examine which elements are of most use. This is summarised in Table 4.13. Al is the best element for assigning samples to a country (75.3 % correctly assigned). It has better success than all elements combined and all elements plus RI. However it does not have a high success for South Korea or Thailand.

Rb can categorise more samples correctly than using all elements combined (73.2 % compared to 72.2 %), but is unable to place any samples from South Korea or Thailand.
Most elements have a high categorising power for samples originating from Australia. It is likely that so many elements are able to correctly categorise samples from Australia as Australian samples are likely to have very different trace element composition in their raw materials, compared to samples from all the other countries which are located in the Northern Hemisphere.

The ability of any single element to assign Germany, South Korea and Thailand samples is very limited, with most elements having less than 50 % success. Li is the best element for categorising German samples (61.5 %), while Sn (64.7 %) is the best element for categorising South Korean samples and Fe (83.3 %) is the

best element for categorising samples from Thailand. Of interest is the strong ability of RI alone to assign 83.3 % of samples from Thailand and 47.1 % of samples from South Korea.

Table 4.13 LDA of individual elements

Element	Proportion correctly assigned	Australia	Germany	Japan	South Korea	Thailand
RI	21.7	16.4	0	15.8	47.1	83.3
^{49}Ti	27.3	76.4	0	3.0	52.9	0
^{55}Mn	33.3	87.3	23.1	5.9	47.1	8.3
^{57}Fe	33.3	58.2	0	15.8	47.1	83.3
^{88}Sr	35.9	16.4	7.7	58.4	0	16.7
^{139}La	36.4	87.3	15.4	14.9	41.2	0
^{25}Mg	38.4	61.8	7.7	37.6	0	25
^{7}Li	39.9	83.6	61.5	18.8	23.5	16.7
^{140}Ce	47.0	16.4	53.8	70.3	11.8	33.3
^{118}Sn	51.5	25.5	7.7	74.3	64.7	8.3
^{90}Zr	57.1	83.6	46.2	58.4	11.8	0
^{137}Ba	65.7	80.0	7.7	77.2	5.9	50.0
All	71.2	83.6	38.5	75.2	47.1	50.0
^{85}Rb	73.2	87.3	46.2	90.1	0	0
All + RI	74.2	81.8	46.2	79.2	58.8	50.0
^{27}Al	75.3	87.3	53.8	86.1	29.4	16.7

4.8.2 Multiclass classifier

A Multiclass classifier using classification by regression with Gaussian processes was used as a model to separate samples into their correct country of origin. This was the best algorithm used, correctly classifying 86.87 % (172/198) of samples. Using this method only 26 instances were incorrectly assigned; the classification of some of these samples has been previously discussed (see section 4.7.3).

The confusion matrix (Figure 4.15) shows the classification of each sample. 49 Australian samples were correctly classified; five Australian samples were classified as Japanese and one was classified as originating from Thailand. Going down column ‘a’, two Japanese, one German and two Thailand samples were classified as Australian.

```
  a  b  c  d  e   <-- classified as
 49  5  0  1  0 |  a = Australia
  2 94  1  2  2 |  b = Japan
  1  1 10  1  0 |  c = Germany
  2  2  0  8  0 |  d = Thailand
  0  4  1  1 11 |  e = South Korea
```

Figure 4.15 Confusion matrix for multiclass classifier.

4.8.3 J4.8 algorithm

J4.8 was used as a model; this builds a decision tree. This algorithm was able to correctly classify 81.31 % (161/198) of samples. Using this method, only 37 samples (18.89 %) were incorrectly assigned. The confusion matrix (Figure 4.16) shows the classification of each sample.

```
  a  b  c  d  e   <-- classified as
 48  1  1  1  4 |  a = Australia
  1 10  1  0  1 |  b = Germany
  5  0 90  2  4 |  c = Japan
  1  0  6 10  0 |  d = South Korea
  6  1  2  0  3 |  e = Thailand
```

Figure 4.16 Confusion matrix for J4.8 algorithm.

The decision tree has 14 leaves. A colon shows the class label. Therefore using the J4.8 algorithm, if Rb is less than or equal to 10.585, Mn is less than or equal to 43.11 and Fe is less than or equal to 3715.9675, Japan and Australia can be categorised on the amount of Mn in the sample; if there is >18.235 it is classed as Australian and if there is less then it is of Japanese origin. The numbers in brackets show the instances which have been incorrectly assigned. For example, (52.0/3.0) on the fifth line shows that out of 52 instances, three were incorrectly assigned.

```
Rb85 <= 10.585
| Mn55 <= 43.11
| | Fe57 <= 3715.9675
| | | Mn55 <= 18.235: Japan (7.0)
| | | Mn55 > 18.235: Australia (52.0/3.0)
| | Fe57 > 3715.9675
| | | Na23 <= 104404.595: Germany (6.0/1.0)
| | | Na23 > 104404.595: Thailand (3.0/1.0)
| Mn55 > 43.11
| | Al27 <= 4769.995: Germany (8.0)
| | Al27 > 4769.995: South Korea (12.0)
Rb85 > 10.585
| Ce140 <= 23.98
| | Rb85 <= 25.005
| | | Ce140 <= 5.52
| | | | Ca42_1 <= 61470.5175: Australia (3.0)
| | | | Ca42_1 > 61470.5175: Japan (3.0/1.0)
| | | Ce140 > 5.52
| | | | RI 1 <= 1.52: Japan (13.0/2.0)
| | | | RI 1 > 1.52
| | | | | Li7 <= 7.4625: Japan (2.0)
| | | | | Li7 > 7.4625: South Korea (3.0)
| | Rb85 > 25.005
| | | Li7 <= 8.8225: Thailand (6.0)
| | | Li7 > 8.8225: Australia (2.0/1.0)
| Ce140 > 23.98: Japan (78.0/1.0)

Number of Leaves:  14
Size of the tree:  27
```

Figure 4.17 Decision tree for J4.8 algorithm.

4.8.4 Sequential minimal optimisation (SMO)

Sequential Minimal Optimisation (SMO) is an algorithm for support vector classification. 76.26 % (151/198) samples were correctly placed into country of origin, while 23.74 % (47/198) were incorrectly categorised. This algorithm increases classification of Japanese samples by 4. However, it is unable to correctly place any of the 12 Thailand samples.

```
  a  b  c  d  e   <-- classified as
 48  0  7  0  0 |  a = Australia
  5  1  7  0  0 |  b = Germany
  7  0 94  0  0 |  c = Japan
  0  0  9  8  0 |  d = South Korea
  2  0 10  0  0 |  e = Thailand
```

Figure 4.18 Confusion Matrix for SMO algorithm.

4.8.5 Naive Bayes

Naive Bayes is a standard probabilistic Naive Bayes classifier. 71.21 % (141/198) samples were correctly categorised. 57 samples (28.79 %) were incorrectly classified. This algorithm is not as good for classification, and severely lowers the accuracy for categorisation of Japanese samples. However, it slightly increases the output for South Korea and Thailand samples.

```
  a  b  c  d  e   <-- classified as
 47  2  2  0  4 |  a = Australia
  0  8  1  0  4 |  b = Germany
  4  4 70 11 12 |  c = Japan
  0  4  2  8  3 |  d = South Korea
  2  0  1  1  8 |  e = Thailand
```

Figure 4.19 Confusion matrix for Naive Bayes algorithm.

4.8.6 Use of multiclass classifier to classify unknown samples

The samples in the ESR database that could not have their country of origin traced and the samples from the homogeneity study were used as a test set against the multiclass classifier algorithm. These samples were used as they had not been seen by the training set. Therefore their classification would not be influenced. As the make and model are known, an educated guess can be taken to decide from which country the vehicle originates.

12 of the 15 samples were assigned to the country of origin from which they most likely originated (Table 4.14). However, three of the samples did not appear to be correctly assigned. The two Ford Territory samples (from the same vehicle) were assigned to different countries. The windscreen was categorised as Australian and the tempered glass was categorised as Japanese. These results reflect their placement on the score plot. Even though the samples are from the same vehicle, there is a plausible explanation for their differing categorisation. As previously mentioned, Australian glass is exported for the Ford Territory range; therefore it is possible that Australia only exports windscreens and that the tempered panes are made in Thailand for the Territory range. The Toyota Hilux was assigned as South Korean. This sample is most likely to be of Japanese origin. However, it sits on the edge of the Japanese and South Korean regions on the score plot. Therefore the algorithm assigned it to the wrong country. The confusion matrix for the multiclass classifier shows that 4 samples that were known to originate from Japan were also incorrectly assigned as originating from South Korea.

These results show that classification of glass samples into country of origin must be treated with caution, due to some manufacturers importing glass. In addition, some countries are not clearly defined from other countries, which may place samples in their overlapping regions in the wrong country. However, for most samples, it is able to give a reasonable indication of the country in which the glass was produced.

Table 4.14 Samples with unknown origin and the country they were assigned to using the multi-class classifier

Sample	Make	Model	Notes	Country assigned
33 LF & 38 WS	Holden	Adventra	Number plate does not match ESR's information	Australia
45 R, 49 WS & 51 R	Toyota	Echo	No number plate provided	Japan
62 LF	Holden	Clubsport	No number plate provided	Australia
63 WS	Holden	Astra	Number plate does not match ESR's information	Australia
74 RF & 78 WS	Hyundai	Not supplied by ESR	No number plate provided	South Korea
124 RF	Ford	Territory	Number plate does not match ESR's information	Japan
125 WS	Ford	Territory	Number plate does not match ESR's information	Australia
146 WS	Nissan	March	Personalised number plate cannot be traced	Japan
175 RF	Toyota	Hilux	No number plate provided	South Korea
-	Holden	Commodore	Obtained for homogeneity test	Australia
-	Toyota	Corolla	Obtained for homogeneity test	Japan

4.9 Front and back panes of laminated glass

A windscreen is made up of two sheets of glass with a plastic sheet in the middle. The two sheets of glass are produced in the plant then undergo a series of steps to bind them to the plastic sheet. If these sheets are bound in the same plant in which they are produced in, it is likely that the front and back sheets of glass will have a very similar elemental composition due to the close timing of their manufacture. However, some automotive windscreen plants buy the glass which is then fabricated into finished windscreens; in these cases the two sheets of glass may not be similar in elemental composition. Control glass is collected for analysis from both the front and back pane at the crime scene if both panes are broken. In these cases the origin of the recovered glass could be from the front or back pane. The aim of this section was to examine the variation of the front and back panes of a windscreen to see whether the two panes of glass are indistinguishable from each other. 77 samples in the database had a front and back pane analysed.

A principal component analysis was conducted on the clr transformed means and the scores were obtained; score 1 of the front pane was plotted against score 1 of the back pane (Figure 4.20). About half of the samples lie within the 95 % confidence level (CI). All remaining samples, apart from three, lie in the 95 % prediction interval (PI). The samples that lie outside the PI are listed in Table 4.15. The replicates of these samples were examined to see if one was classed as an outlier and influencing the mean, however, no outliers were found.

Trejos and Almirall reported that the front and back panes of windscreens were significantly different ($p>0.01$). However, these vehicles (Chevy, 1985 and Jeep Wrangler, 1988) are prior to the years sampled in this research.

The results show the importance of good collection practice of fragments at the crime scene as not all front and back panes have a similar elemental composition.

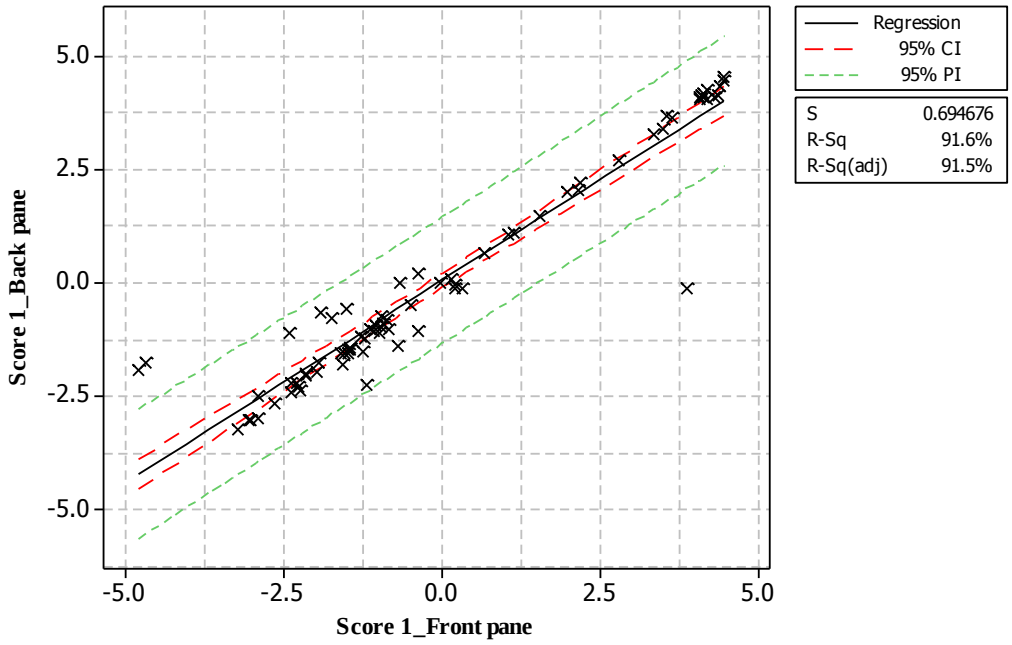

Figure 4.20 Fitted line plot for score 1 of front and back panes. Samples 7, 35 and 41 lie outside the 95 % prediction interval limit.

Table 4.15 Windscreens which have variation exceeding 95 % predicted interval in front and back panes for score 1

Sample	Make	Model	Year	Country
7	Honda	CRV	2002	Japan
35	Lotus	Elise	2004	England
41	Honda	CRV	2003	Japan

4.10 Distinguishing samples

Forensic work requires the comparison of an unknown recovered sample to a control sample. For casework analysis it is beneficial to have a statistical method which is easy to interpret and display in court. PCA, range overlap and the three step method were compared for their ability to distinguish samples.

Usually forensic laboratories analyse control and recovered samples on the same day. This section of research also studied the ability of the PCA and range overlap techniques to report a match if samples were analysed on different days or different instruments. This is beneficial as it will allow the database to be used.

4.10.1 PCA

4.10.1.1 Samples analysed on different days

Section 4.2.3 reported that replicates of samples analysed on different days showed no difference in their analyses. Therefore control and recovered samples analysed on different days should show a match if there is one. Four samples (Table 4.16) were analysed on separate days to investigate the variation found in a score plot.

Table 4.16 Details of samples analysed on different days

Sample	Make	Model	Year	Country
80 RR	Holden	Commodore	2005	Australia
16 R	Toyota	Corolla	2003	Japan
42 WS_F	Mazda	626	2003	Japan
130 WS_F	Audi	S6V10	2006	Germany

The different days are identified by an A or B after the sample name in the score plot (Figure 4.21). All replicates are grouped together apart from sample 80 A. It is unclear why sample 80 A has a large spread, but it could be due either to variation arising from the pane or to measurement error. In comparison, the replicates for day B are very close together; two replicates are directly on top of each other.

The results show that control and recovered samples analysed on different days are visually close on the score plot for most samples. Days A and B sit close together on the score plot for samples 42 and 130. Days A and B for sample 16 (top left corner) have a larger separation than the previous two samples, but are still close together. Two replicates from 80 A sit close to 80 B; however, the other two replicates are further away.

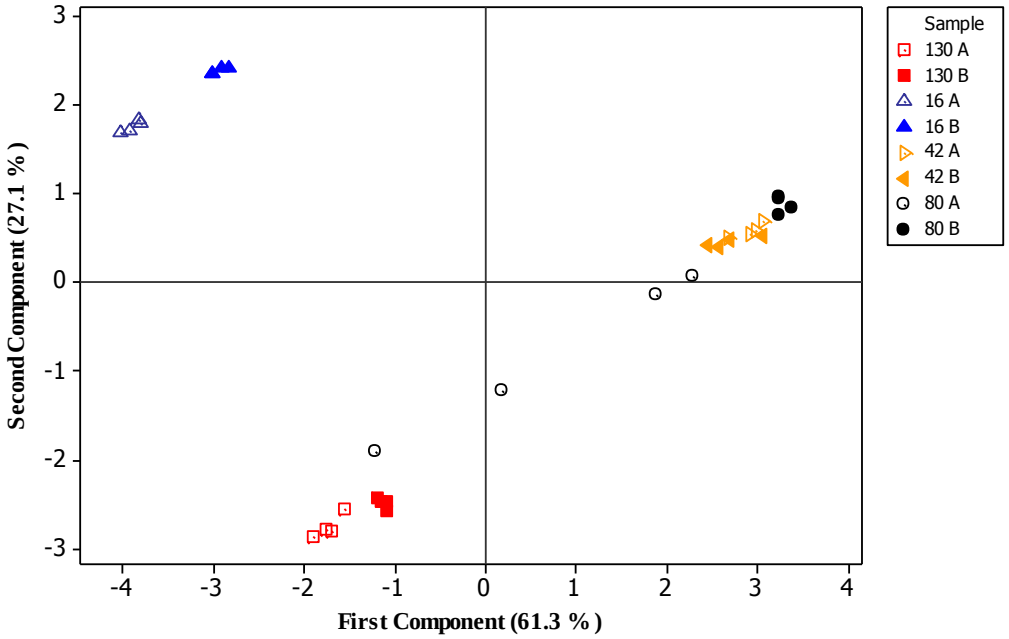

Figure 4.21 Score plot of samples analysed on different days. The days are identified by A and B after the sample name. All replicates are grouped together apart from sample 80 A. Days A and B are positioned the closest for samples 42 and 130.

The results demonstrate PCA can be used to examine samples analysed on different days as samples with a similar elemental composition will sit close together. However, it is noted that the distance between matching samples varies.

As PCA has already been discussed for the whole database (section 4.7) only sets of samples that were unable to be distinguished using RI are discussed here. For simplicity, the ± 0.0005 range was not considered; only samples that had exactly the same RI (to 5.d.p) were analysed to illustrate the ability of PCA.

Five windscreen samples with the same RI (1.52117) were analysed (Table 4.17). The samples cannot be further distinguished by delta RI as they are all laminated samples.

Table 4.17 Samples with RI = 1.52117

Sample ID	Year	Make	Model	Country of Origin	Lam/ non	RI	Delta RI
14 WS_F	2003	Holden	Commodore	Australia	Lam	1.52117	55
17 WS_F	2003	Audi	Cabriolet	Germany	Lam	1.52117	49
58 WS_B	2003	Mitsubishi	Airtrek	Japan	Lam	1.52117	71
58 WS_F	2003	Mitsubishi	Airtrek	Japan	Lam	1.52117	63
106 WS_B	2004	Holden	Clubsport	Australia	Lam	1.52117	45

The four replicates of each sample are clustered together (Figure 4.22). The four different samples are all visually distinguished from each other. 70.8 % of the variance is accounted for in the first principal component and 25.40 % in the second principal component. Therefore 96.2 % of the variance can be explained in the first two principal components. The front and back panes from the windscreen of sample 58 (Mitsubishi Airtrek, 2003) are shown to be indistinguishable. These two panes of glass are unable to be discriminated when these two samples are analysed by themselves (Figure 4.23). This is most likely due to the panes of glass being produced at the same time and cut for lamination.

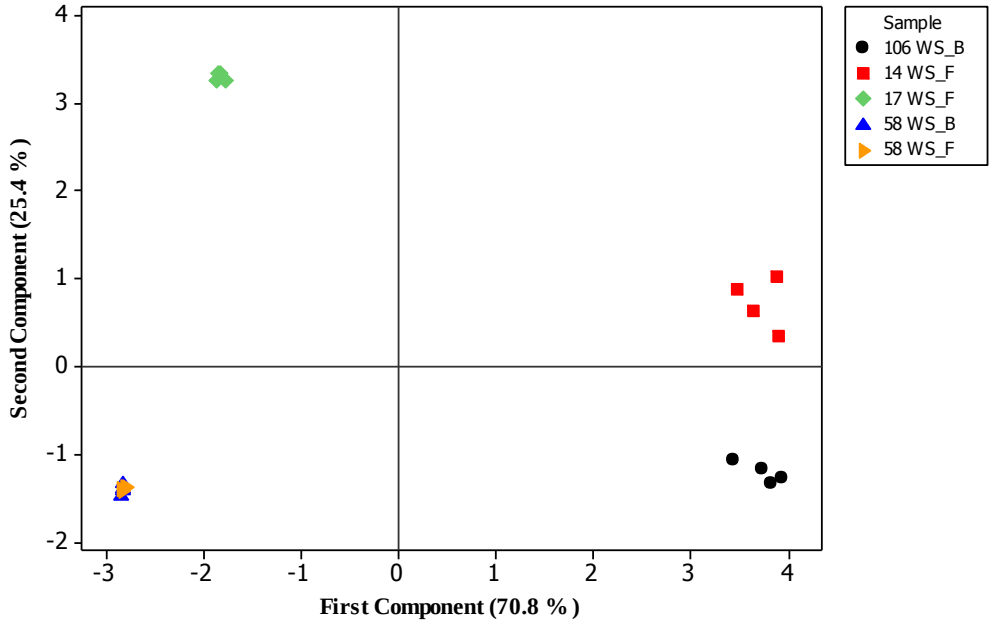

Figure 4.22 Score plot of the five samples with indistinguishable RI. 96.2 % of variance is captured in the first two PC. The different samples are able to be distinguished from each other. The front and back panes of the windscreen from sample 58 are indistinguishable (bottom left hand corner).

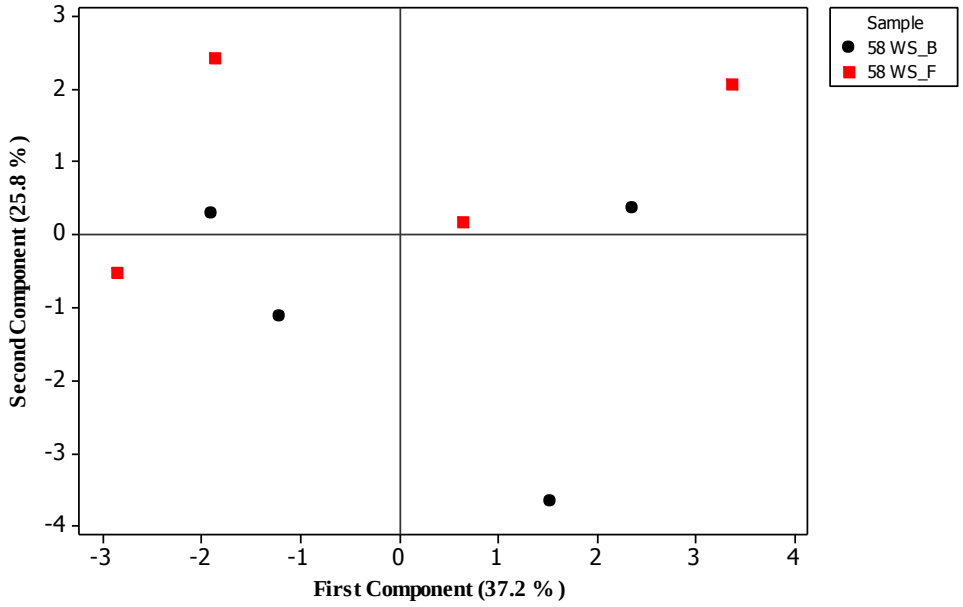

Figure 4.23 Score plot of front and back samples from windscreen 58. They are indistinguishable from each other.

Four windscreen samples, all originating from Japan, with a RI value of 1.52046 were also examined (Table 4.18). PCA is able to discriminate all 4 samples from each other (Figure 4.24). 92.1 % of the variation is in the first two principal components. This example also shows the clustering of replicates and the visual separation of different samples.

Table 4.18 Samples with RI = 1.52046

Sample ID	Year	Make	Model	Country of Origin	Lam/ non	RI	Delta RI
15 WS_F	2003	Toyota	Corolla	Japan	Lam	1.52046	77
20 WS_F	2004	Toyota	Rav4	Japan	Lam	1.52046	70
54 WS_B	2004	Toyota	Prius	Japan	Lam	1.52046	91
140 WS_B	2003	Mitsubishi	Lancer	Japan	Lam	1.52046	53

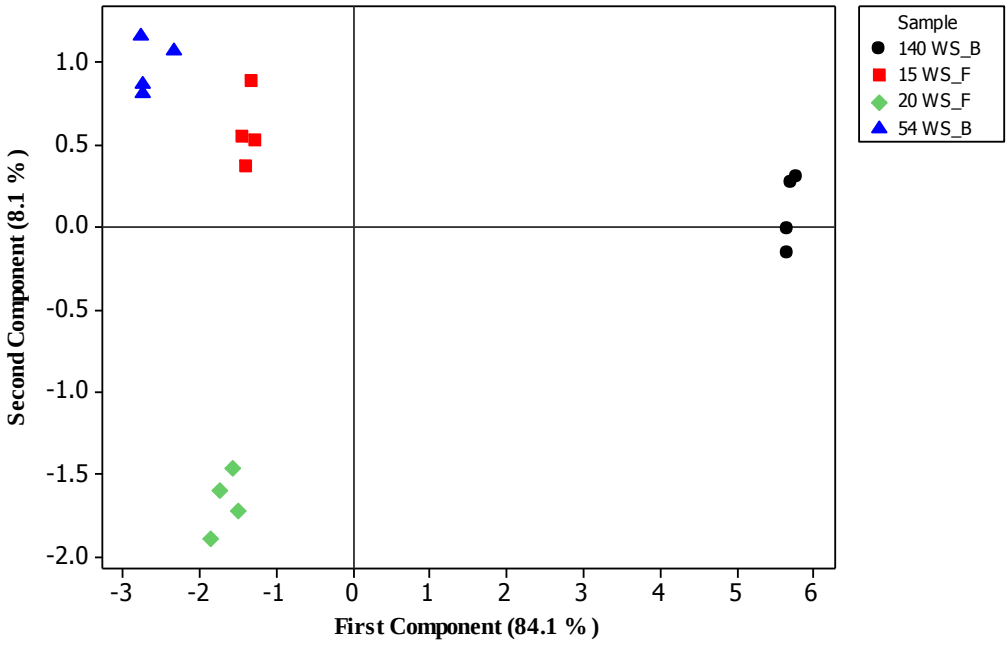

Figure 4.24 Score plot of samples with RI = 1.52046. The samples are able to be distinguished from each other. There is 92.1 % variation in the first two PC.

4.10.1.2 Samples analysed by different laboratories

For the database to have maximum use, it would be valuable if it could be used by many laboratories. This section of research explores the possibility that the

database can be used in different laboratories. As mentioned in section 3.9, a set of four samples were tested by UoW and CFS. The replicates were clr transformed and analysed by PCA.

The score plot (Figure 4.25) shows that the same samples from the two laboratories sit together. Replicates from samples 50, 92 and 153 overlap for the two laboratories; sample 112 has slightly more separation between the replicates from the two laboratories, but they sit very close together. Therefore it is possible for the same sample to be analysed on two different instruments using the method validated in chapter three and still show a visual match.

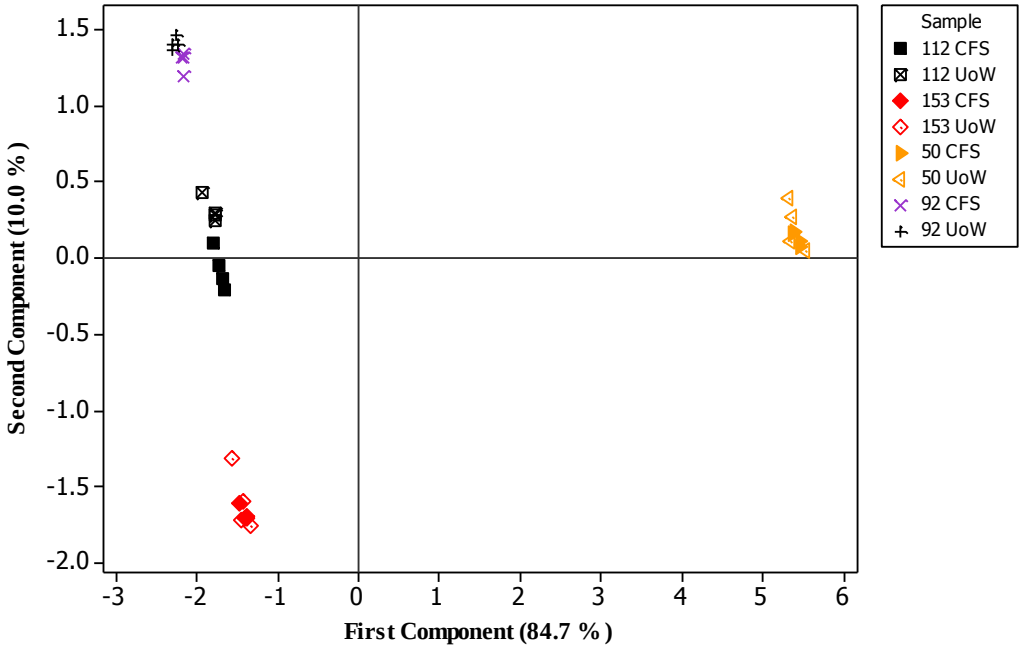

Figure 4.25 Score plot of samples analysed by UoW and CFS. Replicates of samples 50, 92 and 153 overlap between the two laboratories. Replicates of sample 112 for the two laboratories are positioned close together but do not overlap.

4.10.1.3 Conclusion of PCA as a discriminatory technique

This section has shown that samples analysed on different days in one laboratory or in a different laboratory lie close together on the score plot. Therefore a database of samples could be used in many laboratories to show how close the elemental compositions of two samples are.

If PCA was to be used as the sole discriminatory technique, a rule would need to be set to specify how far apart two samples could be and still be classified as originating from the same source. However, this was not explored as there are other methods that can be used for matching samples; the range overlap method is discussed in section 4.10.2.

It was decided that PCA is best suited as an initial exploratory tool to visually assess how different the elemental compositions of samples are. It could be used as a quick analysis to see if the recovered and the control samples are similar in elemental composition. In addition, it may be useful for casework in which many fragments are found on a suspect to gain an idea of whether they are from one or more sources. This is similar to the initial examination of RI range (see section 4.1). Samples which have a similar elemental composition are assumed to originate from the same source and can undergo further testing to see if they match.

4.10.2 Range overlap method

As reported in chapter 1, NFI use the range overlap method. NFI stated that nine or more of ten elements must have ranges which are within two times a standard deviation measure for two glass samples to be classed as matching[23]. This process provides a match/non-match between two samples.

The range overlap method was used to compare samples in the database. For this data, the range of 12 or 13 of the 13 elements had to match for two panes to be classed as indistinguishable. A standard deviation range of ± 2 was used for the range. The average standard deviation from the two homogeneity studies was used as the standard deviation for each element. However, it is noted that these values may not be the most representative values to use. As mentioned in section 4.4.2, the standard deviation for Mg, Fe and Ce in the database are much larger than the standard deviation found in the analysis of the entire window panes. Therefore the range may be under-estimated and type I errors (false exclusions) may occur. The pooled standard deviation of the database for each element would have been a more representative set of values to use as they have been calculated from a long-

term investigation; their values are larger than the standard deviations for samples analysed in a single day. Therefore they would have provided more matches for Mg, Fe and Ce. However careful selection of the range is required as, if the range is too large, more type II errors will occur.

4.10.2.1 Samples analysed on the same day

Forensic laboratories are most likely to analyse recovered and control samples on the same day. This would eliminate day-to-day variation. To illustrate the ability of the range overlap method to match samples analysed on the same day, sets of four ablations from the Holden and Mitsubishi panes were chosen at random. These were averaged and the range overlap method was applied. The samples were shown to match. Therefore this method can be used to compare samples analysed on the same day and a match will be shown if there is one.

4.10.2.2 Samples analysed on different days

The creation of a database would allow recovered samples to be compared with all samples in the database. This would be able to estimate how common the elemental composition of the recovered glass is; if it matches only one control sample there is a high chance the two samples originate from the same place. However, if the recovered sample matches many control samples it does not provide strong evidence of a match.

To use a database, samples would have to be continuously added to keep it updated. Therefore it is necessary to ensure that samples analysed on different days that originate from the same source show a match. One set of the samples from section 4.10.1.1 were labelled as unknown A-D and compared to the database. Details of the samples and the results are shown in Table 4.19.

Table 4.19 Details of samples analysed on different days

Unknown sample	Sample	Make	Model	Year	Country	Correctly matched?
A	80 RR	Holden	Commodore	2005	Australia	Yes
B	16 R	Toyota	Corolla	2003	Japan	No
C	42 WS_F	Mazda	626	2003	Japan	Yes
D	130 WS_F	Audi	S6V10	2006	Germany	Yes

Unknown A matched 11 samples in the database, including sample 80, which is the correct control sample. Unknown C matched nine samples in the database including sample 42 which is the correct control sample. Unknown D only matched the front and back panes of sample 130 in the database which is the correct control sample and allows a conclusive match. Unknown B did not match any of the samples in the database, and only matched Rb, La and Ce, in sample 16; this is a type I error (false exclusion). This sample had a larger gap than other samples between days A and B on the PCA plot. Therefore the ± error was too small to allow the samples to match.

The bias between the unknown and control samples was calculated. Unknown A, C and D had a bias between -5 and 5 % for most elements. However, unknown B had a large bias between most elements. This was larger than 10 % for most elements. This could have occurred from incorrect sampling or day-to-day variation. Figure 4.26 shows the bias of the four samples.

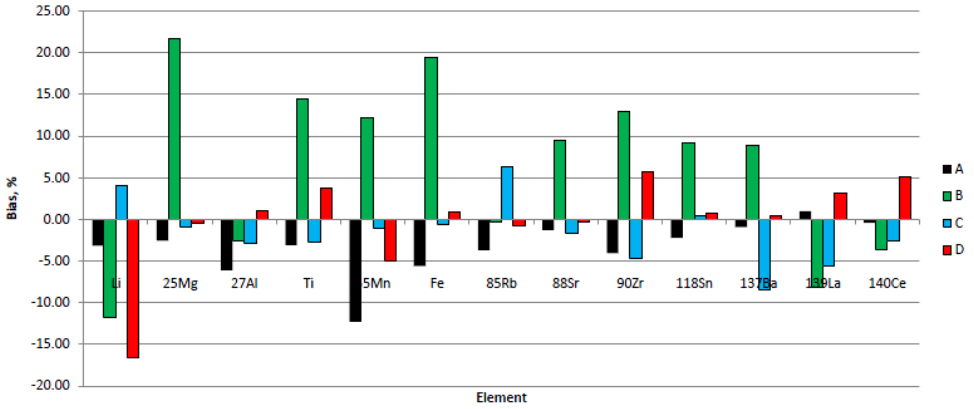

Figure 4.26 Bias of each element for the samples that were analysed on different days. Sample B had more than 10 % bias for most elements between the two days.

The results from sample B show the range overlap method requires further work to minimise the number of type I errors. A larger ± range may be required to tolerate day-to-day variation and measurement errors. This will allow samples originating from the same pane to match even if they are analysed on different days. However, the range must be chosen carefully as if it is too large the number of type II errors (false inclusions) will increase. Type I errors could not be examined for the other samples as they were only analysed once.

Each sample in the database was compared to every other sample using the range overlap method. This shows the number of unique samples and gives an estimation of the number of type II errors that occur. The results can be seen in appendix 6.13; each row of the table contains an individual sample (recovered sample) and shows the percentage of samples that were indistinguishable by elemental composition and also RI. A list of control samples that were indistinguishable from the recovered samples is also given.

If the front and back panes of a windscreen did not match they were treated as two separate samples; if they matched they were classified as the same sample. There were 40 windscreens that had indistinguishable front and back panes. These did not always have the same relativity to other samples. An example of this can be seen in Table 4.20 where the front and back panes of the windscreen of sample 132 were indistinguishable. However, the back pane matched more samples in the

database than the front pane did. In such cases the pane which matched the most samples was used; therefore, in this case, the back pane was used.

Table 4.20 Example of indistinguishable front and back panes from a windscreen using the range overlap method. Samples in bold text are common for both panes

Sample	Number of matching samples	Samples that matched the recovered sample
132 front pane	4	**1, 13, 66, 110**,
132 back pane	10	**1, 13**, 42, **66**, 76, 87F, 102, **110**, 121, 123

There were 204 samples available for comparison. When these were compared using the range overlap method for elemental composition, 80.39 % (164/204) of the samples could be distinguished from all other samples.

The 40 indistinguishable samples had 1 to 17 false inclusions (type II errors). Figure 4.27 shows the frequency of samples that had 1 to 17 false inclusions. All samples that had more than one type II error were categorised as Australian origin using the multiclass classifier algorithm (see section 4.8.2). Samples 66 and 123 had the highest type II errors (8.33 and 7.84 % respectively). The matching samples are seen in Table 4.21; the samples in bold are common to both samples.

Only 41.67 % (20/48) of samples assigned as Australian were able to be distinguished using elemental composition. Australian glass was the hardest to distinguish due to its low variation in elemental concentration. This is due to the localised sourcing of raw materials compared to Northern Hemisphere glass manufacturers. The difficulty in distinguishing Australian glass was also noted by Zurhaar and Mullings using solution ICP-MS[68]. These 40 samples are discussed further in section 4.10.3.

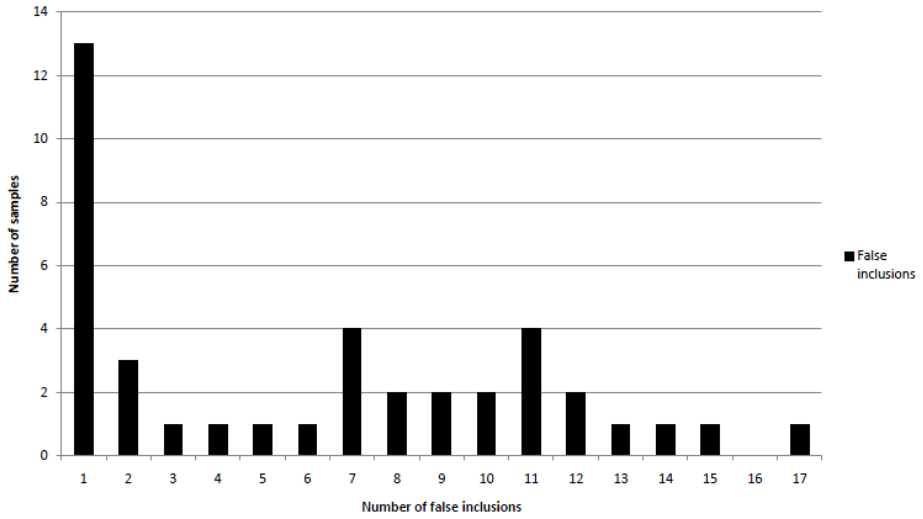

Figure 4.27 Frequency of false inclusions (type II errors) that occurred in the database.

Table 4.21 Examples of Australian samples that had low discrimination. Samples in bold are common for the two samples

ID	Make and Model	Year	Type of window	Number of false inclusions	Samples the elemental composition matched
66	Holden Commodore	2002	R	17	**1**, 11, **13**, 42, 52, 62, **68**, 69, **87**, **101**, **102**, **110**, **120**, **122**, 123, **132**,**144**
123	Holden Commodore	2003	RRQ	15	**1**, **13**, 66, **68**, **87**, **101**, **102**, **110**, **120**, 121, **122**, 125, **132**, **144**, 161

When samples that were assigned as Australian were removed from analysis, 93.59 % (146/156) of samples were distinguishable using elemental composition. There were five remaining indistinguishable pairs (0.64 % type II error). These are discussed further in section 4.10.3.

4.10.2.3 Samples analysed by different instruments

As mentioned in section 4.10.1.2, it would be beneficial for the database to be used in many laboratories. The four samples measured by CFS were compared to the database. The criterion was that 11 or 12 elements had to match, as Zr data was not available. None of the four samples were matched with the correct control sample. The number of elements which matched the correct control sample ranged from 6 to 8 (Table 4.22). All four samples correctly matched Ti, Ba, La and Ce.

Table 4.22 Recovered samples, analysed by CFS, that were compared to the database. Elements that had an overlapping range have a '1' in their column

Sample	^{7}Li	^{25}Mg	^{27}Al	^{49}Ti	^{55}Mn	^{54}Fe
50 WS_F			1	1	1	
92 LF	1		1	1		
112 WS_B	1			1		1
153 WS_F	1			1	1	1

Sample	^{85}Rb	^{88}Sr	^{118}Sn	^{137}Ba	^{139}La	^{140}Ce
50 WS_F	1	1		1	1	1
92 LF		1		1	1	1
112 WS_B				1	1	1
153 WS_F				1	1	1

No samples have an overlapping range for Mg. The bias of the measurements for the two laboratories ranges from -7.28 to 3.84 %. Therefore they would be expected to match. As mentioned in section 4.10.2 the use of the standard deviation from the homogeneity tests may not be representative of the spread in the database. Therefore the range available for overlap may be too small for Mg. However, by using the standard deviation from the database, almost all of the control samples match the recovered sample due to the large range. As Mg is not a trace element, it may not be as useful for discrimination of glass samples. In addition, no samples have an overlapping range for Sn. The bias between the two laboratories for Sn is very large; therefore they would not be expected to match. The large bias most likely arises from the use of Sn in the float glass process.

These results show the analysis of Sn in automotive glass should only be used with caution or it should be removed from analyses due to the large bias in the measurements between laboratories.

Due to the relatively good bias between the measurements for the two laboratories, it was expected that the range overlap method would provide good results. However, the results show that further work is required if a database is to be used between laboratories for analysis of samples. It is possible that the ± 2 σ limit is too tight for some elements. Therefore, a larger range that would allow for day-to-day variation and variation between instruments would need to be found. However, this would need to be carefully chosen to minimise type II errors.

4.10.2.4 Conclusion of range overlap method

The range overlap method has been shown to work well for samples analysed on the same instrument on the same day. It is also able to match samples analysed on the same instrument on different days. However, some type I and type II errors occur. The ± 2σ range may need to be modified to minimise these.

80.30 % of the database was able to be distinguished using the range overlap method. 1 to 17 type II errors occurred (0.49 to 8.33 %). The discrimination was increased to 93.59 % when Australian data was removed. Australian samples were hard to distinguish due to their low elemental variation. Type I errors could not be calculated with the data set as each sample was only analysed once.

4.10.3 Three step method

A three-step procedure was created to increase the discrimination power. This used the range overlap of elemental composition first, due to its greater discriminating ability, followed by comparison of delta RI then RI range. The sample that was compared to all other samples in the database was called the recovered sample; the rest of the samples were called the control samples. At each step, control samples that did not match the recovered sample were removed from

the comparison before undertaking the next step; this allowed a greater opportunity to distinguish samples by RI.

The steps for discrimination were as follows:

1. The recovered sample was compared to the control samples using the elemental range overlap method.
   If the recovered sample was unique, the process stopped.
   If the recovered sample matched one or more control samples, step 2 was undertaken.
2. Delta RI of the recovered sample was compared to each control sample that matched in step 1.
   If delta RI of the recovered and control samples were different (i.e. tempered or laminated glass), the recovered sample was distinguishable from that control sample.
   If delta RI was the same, the samples were indistinguishable at this point and step 3 was undertaken.
3. The RI range (± 0.0005) of the recovered sample was compared to the remaining control samples.
   If the RI range overlapped, the samples were indistinguishable.
   If the RI range did not overlap, the control sample was distinguishable from that control sample.

The three-step procedure is also set out in a flow diagram (Figure 4.28).

The three-step procedure was applied to the 40 samples that were unable to be distinguished using only elemental composition in section 4.10.2.2. Each of these samples is presented in Table 4.23 with the number of matches to the control samples at each of the three steps. Samples in bold text are able to be discriminated using the three-step procedure; samples that are underlined are not classified as Australian and are discussed further on in this section.

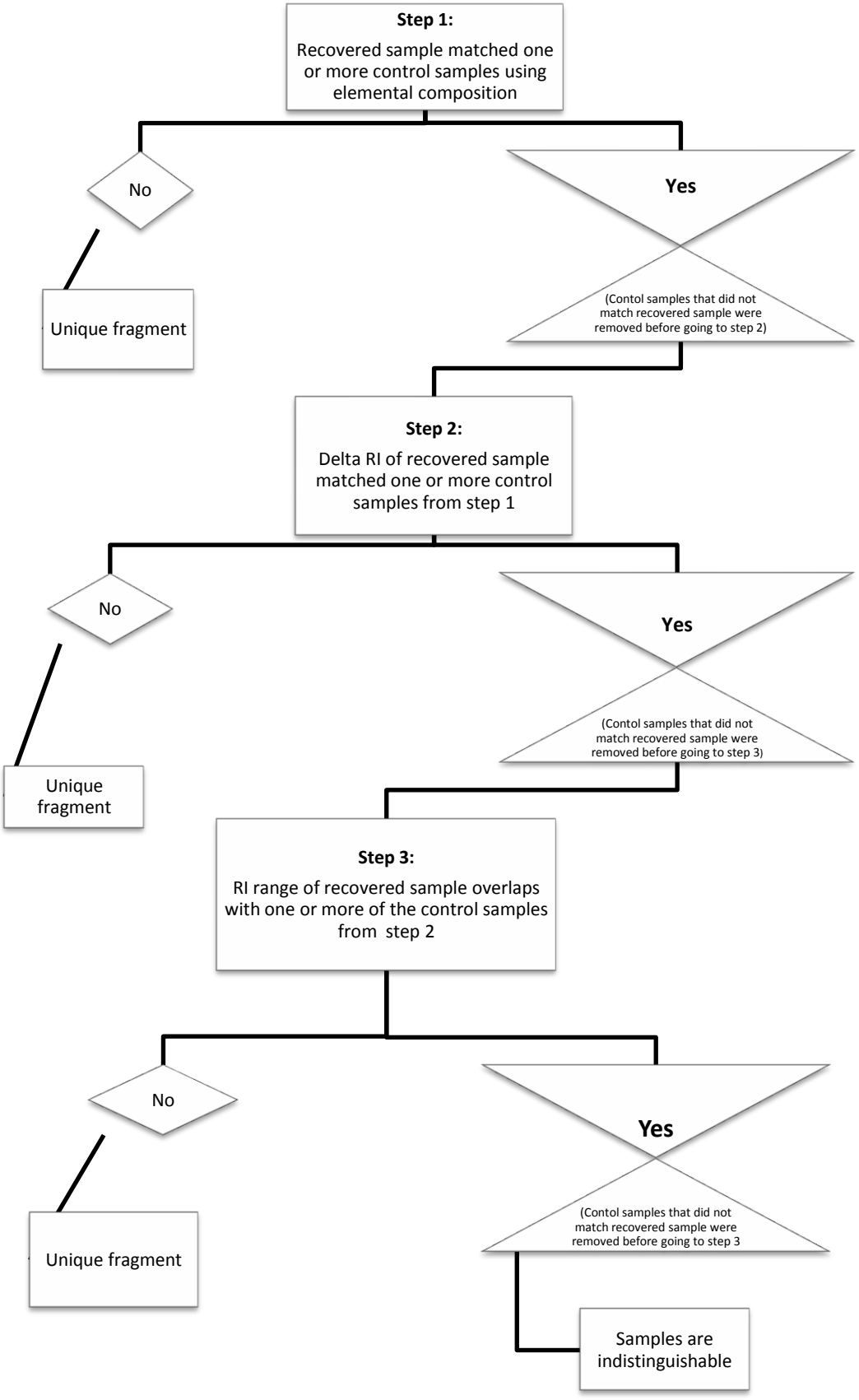

Figure 4.28 Flow diagram of the three-step procedure for distinguishing samples

Table 4.23 Samples that required analysis by the three-step process. Samples in bold are able to be distinguished using this process; underlined samples are not of Australian origin

Sample	Number of samples indistinguishable by elemental composition (Step 1)	Number of samples indistinguishable after Delta RI consideration (Step 2)	Number of samples indistinguishable after RI range overlap (Step 3)
1	8	5	3
11	9	8	7
13	11	4	3
14	7	2	2
35	1	1	1
37	**1**	**1**	**0**
38	7	4	3
42*	5	2	1
49	1	1	1
50	1	1	1
52	7	2	2
61	**2**	**0**	**0**
62	9	3	1
65	1	1	1
66	17	8	7
68	13	4	3
69	12	5	5
76	8	4	4
78	1	1	1
80	4	1	1
87	12	6	5
101	11	5	4
102	14	6	5
106	1	1	1
107	**1**	**0**	**0**
110	13	7	6
113	1	1	1
119	2	2	2
120	**10**	**5**	**0**
121	11	7	7
122	**11**	**4**	**0**
123	16	8	6
125	**2**	**0**	**0**
132	10	2	1
144	**7**	**4**	**0**
145	1	1	1
161†	7	4	4
171	1	1	1

* This is a Mazda 626 from Japan, but is classified as Australian
† This is a Toyota Hilux from Japan, but is classified as Australian

Sample	Number of samples indistinguishable by elemental composition (Step 1)	Number of samples indistinguishable after Delta RI consideration (Step 2)	Number of samples indistinguishable after RI range overlap (Step 3)
172	**1**	**1**	**0**
174	1	1	1

The three step method can distinguish 84.31 % (172/204) of samples from all other samples in the database, which is an extra eight samples. Five of these are of Australian origin, one is a Ford Territory of unknown origin, but was classed as Australian by the multiclass classifier. Therefore this procedure allows slightly better discrimination of Australian samples.
Of interest are samples 120, 122 and 144 which had 10, 11 and 7 matches in the database using only elemental composition. The use of RI as well allowed these samples to be uniquely distinguished.

Samples 66 and 123, which had the highest type II error rates in the range overlap method, ended up with only seven and six matching samples respectively in the three step method, thus greatly reducing the type II errors observed. Figure 4.29 shows the frequency of type II errors using the three step method.

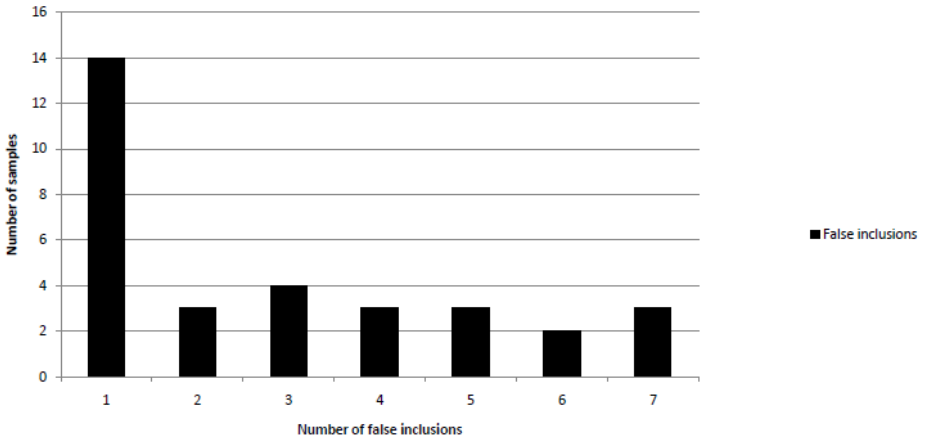

Figure 4.29 Frequency of false inclusions (type II errors) that occurred in the database for the three step method.

As mentioned in section 4.10.2.2, when samples from Australia are removed, only five pairs of windscreen samples are indistinguishable. The details of these

samples are in Table 4.24, with each pair separated by a line. The three step method was applied to these samples; delta RI (step 2) was unable to provide any further discrimination as all samples were of laminated origin. But comparison of the RI range (step 3) was able to discriminate one further pair. These samples both originated from vehicles produced in 2004 in Japan. Therefore by using elemental composition followed by RI determination, 94.87 % (148/156) of samples that were not assigned to Australian origin were able to be discriminated.

4.10.3.1 Conclusion of three step method

The three step method provides marginally better discrimination than elemental comparison alone. A further eight samples were able to be distinguished by using elemental composition and RI analysis. Five of these were Australian glass samples. 84.31 % of samples in the database are able to be distinguished. When Australian data is removed 94.87 % of samples are able to be distinguished. The type II error rate was substantially reduced by including RI in the discriminating method. As RI is a cheap and fast technique to use it is beneficial to use the three step method over the range overlap method.

Table 4.24 Samples that are indistinguishable by the range overlap method (excluding Australian samples). These samples were analysed using the three step method, which allowed one extra pair to be discriminated

ID	Make and Model	Country	Year	Lam/T	RI	Delta RI	Number of laminated samples that are indistinguishable by RI*	Is pair distinguishable by RI?
35	Lotus Elise	England	2004	WS_F	1.52026	31	39 (24.1 %)	No
171	Ford Explorer	USA	2004	WS_F	1.52007	57	29 (17.9 %)	
37	Mitsubishi Lancer	Japan	2004	WS_B	1.51925	96	19 (11.7 %)	Yes
172	Mazda 3	Japan	2004	WS_F	1.51992	36		
49	Toyota Echo	Unknown	Unknown	WS_B	1.51965	67	28 (17.3 %)	No
65	Daihatsu Terios	Japan	2004	WS_B	1.51963	63		

* The percentage listed is only for indistinguishable laminated samples, not the entire database.

ID	Make and Model	Country	Year	Lam/T	RI	Delta RI	Number of laminated samples that are indistinguishable by RI*	Is pair distinguishable by RI?
78	Hyundai (unknown model)	Unknown	Unknown	WS_F	1.52349	82	6 (3.6 %)	No
174	Hyundai Tucson	South Korea	2005	WS_F	1.52346	64	6 (3.6 %)	
				WS_B	1.52343	70	6 (3.6 %)	
113	Toyota Corolla	Japan	2005	WS_F	1.51956	59	27 (16.7 %)	No
				WS_B	1.51942	72	24 (14.8 %)	
145	Toyota Corolla	Japan	2006	WS_F	1.51947	79	24 (14.8 %)	
				WS_B	1.51944	68	24 (14.8 %)	

* The percentage listed is only for indistinguishable laminated samples, not the entire database.

5 Conclusion and recommendations for future work

This research validated a LA-ICP-MS method for automotive glass analysis which included the use of FGS 2 as a viable standard. A database of automotive glass samples from around the world was established which was used to categorise samples into country of origin and to discriminate samples.

5.1 Evaluation and summary of findings

The method developed is relatively robust and is stable over time. The method is suitable for analysis of glass that will be compared to samples that were analysed on different days.

FGS 2 was found to have a small bias relative to the literature values for most elements and low RSDs. It is a feasible standard to use for calibration of the LA-ICP-MS. In addition, it has a higher concentration of Fe and Ti than NIST 612, so is able to detect these elements.

An inter-laboratory comparison was conducted with CFS. Four samples were compared and the bias of most elements was below 10 %. Sn had the highest bias, with all samples having more than 25 % bias between the laboratories.

Most elements are homogeneous in automotive panes. However, K and Pb were shown to have spatial variation. Therefore these elements are not useful for the discrimination of automotive glass as two samples originating from the same pane may be classed as different due to this large concentration difference.

To our knowledge this is the first time a large database of samples from across the globe has been produced. This allowed the difference in elemental composition throughout the world to be studied. A categorisation method was created that places samples into the country of origin of the glass. Australian data was easily classified into its country of origin, as the elemental composition differs greatly from that of countries in the Northern Hemisphere.

The use of elemental composition followed by RI (three step method) for discrimination of samples was slightly better than using elemental composition alone and decreased the type II error rate. 84.31 % of samples were distinguished from all other samples. However, there is very little variation within the Australian glass which makes it hard to distinguish samples. With Australian samples removed, 94.87 % of samples were able to be distinguished.

This research demonstrates the utility of the method, the ability to categorise samples into country of origin and the prospect of using it to discriminate glass fragments. However, it is noted that LA-ICP-MS is costly to run and requires a trained technique for optimum results. Therefore LA-ICP-MS may be restricted to high profile cases and routine forensic casework will most likely continue to use RI as the method of choice for the near future. However, as the use of elemental composition analysis over RI was shown to be superior for discrimination of glass, a further possibility is to find an alternative, cheaper instrument to analyse the elemental composition of glass.

5.2 Recommendations for future work

5.2.1 Method development

As it is costly to run LA-ICP-MS, it may be beneficial to investigate if the method can be shortened. This could take the form of:

- Shortened ablation, initial background and post ablation wash out times
- Reducing the number of replicates required per sample

A larger round-robin study would be of use to gain more information of the variation between instruments. This information could be used to find an appropriate range for each element to allow samples from the same origin to match. This is critical if a range of laboratories are to contribute to the extension of the database.

The front and back panes of windscreens were not always indistinguishable from each other. Additional research could be undertaken to examine this further.

5.2.2 Statistical analysis

It was noted in section 4.10.2 that using the standard deviation from the homogeneity test may not be the most representative value. Therefore the standard deviation from the database could be tested. However, this will cause more matches due to the wider standard deviation for Mg, Fe and Ce. In addition, a ± 2 σ interval may not be the best interval to use. Therefore alternative intervals could be trialled to see if they improve the discrimination.

The type II error rate was considered in this research. However, the samples in the database were not analysed more than once so the type I error could not be estimated for the range overlap method. Future research could include re-analysing samples in the database to estimate the type I error rate.

While the three step method allows good discrimination for non-Australian glass, it would be interesting to see if a different statistical technique would allow better discrimination of Australian glass samples. A continuous approach is a possible technique for discrimination as it gives the strength of the match, not a match/non-match result.

Due to the limitation of time, the sample size of some countries was not increased. A larger sample set from Spain, South Africa, Belgium, England, France, USA and Italy would be useful to allow a better picture of their elemental composition for categorising samples into these countries.

5.2.3 Ongoing work

The samples analysed during this research were from the years 2002 -2006.
The database would have to be updated with samples from newer vehicles for it to still be valid. This may require adding a set number of samples to the database every year.

A study of new vehicles could be undertaken to see if there is a large variation in the elemental composition from each country. The country of origin will require

periodic testing as new raw material mine sites may be sourced once the original mines are exhausted. They may have a different composition of elements which will affect the categorisation of samples into country of origin.

Finally, legislation to introduce marker elements into glass could be investigated. This could be established to have a unique elemental set for different manufacturers.

References

1. Mysen, B. O.; Richet, P., *Silicate glasses and melts – properties and structure*. Elsevier: The Netherlands, 2005.
2. Leadbetter, A. J., *Solid liquids and liquid crystals*. The Printing Unit of the University of Exeter: Great Britian, 1976.
3. In *Van Nostrand's Scientific Encyclopedia*, Ninth ed.; Considine, G. D., Ed. Wiley Interscience: New York, 2002; Vol. 1.
4. American Society for Testing and Materials Method (C0162-04) - Standard terminology of glass and glass products. In *ASTM Annual Book if ASTM Standards*, American Society for Testing and Materials: West Conshohocken, 2004; Vol. 15.02.
5. Macfarlane, A.; Martin, G., *The glass bathyscaphe – how glass changed the world*. Profile Books Ltd: Great Britain, 2003.
6. The World Book Encyclopedia. In World Book: Chicago, 2001; Vol. 8.
7. Glass. In *Encyclopædia Britannica*, Encyclopædia Britannica, Inc.: 1970; Vol. 10.
8. Glass. In *The Encyclopædia Britannica - A dictionary of arts, sciences, literature and general information*, 11th ed.; 1910; Vol. XII.
9. Curran, J. M.; Hicks, T. N.; Buckleton, J. S., *Forensic Interpretation of Glass Evidence*. CRC Press: 2000; p 178.
10. Freitag, D. W., Glass Industry. In *Opportunities for Advanced Ceramics to Meet the Needs of the Industries of the Future* [Online] U.S. Advanced Ceramics Associated and Oak Ridge National Laboratory: United States of America, 1998. http://www.ms.ornl.gov/programs/energyeff/cfcc/iof/chap6.pdf.
11. Fibreglass. http://www.einstein.yu.edu/ehs/Industrial%20Hygiene/Fs_Fibergls.htm (27 June 2010),
12. Montero, S.; Hobbs, A. L.; French, T. A.; Almirall, J. R., Elemental analysis of glass fragments by ICP-MS as evidence of association: analysis of a case. *Journal of Forensic Sciences* **2003,** 48, (5), 1101-1107.
13. http://www.agc.jp/english/csr/environment/products/images/env_sp01_08a.jpg (9 March 2010),
14. Carr, N. Encyclopædia Britannica. http://www.britannica.com/EBchecked/topic/210354/float-glass-method (23 Novemeber 2009),
15. Becker, S.; Weis, P. Laser ablation ICP-MS in forensic glass analysis: A decade of Experience. http://projects.nfstc.org/trace/docs/final/Becker.pdf
16. Knapp, B., *Silicon*. Atlantic Europe Publishing: UK, 1996.
17. Coumbaros, J.; Denman, J.; Kirkbride, K. P.; Walker, G. S.; Skinner, W., An investigation into the spatial elemental distribution within a pane of glass by time of flight secondary ion mass spectrometry. *Journal of Forensic Sciences* **2008,** 53, (2), 312-320.
18. Rendle, D. F., Advances in chemistry applied to forensic science. *Chemical Society Reviews* **2005,** 34, (12), 1021-1030.
19. Castro, W.; Trejos, T.; Naes, B.; Almirall, J., Comparison of high-resolution and dynamic reaction cell ICP-MS capabilities for forensic analysis of iron in glass. *Analytical and Bioanalytical Chemistry* **2008,** 392, (4), 663-672.

20. Holloway, D. G., *The physical properties of glass*. Wykeham Publications LTD: London, 1973.
21. Watling, R. J.; Lynch, B. F.; Herring, D., Use of laser ablation inductively coupled plasma mass spectrometry for fingerprinting scene of crime evidence. *Journal of Analytical Atomic Spectrometry* **1997,** 12, 195–203.
22. Wagner, B.; Nowak, A.; Bulska, E.; Kunicki-Goldfinger, J.; Schalm, O.; Janssens, K., Complementary analysis of historical glass by scanning electron microscopy with energy dispersive X-ray spectroscopy and laser ablation inductively coupled plasma mass spectrometry. *Microchimica Acta* **2008,** 162, 415–424.
23. Koons, R. D. In *Paint and glass - a review: 2004 to 2007*, 15th International Forensic Science Symposium, Lyon, 2007; Lyon, 2007.
24. Curran, J. M.; Triggs, C. M.; Almirall, J. R.; Buckleton, J. S.; Walsh, K. A. J., The interpretation of elemental composition measurements from forensic glass evidence: I. *Science & Justice* **1997,** 37, (4), 241-244.
25. Almirall, J.; Trejos, T., Advances in the forensic analysis of glass fragments with a focus on refractive index and elemental analysis. *Forensic Science Review* **2006,** 18, (2).
26. Rincon, R., *Characterisation techniques of glasses and ceramics*. 1999.
27. Hickman, D. A., Linking criminals to the scene of the crime with glass analysis. *Analytical Chemistry* **1984,** 56, (7), 844A-852A.
28. Corbin, G. Kiwi Iconz. http://kiwiiconz.tripod.com (29 April 2010),
29. Bowey, A. M. Glass Museum On Line. http://www.theglassmuseum.com (29 April 2010),
30. Isaacs, N., The changing shape of window glass. *Build* 2007, pp 118-119.
31. *Toyota's commitment to New Zealanders*; Toyota New Zealand: 2009.
32. *New Zealand motor vehicle registration statistics 2008*; NZ Transport Agency: Palmerston North, 2009.
33. Grzegorz, Z., Glass analysis for forensic purposes - a comparison of classification methods. *Journal of Chemometrics* **2007,** 21, (5-6), 174-186.
34. Almirall, J. R.; Cole, M. D.; Gettinby, G.; Furton, K. G., Discrimination of glass sources using elemental composition and refractive index: development of predictive models. *Science & Justice* **1998,** 38, (2), 93-100.
35. Almirall, J., Forensic chemistry education. *Analytical Chemistry* **2005,** 77, (2).
36. Petterd, C. I.; Hamshere, J.; Stewart, S.; Brinch, K.; Masi, T.; Roux, C., Glass particles in the clothing of members of the public in South-Eastern Australia - a survey. *Forensic Science International* **1999,** 103, (3), 193-198.
37. Bennett, R. L.; Kim, N. D.; Curran, J. M.; Coulson, S. A.; Newton, A. W. N., Spatial variation of refractive index in a pane of float glass. *Science & Justice* **2003,** 43, (2), 71-76.
38. Coulson, S. A.; Buckleton, J. S.; Gummer, A. B.; Triggs, C. M., Glass on clothing and shoes of members of the general population and people suspected of breaking crimes. *Science & Justice* **2001,** 41, (1), 39-48.
39. Brettell, T. A.; Saferstein, R., Forensic science. *Analytical Chemistry* **1987,** 59, (12), R162-R174.
40. Underhill, M., The acquisition of breaking and broken glass *Science & Justice* **1997,** 37, 121-127.

41. Lambert, J. A.; Satterthwaite, M. J.; Harrison, P. H., A survey of glass fragments recovered from clothing of persons suspected of involvement in crime. *Science & Justice* **1995,** 35, (4), 273-281.
42. Hicks, T.; Vanina, R.; Margot, P., Transfer and persistence of glass fragments on garments. *Science & Justice* **1996,** 36, (2), 101-107.
43. Allen, T. J.; Scranage, J. K., The transfer of glass-part 1: Transfer of glass to individuals at different distances. *Forensic Science International* **1998,** 93, (2-3), 167-174.
44. Allen, T. J.; Hoefler, K.; Rose, S. J., The transfer of glass-part 2: A study of the transfer of glass to a person by various methods. *Forensic Science International* **1998,** 93, (2-3), 175-193.
45. Allen, T. J.; Hoefler, K.; Rose, S., The transfer of glass-part 3: The transfer of glass from a contaminated person to another uncontaminated person during a ride in a car. *Forensic Science International* **1998,** 93, (2-3), 195-200.
46. Allen, T. J.; Cox, A. R.; Barton, S.; Messam, P.; Lambert, J. A., The transfer of glass-part 4 The transfer of glass fragments from the surface of an item to the person carrying it. *Forensic Science International* **1998,** 93, 201-208.
47. Roux, C.; Kirk, R.; Benson, S.; Van Haren, T.; Petterd, C. I., Glass particles in footwear of members of the public in South-Eastern Australia - a survey. *Forensic Science International* **2001,** 116, (2-3), 149-156.
48. Trejos, T.; Almirall, J. R., Sampling strategies for the analysis of glass fragments by LA-ICP-MS: Part II: Sample size and sample shape considerations. *Talanta* **2005,** 67, (2), 396-401.
49. Guin, J.-P.; Wiederhon, S., M., Fracture of silicate glasses: ductile or brittle? *Physical Review Letters* **2004,** 92.
50. Brown, G., A *Thickness and refractive index data of a population of Christchurch window glasses*; CD2354; Department of Scientific and Industrial Research: Christchurch, 1985.
51. May, C. D.; Watling, R. J. In *A comparison of the use of refractive index (RI) and laser ablation inductively coupled plasma mass spectrometry (LA-ICP-MS) for the provenance establishment of glass bottles*, 10th SIDS International Conference, Portsmouth, England, June 23-26, 2008; Humana Press Inc: Portsmouth, England, 2008; pp 66-76.
52. Brettell, T. A.; Saferstein, R., Forensic science. *Analytical Chemistry* **1983,** 55, 19R-31R.
53. Newton, A. W. N.; Buckleton, J. S., An investigation into the relationship between edge counts and the variability of the refractive index of glass: Part I: Edge morphology. *Forensic Science International* **2008,** 177, (1), 24-31.
54. Brettell, T. A.; Saferstein, R., Forensic science. *Analytical Chemistry* **1985,** 57, 175R-187R.
55. Brettell, T. A.; Saferstein, R., Forensic science. *Analytical Chemistry* **1995,** 67, 273-294.
56. Suzuki, Y.; Kikkawa, H. S.; Kasamatsu, M.; Higashikawa, Y.; Suzuki, S., Forensic discrimination of sheet glass exposed to high temperature by the determination of trace impurities using ICP-MS. *Analytical Sciences* **2008,** 24, (6), 745-749.
57. Naes, B. E.; Umpierrez, S.; Ryland, S.; Varnett, C.; Almirall, J. R., A comparison of laser ablation inductively coupled plasma mass spectrometry, micro X-ray fluorescence spectroscopy, and laser induced breakdown

spectroscopy for the discrimination of automotive glass. *Spectrochimica Acta Part B: Atomic Spectroscopy* **2008,** 63, 1145-1150.
58. Neufeld, L. M. *Analysis of forensic glass samples by laser ablation ICP-MS*; Agilent Technologies: 2004.
59. Coulson, S.; Kitto, L.; Campbell, G. P., An update of vehicle glass in New Zealand:The 2002-2006 vehicle glass survey. In ESR: Auckland, 2009.
60. Coulson, S. A.; Newton, A. W. N.; Curran, J. M.; Rushton, K. In *Analysis of the variation of glass refractive index with respect to annealing*, The 20th International Symposium on the Forensic Sceicnes (ANZFSS) - Forensic Science on Trial, Sydney, 2010; Sydney, 2010.
61. Nishiwaki, Y.; Shimoyama, M.; Nakanishi, T.; Ninomiya, T.; Nakai, I., Application of total reflection X-ray fluorescence spectrometry to small glass fragments. *Analytical Sciences* **2006,** 22, (10), 1297-1300.
62. Roedel, T. C.; Bronk, H.; Haschke, M., Investigation of the influence of particle size on the quantitative analysis of glasses by energy-dispersive micro X-ray fluorescence spectrometry. *X-Ray Spectrometry* **2002,** 31, (1), 16-26.
63. Padilla, R.; Van Espen, P.; Abrahantes, A.; Janssens, K., Semiempirical approach for standardless calibration in μ-XRF spectrometry using capillary lenses. *X-Ray Spectrometry* **2004,** 34, 19-27.
64. Rodriguez-Celis, E.; Gornushkin, I.; Heitmann, U.; Almirall, J.; Smith, B.; Winefordner, J.; Omenetto, N., Laser induced breakdown spectroscopy as a tool for discrimination of glass for forensic applications. *Analytical and Bioanalytical Chemistry* **2008,** 391, (5), 1961-1968.
65. Bridge, C. M.; Powell, L. J.; Steele, K. L.; Williams, M.; MacInnis, J. M.; Sigman, M. E., Characterisation of automobile float glass with laser-induced breakdown spectroscopy and laser ablation inductively coupled plasma mass spectrometry *Applied Spectroscopy* **2006,** 60, (10), 1181-1187.
66. Bridge, C. M.; Powell, L. J.; Steele, K. L.; Sigman, M. E., Forensic comparative glass analysis by laser-induced breakdown spectroscopy *Spectrochimica Acta Part B* **2007,** 62, 1419-1425.
67. Günther, D.; Hattendorf, B., Solid sample analysis using laser ablation inductively coupled plasma mass spectrometry. *TrAC Trends in Analytical Chemistry* **2005,** 24, (3), 255-265.
68. Zurhaar, A.; Mullings, L., Characterisation of forensic glass samples using inductively coupled plasma mass spectrometry. *Journal of Analytical Atomic Spectrometry* **1990,** 5, 611-617.
69. Duckworth, D. C.; Morton, S. J.; Bayne, C. K.; Koons, R. D.; Montero, S.; Almirall, J. R., Forensic glass analysis by ICP-MS: a multi-element assessment of discriminating power via analysis of variance and pairwise comparisons. *Journal of Analytical Atomic Spectrometry* **2002,** 17, 662-668.
70. Suzuki, Y.; Sugita, R.; Suzuki, S.; Marumo, Y., Forensic discrimination of bottle glass by refractive index measurement and analysis of trace elements with ICP-MS. *Analytical Sciences* **2000,** 16, (11), 1195.
71. Almirall, J. R.; Trejos, T.; Hobbs, A.; Furton, K. In *Trace elemental analysis of glass and paint samples of forensic interest by ICP-MS using Laser Ablation solid sample introduction*, Conference on Sensors, and Command, Control, Communications, and Intelligence (C3I) Technologies for Homeland Defense and Law Enforcement II, Orlando, Fl, Apr 21-25, 2003; Carapezza, E. M., Ed. Orlando, Fl, 2003; pp 193-204.

72. Neufeld, L. M., Application of laser ablation ICP-MS to the analysis of forensic glass samples. *Spectrosopy* 2005, pp 31-36.
73. Durrant, S. F., Laser ablation inductively coupled plasma mass spectrometry: achievements, problems, prospects. *Journal of Analytical Atomic Spectrometry* **1999,** 14, 1385–1403.
74. Günther, D.; Horn, I.; Hattendorf, B., Recent trends and developments in laser ablation-ICP-mass spectrometry. *Fresenius J Anal Chem* **2000,** 368, 4-14.
75. Russo, R. E.; Mao, X.; Liu, H.; Gonzalez, J.; Mao, S. S., Laser ablation in analytical chemistry-a review. *Talanta* **2002,** 57, (3), 425-451.
76. Thomas, R., *Practical guide to ICP-MS*. Marcel Dekker, Inc: New York, 2004.
77. van Elteren, J. T.; Tennent, N. H.; Selih, V. S., Multi-element quantification of ancient/historic glasses by laser ablation inductively coupled plasma mass spectrometry using sum normalization calibration. *Analytica Chimica Acta* **2009,** 644, (1-2), 1-9.
78. Jackson, S. E., The application of Nd:YAG lasersing in LA-ICP-MS. In *Laser-Ablation ICPMS in the Earth Sciences - Principles and applications*, Sylvester, P., Ed. Mineralogical Associsation of Canada: 2001; Vol. 29.
79. Schroeder, E.; Hamester, M.; Kaiser, M., Properties and characteristics of a laser ablation ICP-MS system for the quantitative elemental analysis of glasses. *Applied Surface Science* **1998,** 127-129, 292-298.
80. Smith, K.; Trejos, T.; Watling, J. R.; Almirall, J. R., A guide for the quantitative elemental analysis of glass using laser ablation inductively coupled plasma mass spectrometry. *Atomic Spectroscopy* **2006,** 27, (3), 69-75.
81. Moenke-Blankenburg, L.; Schumann, T.; Günther, D.; Kuss, H.; Paul, M., Quantitative analysis of glass using inductively coupled plasma atomic emission and mass spectrometry, laser micro-analysis inductively coupled plasma atomic emission spectrometry and laser ablation inductively coupled plasma mass spectrometry. *Journal of Analytical Atomic Spectrometry* **1992,** 7, 251-254.
82. Trejos, T.; Montero, S.; Almirall, J. R., Analysis and comparison of glass fragments by laser ablation inductively coupled plasma mass spectrometry (LA-ICP-MS) and ICP-MS. In *Analytical & Bioanalytical Chemistry*, Springer Science & Business Media B.V.: 2003; Vol. 376, pp 1255-1264.
83. Oxford English Dictionary. http://www.oed.com/ (7 April 2010),
84. Berends-Montero, S.; Wiarda, W.; de Joode, P.; van der Peijl, G., Forensic analysis of float glass using laser ablation inductively coupled plasma mass spectrometry (LA-ICP-MS): validation of a method. *Journal of Analytical Atomic Spectrometry* **2006,** 21, (11), 1185-1193.
85. Jackson, S. E., Calibration strategies for elemental analysis by LA-ICP-MS. In *Laser Ablation ICP-MS in the Earth Sciences: Current Practices and Outstanding Issues*, Sylvester, P., Ed. Mineralogical Association of Canada: Vancouver, 2008; Vol. 40.
86. Günther, D.; Cousin, H.; Magyar, B.; Leopold, I., Calibration Studies on Dried Aerosols for Laser Ablation–Inductively Coupled Plasma Mass Spectrometry. *Journal of Analytical Atomic Spectrometry* **1997,** 12, 165-170.
87. Latkoczy, C.; Becker, S.; Dücking, M.; Günther, D.; Hoogewerff, J. A.; Almirall, J. R.; Buscaglia, J.; Dobney, A.; Koons, R. D.; Montero, S.; Peijl, G. J. Q. v. d.; Stoecklein, W. R. S.; Trejos, T.; Watling, J. R.; Zdanowicz, V. S., Development and evaluation of a standard method for the quantitative

determination of elements in float glass samples by LA-ICP-MS. *Journal of Forensic Sciences* **2005,** 50, (6), 1-15.
88. Trejos, T.; Almirall, J. R., Sampling strategies for the analysis of glass fragments by LA-ICP-MS: Part I. Micro-homogeneity study of glass and its application to the interpretation of forensic evidence. *Talanta* **2005,** 67, (2), 388-395.
89. Montero, S. Trace elemental analysis of glass by indicutively coupled plasma-mass spectrometry (ICP-MS) and laser abalation inductively coupled plasma-mass spectrometry (LA-ICP-MS). Florida International University, Miami, 2002.
90. González, J. J.; Fernández, A.; Mao, X.; Russo, R. E., Scanning vs. single spot laser ablation (λ=213 nm) inductively coupled plasma mass spectrometry. *Spectrochimica Acta Part B: Atomic Spectroscopy* **2004,** 59, (3), 369-374.
91. Kuhn, H.-R.; Guillong, M.; Günther, D., Size-related vaporisation and ionisation of laser-induced glass particles in the inductively coupled plasma. *Analytical and Bioanalytical Chemistry* **2004,** 378, (4), 1069-1074.
92. Aeschliman, D. B.; Bajic, S. J.; Baldwin, D., P.; Houk, R., S., Multivariate pattern matching of trace elements in solids by laser ablation inductively coupled plasma-mass spectrometry: source attribution and preliminary diagnosis of fractionation. *Analytical Chemistry* **2004,** 76, (11), 3119-3125.
93. De Roy, G., *ENFSI best practice manual for forensic glass examination: Appendix G. Quantitative forensic float glass analysis using LA-ICP-MS Ref.Code: EPG-BPM-002 App. F.* ENSFI: 2009.
94. May, C. D. Development of novel analytical and interpretational protocolss to facilitate the provenance establishment of glass and plastic evidence. The University of Western Australia, 2009.
95. Montero, S. *Forensic float-glass analysis using laser ablation inductively coupled plasma mass spectrometry (LA-ICP-MS)*; 2005.
96. Gonzalez, J.; Mao, X., L.; Roy, J.; Mao, S. S.; Russo, R. E., Comparison of 193, 213 and 266 nm laser ablation ICP-MS. *Journal of Analytical Atomic Spectrometry* **2002,** 17, 1108-1113.
97. González, J.; Liu, C.; Yoo, J.; Mao, X.; Russo, R. E., Double-pulse laser ablation inductively coupled plasma mass spectrometry. *Spectrochimica Acta Part B: Atomic Spectroscopy* **2005,** 60, (1), 27-31.
98. Campbell, G. P.; Curran, J. M., The interpretation of elemental composition measurements from forensic glass evidence III. *Science & Justice* **2009,** 49, (1), 2-7.
99. Günther, D.; Heinrich, C., A., Enhanced sensitivity in laser ablation-ICP mass spectrometry using helium-argon mixtures as aerosol carrier. *Journal of Analytical Atomic Spectrometry* **1999,** 14, 1369-1368.
100. Horn, I.; Gunther, D., The influence of ablation carrier gasses Ar, He and Ne on the particle size distribution and transport efficiencies of laser ablation-induced aerosols: implications of LA-ICP-MS. *Applied Surface Science* **2003,** 207, 144-157.
101. Gunther, D.; Heinrich, C., A., Comparison of the ablation behaviour of 266 nm Nd:YAG and 193 nm ArF excimer lasers for LA-ICP-MS analysis. *Journal of Analytical Atomic Spectrometry* **1999,** 14, 1369-1374.
102. Günther, D.; Hattendorf, B.; Audétat, A., Multi-element analysis of melt and fluid inclusions with improved detection capabilities for Ca and Fe using laser

ablation with a dynamic reaction cell ICP-MS. *Journal of Analytical Atomic Spectrometry* **2001,** 16, 1085-1090.
103. Umpierrez, S.; Trejos, T.; Neubauer, K.; Almirall, J. *Determination of iron in glass by solution and laser ablation using dynamic reaction cell ICP-MS*; PerkinElmer.
104. Scheer, S. *The evidential value of elemental composition in forensic glass examination: the use of multivariate likelihood ratio methods*; Netherlands Forensic Institute: 2006.
105. Campbell, G. P. Characterisation of New Zealand nephrite for forensic purposes. The University of Auckland, Auckland, 2009.
106. Pearce, N. J. G.; Perkins, W. T.; Westgate, J. A.; Gorton, M. P.; Jackson, S. E.; Neal, C. R.; Chenery, S. P., A compilation of new and published major and trace element data for NIST SRM 610 and NIST SRM 612 glass reference materials. *Geostandards Newsletter* **1997,** 21, 115-144.
107. van Achterbergh, E.; Ryan, C. G.; Griffin, W. L. *GLITTER! User's manual - on-line interactive data reduction for the LA-ICP-MS microprobe*, GEMOC National Key Centre, Macquarie University.
108. Lee, C.-T. A. Laser ablation ICP-MS: Data reduction. http://www.ruf.rice.edu/~ctlee/LASERABLATIONICP.pdf
109. Montero, S.; Wiarda, W.; de Joode, P.; van der Peijl, G., Forensic analysis of float glass using laser ablation inductively coupled plasma mass spectrometry (LA-ICP-MS): validation of a method. *Journal of Analytical Atomic Spectrometry* **2006,** 21, 1185-1193.
110. Gao, S.; Liu, X. L.; Yuan, H.; Hattendorf, B.; Detlef, G.; Chen, L.; Hu, S., Determination of forty two major and trace elements in USGS and NIST SRM glasses by laser ablation-inductively coupled plasma-mass spectrometry. *Geostandards Newsletter* **2002,** 26, (2).

6 Appendices

Appendix	Title	Print/ Electronic
6.1	ESR database information	Print
6.2	Placket-Burman run sequence	Print
6.3	Main effects plots for Plackett-Burman test	Electronic
6.4	Normal plot of the standardised effects for Plackett-Burman test	Electronic
6.5	Quality control charts using NIST 612 as calibration standard	Electronic
6.6	Quality control charts using FGS 2 as calibration standard	Electronic
6.7	Contour plots for Toyota Corolla side window	Electronic
6.8	Surface plots for Toyota Corolla side window	Electronic
6.9	Contour plots for Mitsubishi Cedia side window	Electronic
6.10	Contour plots for Holden Commodore windscreen	Electronic
6.11	Surface plots for Mitsubishi Cedia side window	Electronic
6.12	Surface plots for Holden Commodore windscreen	Electronic
6.13	Summary of range overlap method	Print

6.1 ESR database information

Sheet ID	Registration Number	Year	Make	Model	Country	Lam /non	Pane	Origin	Colour	Width	Float	Match Temp	RI	Match Temp (Post Annealed)	RI (Post Annealed)	Delta RI
1 LF	BMS865	2003	Holden	Calais	Australia	T	LF	LF	Pale Green	3.85	Float	63.32	1.52036	59.7	1.52169	133
2 WS_B	BMS865	2003	Holden	Calais	Australia	Lam	WS	Lam/B	Clear	2.05	Float	70.12	1.51818	68.1	1.51893	75
2 WS_F	BMS865	2003	Holden	Calais	Australia	Lam	WS	Lam/F	Blue/Green	2.4	Float	63.69	1.52054	65.07	1.52004	50
3 RR	AQB491	2002	Nissan	Pulsar	Japan	T	RR	RR	Green	3.15	Float	68.16	1.51858	62.9	1.52052	194
4 LF	ASC435	2002	Honda	CRV	Japan	T	LF	LF	Green	3.45	Float	64.39	1.51997	60.02	1.52158	161
5 RF	AUA428	2002	Mitsubishi	Galant	Japan	T	RF	RF	Blue/Green	3.39	Float	63.77	1.5202	59.44	1.52179	159
6 WS_B	AYS519	2002	Nissan	Primera	Japan	Lam	WS	Lam/B	Clear	?	NOS	66.82	1.51939	63.35	1.51993	54
6 WS_F	AYS519	2002	Nissan	Primera	Japan	Lam	WS	Lam/F	Clear	?	NOS	67.86	1.51901	66.13	1.51965	64
7 WS_B	ASC435	2002	Honda	CRV	Japan	Lam	WS	Lam/B	Clear	?	NOS	71.93	1.51751	70.08	1.51819	68
7 WS_F	ASC435	2002	Honda	CRV	Japan	Lam	WS	Lam/F	Clear	?	NOS	55.21	1.52365	52.65	1.5246	95
8 RRQ	AUM763	2002	Holden	Commodore Executive s/w	Australia	T	RRQ	RRQ	Green	3.42	Float	62.74	1.52057	58.02	1.52231	174
9 WS_B	AUM763	2002	Holden	Commodore Executive s/w	Australia	Lam	WS	Lam/B	Blue/Green	2.27	Float	59.89	1.52194	58.33	1.52251	57
9 WS_F	AUM763	2002	Holden	Commodore Executive s/w	Australia	Lam	WS	Lam/F	Blue/Green	2.28	Float	59.96	1.52191	58.34	1.52251	60
11 WS_F	BKS159	2003	Holden	Ute	Australia	Lam	WS	Lam/F	Clear	2.28	Float	61.41	1.52106	60.09	1.52155	49
12 WS_F	BHD628	2003	Mazda	6	Japan	Lam	WS	Lam/F	Blue/Green	2.11	Float	63.22	1.5204	61.62	1.52099	59
13 RF	BEM205	2003	Holden	Commodore	Australia	T	RF	RF	Green	3.93	Float	63.5	1.5203	59.35	1.52183	153
14 WS_F	BEM205	2003	Holden	Commodore	Australia	Lam	WS	Lam/F	Pale Green	2.13	Float	61.97	1.52117	60.49	1.52172	55

Sheet ID	Registration Number	Year	Make	Model	Country	Lam /non	Pane	Origin	Colour	Width	Float	Match Temp	RI	Match Temp (Post Annealed)	RI (Post Annealed)	Delta RI
14 WS_B	BEM205	2003	Holden	Commodore	Australia	Lam	WS	Lam/B	Pale Green	2.18	Float	61.69	1.52128	59.96	1.52191	63
15 WS_F	BJL112	2003	Toyota	Corolla	Japan	Lam	WS	Lam/F	Pale Green	2.04	Float	63.06	1.52046	60.95	1.52123	77
15 WS_B	BJL112	2003	Toyota	Corolla	Japan	Lam	WS	Lam/B	Pale Green	2.02	Float	62.64	1.52062	60.58	1.52138	76
16 R	BJL112	2003	Toyota	Corolla	Japan	T	Rear	Rear	Green	3.1	Float	66.77	1.51909	62.08	1.52082	173
17 WS_F	BCC368	2003	Audi	Cabriolet	Germany	Lam	WS	Lam/F	Green	2.08	Float	61.14	1.52117	59.79	1.52166	49
17 WS_B	BCC368	2003	Audi	Cabriolet	Germany	Lam	WS	Lam/B	Clear	1.64	Float	61.09	1.52118	59.35	1.52182	64
18 WS_B	CFN600	2004	Toyota	Rav4	Japan	Lam	WS	Lam/B	Green	2.05	Float	66.42	1.51954	63.88	1.52047	93
18 WS_F	CFN600	2004	Toyota	Rav4	Japan	Lam	WS	Lam/F	Green	2.02	Float	65.3	1.51963	63.4	1.52034	71
19 LF	CDD228	2004	Toyota	Rav4	Japan	T	LF	LF	Green	3.93	Float	59.61	1.52172	55.6	1.5232	148
20 WS_F	CBE399	2004	Toyota	Rav4	Japan	Lam	WS	Lam/F	Green	2.05	Float	63.92	1.52046	62.01	1.52116	70
21 RRQ	CBE399	2004	Toyota	Rav4	Japan	T	RRQ	RRQ	Green	3.16	Float	56.36	1.52292	51.86	1.52457	165
22 WS_B	BPZ221	2003	Toyota	Corolla	Japan	Lam	WS	Lam/B	Green	2.04	Float	62.23	1.52109	60.51	1.52171	62
22 WS_F	BPZ221	2003	Toyota	Corolla	Japan	Lam	WS	Lam/F	Green	2.01	Float	62.17	1.5211	60.66	1.52165	55
23 WS_F	BRM806	2003	Mazda	6	Japan	Lam	WS	Lam/F	Pale Green	1.97	Float	64.27	1.52033	62.98	1.5208	47
24 LF	BRM806	2003	Mazda	6	Japan	T	LF	LF	Green	3.92	Float	67.15	1.51927	63.15	1.52074	147
25 LF	BLM778	2003	Holden	Commodore	Australia	T	LF	LF	Pale Green	3.89	Float	64.22	1.52003	59.7	1.5217	167
26 LRQ	BZM651	2004	Ford	Explorer	USA	T	LRQ	LRQ	Green	3.81	Float	65.06	1.52004	60.35	1.52177	173
27 R	ANS574	2002	Suzuki	Grand Vitara	Japan	T	Rear	Rear	Green	3.15	Float	64.28	1.52001	60.64	1.52166	165
28 WS_B	BFC541	2003	Nissan	Navara	Japan	Lam	WS	Lam/B	Blue/Green	2.09	Float	64.35	1.5203	63.64	1.52056	26
28 WS_F	BFC541	2003	Nissan	Navara	Japan	Lam	WS	Lam/F	Blue/Green	2.05	Float	63.69	1.52023	62.7	1.52059	36
29 R	CKE20	2004	Toyota	Corolla	Japan	T	Rear	Rear	Clear	3.09	Float	68.82	1.51866	64.02	1.52042	176
30 R	CHF639	2004	Mitsubishi	Lancer	Japan	T	Rear	Rear	Green	3.12	Float	64.93	1.51977	60.79	1.52129	152
31 LR	BTG796	2004	Toyota	Echo	Japan	T	LR	LR	Green	3.14	Float	56.3	1.52295	51.58	1.52468	173

Sheet ID	Registration Number	Year	Make	Model	Country	Lam /non	Pane	Origin	Colour	Width	Float	Match Temp	RI	Match Temp (Post Annealed)	RI (Post Annealed)	Delta RI
32 LF	CEG512	2004	Mitsubishi	Lancer	Japan	T	LF	LF	Green	3.39	Float	64.75	1.51984	61.23	1.52145	161
33 LF	CWBR1	2004	Holden	Adventra	Unknown	T	LF	LF	Pale Green	3.89	Float	64.26	1.52002	59.26	1.52186	184
35 WS_F	CFP134	2004	Lotus	Elise	England	Lam	WS	Lam/F	Green	2	Float	63.61	1.52026	62.75	1.52057	31
35 WS_B	CFP134	2004	Lotus	Elise	England	Lam	WS	Lam/B	Clear	?	Float	70.29	1.51812	68.99	1.5186	48
36 R	BLW412	2003	Toyota	Corolla	Japan	T	Rear	Rear	Green	3.13	Float	66.77	1.5191	62.63	1.52093	183
37 WS_B	CEG512	2004	Mitsubishi	Lancer	Japan	Lam	WS	Lam/B	Green	2.02	Float	67.21	1.51925	64.59	1.52021	96
37 WS_F	CEG512	2004	Mitsubishi	Lancer	Japan	Lam	WS	Lam/F	Green	2.02	Float	66.65	1.51946	64.27	1.52033	87
38 WS_B	CWBR1	2004	Holden	Adventra	Unknown	Lam	WS	Lam/B	Green	2.27	Float	61.66	1.52097	59.96	1.5216	63
38 WS_F	CWBR1	2004	Holden	Adventra	Unknown	Lam	WS	Lam/F	Green	2.28	Float	61.25	1.52112	59.68	1.5217	58
39 WS_F	BLW412	2003	Toyota	Corolla	Japan	Lam	WS	Lam/F	Clear	2.1	Float	62.95	1.5205	61.8	1.52092	42
40 WS_B	BYZ697	2004	Toyota	Hilux	Japan	Lam	WS	Lam/B	Green	2.13	Float	57.7	1.52243	55.08	1.52339	96
40 WS_F	BYZ697	2004	Toyota	Hilux	Japan	Lam	WS	Lam/F	Green	2.11	Float	57.77	1.52241	55.64	1.52319	78
41 WS_B	BMA931	2003	Honda	CRV	Japan	Lam	WS	Lam/B	Clear	1.97	Float	70.33	1.51779	68.82	1.51834	55
41 WS_F	BMA931	2003	Honda	CRV	Japan	Lam	WS	Lam/F	Green	2.1	Float	54.02	1.52379	52.64	1.52429	50
42 WS_F	ATC467	2003	Mazda	626	Japan	Lam	WS	Lam/F	Blue/Green	2.13	Float	61.04	1.52152	59.05	1.52226	74
43 WS_B	CFF390	2004	Toyota	Landcruiser Prado	Japan	Lam	WS	Lam/B	Green	2.1	Float	63.61	1.52057	61.74	1.52126	69
43 WS_F	CFF390	2004	Toyota	Landcruiser Prado	Japan	Lam	WS	Lam/F	Green	2.2	Float	63.52	1.52061	61.96	1.52118	57
44 R	CFF390	2004	Toyota	Landcruiser Prado	Unknown	T	Rear	Rear	Grey	3.17	Float	66.76	1.51942	62.45	1.521	158
45 R	?	?	Toyota	Echo	Japan	T	Rear	Rear	Green	3.2	Float	56.46	1.52289	51.22	1.52481	192
46 LF	BZD876	2004	Mazda	Bounty	Thailand	T	LF	LF	Pale Green	3.88	Float	70.48	1.51773	66.16	1.51932	159
47 WS_B	BZD876	2004	Mazda	Bounty	Thailand	Lam	WS	Lam/B	Blue/Green	?	NOS	65.38	1.5196	63.76	1.5202	60
47 WS_F	BZD876	2004	Mazda	Bounty	Thailand	Lam	WS	Lam/F	Blue/Green	2.09	Float	65.67	1.5195	64.6	1.52021	71

Sheet ID	Registration Number	Year	Make	Model	Country	Lam /non	Pane	Origin	Colour	Width	Float	Match Temp	RI	Match Temp (Post Annealed)	RI (Post Annealed)	Delta RI
48 WS_B	CGM795	2004	Renault	Megane	France	Lam	WS	Lam/B	Clear	2.07	Float	64.47	1.52026	62.88	1.52084	58
48 WS_F	CGM795	2004	Renault	Megane	France	Lam	WS	Lam/F	Clear	2.12	Float	62.63	1.52093	60.56	1.52169	76
49 WS_B	?	?	Toyota	Echo	Unknown	Lam	WS	Lam/B	Green	1.82	Float	66.13	1.51965	64.3	1.52032	67
49 WS_F	?	?	Toyota	Echo	Unknown	Lam	WS	Lam/F	Green	1.97	Float	65.76	1.51978	64.18	1.52036	58
50 WS_B	CFP243	2004	Holden	Commodore Wagon	Australia	Lam	WS	Lam/B	Green	2.3	Float	62.89	1.52084	60.1	1.52186	102
50 WS_F	CFP243	2004	Holden	Commodore Wagon	Australia	Lam	WS	Lam/F	Green	2.29	Float	55.59	1.52352	54.05	1.52409	57
51 R	?	?	Toyota	Echo	Unknown	T	Rear	Rear	Clear	3.11	Float	56.51	1.52286	51.85	1.52458	172
52 RF	BJY270	2003	Holden	Commodore	Australia	T	RF	RF	Green	3.85	Float	63.7	1.52054	59.87	1.52194	140
53 RF	CAH869	2004	Toyota	Prius	Japan	T	RF	RF	Green	3.84	Float	58	1.52232	53.43	1.524	168
54 WS_B	CAH869	2004	Toyota	Prius	Japan	Lam	WS	Lam/B	Pale Green	2.04	Float	63.06	1.52046	60.58	1.52137	91
54 WS_F	CAH869	2004	Toyota	Prius	Japan	Lam	WS	Lam/F	Pale Green	2.03	Float	62.92	1.52051	61.39	1.52108	57
55 LF	CFP243	2004	Holden	Commodore Wagon	Australia	T	LF	LF	Clear	3.92	Float	64.65	1.52019	59.82	1.52165	146
56 WS_B	BFK598	2003	Audi	A6	Germany	Lam	WS	Lam/B	Green	2.06	Float	64.61	1.51989	62.76	1.52057	68
56 WS_F	BFK598	2003	Audi	A6	Germany	Lam	WS	Lam/F	Green	2.08	Float	64.35	1.51998	62.96	1.5205	52
57 RRQ	BJE587	2003	Mitsubishi	Airtrek	Japan	T	RRQ	RRQ	Green	3.17	Float	67.39	1.51918	62.44	1.521	182
58 WS_B	BJE587	2003	Mitsubishi	Airtrek	Japan	Lam	WS	Lam/B	Clear	?	NOS	61.13	1.52117	59.21	1.52188	71
58 WS_F	BJE587	2003	Mitsubishi	Airtrek	Japan	Lam	WS	Lam/F	Clear	?	NOS	61.14	1.52117	59.42	1.5218	63
59 R	AUL886	2002	Peugeot	206	France	T	Rear	Rear	Green	3.85	Float	66.14	1.51933	61.85	1.5209	157
60 R	CJS295	2004	Daihatsu	Terios	Japan	T	Rear	Rear	Clear	3.19	Float	65.69	1.51949	61.02	1.52121	172
61 RRQ	ALU865	2002	Holden	commodore	Australia	T	RRQ	RRQ	Green	3.85	Float	63.19	1.52041	58.17	1.52226	185
62 LF	?	2004	Holden	Clubsport	Unknown	T	LF	LF	Blue/Green	3.87	Float	64.05	1.52009	59.76	1.52167	158
63 WS_F	CFY817	?	Holden	Astra	Unknown	Lam	WS	Lam/F	Clear	?	NOS	63.39	1.52065	61.47	1.52136	71

Sheet ID	Registration Number	Year	Make	Model	Country	Lam /non	Pane	Origin	Colour	Width	Float	Match Temp	RI	Match Temp (Post Annealed)	RI (Post Annealed)	Delta RI
64 R	BQR305	2003	Holden	Barina	Spain	T	Rear	Rear	Blue/Green	3.54	Float	61.41	1.52106	56.33	1.52294	188
65 WS_B	CJS295	2004	Daihatsu	Terios	Japan	Lam	WS	Lam/B	Blue/Green	1.78	Float	65.32	1.51963	63.6	1.52026	63
65 WS_F	CJS295	2004	Daihatsu	Terios	Japan	Lam	WS	Lam/F	Blue/Green	1.97	Float	65.81	1.51945	64.12	1.52007	62
66 R	ASA740	2002	Holden	Commodore	Australia	T	Rear	Rear	Green	3.35	Float	64.56	1.52022	59.81	1.52197	175
67 WS_B	ALU865	2002	Holden	Commodore	Australia	Lam	WS	Lam/B	Clear	2.03	Float	66.4	1.51923	65.29	1.51964	41
67 WS_F	ALU865	2002	Holden	Commodore	Australia	Lam	WS	Lam/F	Blue	2.02	Float	67.5	1.51914	65.59	1.51984	70
68 WS_B	ASA740	2002	Holden	Commodore Clubsport	Australia	Lam	WS	Lam/B	Pale Green	?	NOS	61.73	1.52127	60.45	1.52173	46
68 WS_F	ASA740	2002	Holden	Commodore Clubsport	Australia	Lam	WS	Lam/F	Pale Green	?	NOS	61.79	1.52124	60.05	1.52188	64
69 WS_B	?	2004	Holden	Clubsport	Australia	Lam	WS	Lam/B	Blue/Green	2.32	Float	61.55	1.52102	59.25	1.52186	84
69 WS_F	?	2004	Holden	Clubsport	Australia	Lam	WS	Lam/F	Blue/Green	2.25	Float	62.62	1.52093	60.97	1.52154	61
70 WS_B	BZA317	2004	Peugeot	206	France	Lam	WS	Lam/B	Clear	2.07	Float	64.25	1.52002	62.68	1.5206	58
70 WS_F	BZA317	2004	Peugeot	206	France	Lam	WS	Lam/F	Clear	2.6	Float	67.89	1.519	66.17	1.51963	63
72 WS_F	CTF393	2002	Hyundai	?	South Korea	Lam	WS	Lam/F	Green	2.1	Float	62.19	1.5211	60.46	1.52173	63
73 WS_B	CPQ128	2003	Mini	Cooper	Germany	Lam	WS	Lam/B	Pale Green	1.55	Float	59.22	1.52187	61.25	1.52112	75
73 WS_F	CPQ128	2003	Mini	Cooper	Germany	Lam	WS	Lam/F	Blue/Green	2.1	Float	60.94	1.52124	59.01	1.52195	71
74 RF	?	2005	Hyundai	?	Unknown	T	RF	RF	Green	3.91	Float	57.04	1.52298	52.97	1.52449	151
75 WS_B	BUL468	2004	Mitsubishi	Colt	Japan	Lam	WS	Lam/B	Clear	1.8	Float	62.67	1.5206	60.61	1.52136	76
75 WS_F	BUL468	2004	Mitsubishi	Colt	Japan	Lam	WS	Lam/F	Pale Green	1.8	Float	62.66	1.5206	60.97	1.52123	63
76 LF	CKZ262	2004	Holden	Commodore	Australia	T	LF	LF	Blue/Green	3.9	Float	64.31	1.52	60	1.52158	158
77 LR	BUL468	2004	Mitsubishi	Colt	Japan	T	LR	LR	Green	3.11	Float	58.08	1.52229	53.1	1.52412	183
78 WS_B	?	2005	Hyundai	?	Unknown	Lam	WS	Lam/B	Pale Blue/Green	2.06	Float	55.28	1.52364	52.48	1.52466	102

Sheet ID	Registration Number	Year	Make	Model	Country	Lam /non	Pane	Origin	Colour	Width	Float	Match Temp	RI	Match Temp (Post Annealed)	RI (Post Annealed)	Delta RI
78 WS_F	?	2005	Hyundai	?	Unknown	Lam	WS	Lam/F	Pale Blue/Green	2.07	Float	54.84	1.52349	53.42	1.52431	82
79 LR	BCN265	2003	Hyundai	Santa Fe	South Korea	T	LR	LR	Blue/Green	3.49	Float	54.72	1.52352	50.23	1.52517	165
80 RR	CMK148	2005	Holden	Commodore	Australia	T	RR	RR	Pale Green	3.85	Float	64.18	1.52005	59.21	1.52188	183
81 WS_B	AZM776	2002	Holden	Rodeo	Japan	Lam	WS	Lam/B	Blue/Green	2.11	Float	64.9	1.51978	63.9	1.52015	37
81 WS_F	AZM776	2002	Holden	Rodeo	Japan	Lam	WS	Lam/F	Blue/Green	2.11	Float	64.83	1.51981	63.65	1.52024	43
82 RF	AZM776	2002	Holden	Rodeo	Japan	T	RF	RF	Green	3.35	Float	66.82	1.51908	62.98	1.52081	173
83 RL	AZM776	2002	Holden	Rodeo	Japan	T	R Canopy	R Canopy	Clear	3.89	Float	68.72	1.5187	64.89	1.5201	140
84 WS_B	AYJ272	2002	Toyota	Landcruiser Prado	Japan	Lam	WS	Lam/B	Green	2.08	Float	61.62	1.52099	59.68	1.5217	71
84 WS_F	AYJ272	2002	Toyota	Landcruiser Prado	Japan	Lam	WS	Lam/F	Green	2.01	Float	62.59	1.52095	60.96	1.52154	59
85 LRQ	AYJ272	2002	Toyota	Landcruiser Prado	Japan	T	LRQ	LRQ	Pale Green	3.43	Float	66.87	1.51906	62.67	1.5206	154
86 RRQ	BLB534	2003	Toyota	Echo	Japan	T	RRQ	RRQ	Green	2.8	Float	56.79	1.52276	52.77	1.52425	149
87 WS_B	BSW575	2003	Holden	Ute	Australia	Lam	WS	Lam/B	Green		NOS	60.79	1.52129	59.13	1.52191	62
87 WS_F	BSW575	2003	Holden	Ute	Australia	Lam	WS	Lam/F	Green	2.24	Float	61.77	1.52125	60.28	1.52179	54
88 RF	BSW575	2003	Holden	Ute	Australia	T	RF	RF	Pale Green	3.83	Float	64.76	1.52015	60.49	1.52172	157
89 R	BZD825	2004	Mazda	6	Japan	T	Rear	Rear	Pale Green	3.07	Float	66.8	1.5194	62.03	1.52115	175
90 WS_B	ANY236	2002	Toyota	Rav4	Japan	Lam	WS	Lam/B	Green	1.99	Float	64.04	1.52042	61.94	1.52119	77
90 WS_F	ANY236	2002	Toyota	Rav4	Japan	Lam	WS	Lam/F	Green	1.96	Float	64.14	1.52038	62.24	1.52108	70
91 WS_B	ASR653	2002	Ford	Courier	Thailand	Lam	WS	Lam/B	Green	2.12	Float	65.28	1.51965	63.19	1.52042	77
91 WS_F	ASR653	2002	Ford	Courier	Thailand	Lam	WS	Lam/F	Green	2.13	Float	66.09	1.51966	64.3	1.52032	66
92 LF	ASR653	2002	Ford	Courier	Thailand	T	LF	LF	Green	3.85	Float	66.75	1.51942	62.4	1.52102	160
93 RF	CHP423	2004	Hyundai	Getz	South	T	RF	RF	Green	3.23	Float	69.24	1.51819	64.66	1.51987	168

Sheet ID	Registration Number	Year	Make	Model	Country	Lam /non	Pane	Origin	Colour	Width	Float	Match Temp	RI	Match Temp (Post Annealed)	RI (Post Annealed)	Delta RI
94 WS_B	CHP423	2004	Hyundai	Getz	South Korea	Lam	WS	Lam/B	Clear	1.9	Float	68.63	1.51941	67.42	1.51886	55
94 WS_F	CHP423	2004	Hyundai	Getz	South Korea	Lam	WS	Lam/F	Green	2.2	Float	63.42	1.52033	62.04	1.52083	50
95 R	CZW829	2005	Toyota	Corolla	Japan	T	Rear	Rear	Pale Green	3.11	Float	66.29	1.51927	62.35	1.52072	145
96 WS_B	CHC650	2004	Nissan	Pulsar	England	Lam	WS	Lam/B	Clear	1.77	Float	67.99	1.51897	66.04	1.51968	71
96 WS_F	CHC650	2004	Nissan	Pulsar	England	Lam	WS	Lam/F	Blue/Green	2.12	Float	66.94	1.51903	66.25	1.51929	26
97 LF	BGB667	2003	Ford	Falcon	Australia	T	LF	LF	Green	4.81	Float	66.59	1.51916	62.76	1.52057	141
98 WS_B	CZK773	2005	Ford	Falcon	Australia	Lam	WS	Lam/B	Pale Green		NOS	63.41	1.52033	62.87	1.52053	20
98 WS_F	CZK773	2005	Ford	Falcon	Australia	Lam	WS	LamF	Green	2.1	Float	63.69	1.52023	62.63	1.52062	39
99 WS_B	CMU320	2002	Mitsubishi	Airtrek	Japan	Lam	WS	Lam/B	Green	2.08	Float	65.35	1.51994	63.39	1.52066	72
99 WS_F	CMU320	2002	Mitsubishi	Airtrek	Japan	Lam	WS	Lam/F	Green	2.08	Float	65.09	1.52003	63.44	1.52063	60
100 RF	BEB275	2003	Toyota	Camry	Australia	T	RF	RF	Green	4.83	Float	64.03	1.52042	59.99	1.5219	148
101 WS_F	BEB275	2003	Toyota	Camry	Australia	Lam	WS	Lam/F	Green	2.01	Float	61.04	1.5212	59.6	1.52173	53
101 WS_B	BEB275	2003	Toyota	Camry	Australia	Lam	WS	Lam/B	Green	2.07	Float	60.99	1.52122	59.54	1.52175	53
102 RRQ	CFA18	2004	Holden	Commodore	Australia	T	RRQ	RRQ	Green	3.36	Float	65.68	1.51981	61.13	1.52149	168
103 WS_F	BPF700	2003	Mazda	6	Japan	Lam	WS	Lam/F	Green	2.01	Float	63.57	1.52059	62.25	1.52107	48
103 WS_B	BPF700	2003	Mazda	6	Japan	Lam	WS	Lam/B	Green	2.02	Float	63.75	1.52052	62.15	1.52111	59
104 LF	ALR208	2002	Suzuki	Ignis	Japan	T	LF	LF	Pale Green	3.13	Float	68.21	1.51888	63.5	1.52061	173
105 WS_F	ALR208	2002	Suzuki	Ignis	Japan	Lam	WS	Lam/F	Green	2.08	Float	61.49	1.52104	59.33	1.52183	79
105 WS_B	ALR208	2002	Suzuki	Ignis	Japan	Lam	WS	Lam/B	Green	2.13	Float	61.26	1.52112	59.7	1.52169	57
106 WS_F	CNQ701	2004	Holden	Clubsport	Australia	Lam	WS	Lam/F	Pale Green	2.25	Float	61.02	1.52121	59.51	1.52176	55
106 WS_B	CNQ701	2004	Holden	Clubsport	Australia	Lam	WS	Lam/B	Pale Green	2.22	Float	61.14	1.52117	59.89	1.52162	45

Sheet ID	Registration Number	Year	Make	Model	Country	Lam /non	Pane	Origin	Colour	Width	Float	Match Temp	RI	Match Temp (Post Annealed)	RI (Post Annealed)	Delta RI
107 RR	CNQ701	2004	Holden	Clubsport	Australia	T	RR	RR	Green	3.93	Float	65.01	1.52005	60.74	1.52163	158
108 WS_F	CUU257	2005	Toyota	Corolla	Japan	Lam	WS	Lam/F	Green	2.07	Float	63.44	1.52032	61.67	1.52097	65
109 R	CUU257	2005	Toyota	Corolla	Japan	T	Rear	Rear	Green	3.08	Float	66.94	1.51903	62.53	1.52065	162
110 R	BEQ379	2003	Holden	Commodore	Australia	T	Rear	Rear	Green	3.4	Float	63.72	1.52022	59.47	1.52178	156
111 RF	DDR464	2006	Ford	Focus	South Africa	T	RF	RF	Green	3.82	Float	64.38	1.52029	60.08	1.52187	158
112 WS_F	BSJ633	2003	Hyundai	Elantra	South Korea	Lam	WS	Lam/F	Clear	2.06	Float	64.55	1.52023	62.43	1.52101	78
112 WS_B	BSJ633	2003	Hyundai	Elantra	South Korea	Lam	WS	Lam/B	Clear	2.04	Float	64.99	1.52006	62.76	1.52088	82
113 WS_F	DBZ750	2005	Toyota	Corolla	Japan	Lam	WS	Lam/F	Green	1.99	Float	65.5	1.51956	63.89	1.52015	59
113 WS_B	DBZ750	2005	Toyota	Corolla	Japan	Lam	WS	Lam/B	Green	2.01	Float	65.89	1.51942	63.92	1.52014	72
114 R	CSL311	2005	Ford	Transit	England	T	Rear	Rear	Pale Green	3.26	Float	62.86	1.52085	58.05	1.52262	177
115 RF	CSM484	2005	BMW		Germany	T	RF	RF	Pale Green	3.84	Float	67.5	1.51915	63.2	1.52072	157
116 RF	BSJ633	2003	Hyundai	Elantra	South Korea	T	RF	RF	Green	3.49	Float	58.21	1.52256	53.88	1.52415	159
117 R	CPC999	2005	Toyota	Corolla	Japan	T	Rear	Rear	Blue/Green	3.13	Float	66.31	1.51926	62.05	1.52083	157
118 WS_F	CPC999	2005	Toyota	Corolla	Japan	Lam	WS	Lam/F	Green	2.02	Float	67.21	1.51925	64.9	1.5201	85
118 WS_B	CPC999	2005	Toyota	Corolla	Japan	Lam	WS	Lam/B	Blue/Green	1.97	Float	66.92	1.51935	64.88	1.52011	76
119 RR	CDQ698	2004	Holden	Commodore	Australia	T	RR	RR	Green	3.39	Float	64.7	1.52017	60.47	1.52173	156
120 R	DKN437	2006	Holden	Commodore	Australia	T	Rear	Rear	Pale Green	3.37	Float	66.6	1.51916	62.19	1.52078	162
121 LF	BZA736	2004	Holden	Commodore Ute	Australia	T	LF	LF	Clear	3.75	Float	65.03	1.52005	60.54	1.5217	165
122 WS_F	DKN437	2006	Holden	Commodore	Australia	Lam	WS	Lam/F	Pale Blue/Green	1.58	Float	63.87	1.52016	62.39	1.5207	54
122 WS_B	DKN437	2006	Holden	Commodore	Australia	Lam	WS	Lam/B	Pale Green	1.61	Float	64.7	1.52017	63.23	1.52071	54

Sheet ID	Registration Number	Year	Make	Model	Country	Lam /non	Pane	Origin	Colour	Width	Float	Match Temp	RI	Match Temp (Post Annealed)	RI (Post Annealed)	Delta RI
123 RRQ	CNA302	2003	Holden	Commodore Clubsport	Australia	T	RRQ	RRQ	Pale Green	3.75	Float	64.52	1.52024	59.99	1.5219	166
124 RF	DTC875	2006	Ford	Territory	Unknown	T	RF	RF	Green	3.79	Float	67.52	1.51914	63.04	1.52078	164
125 WS_B	DTC875	2006	Ford	Territory	Unknown	Lam	WS	Lam/B	Green	2.06	Float	63.89	1.52048	61.96	1.52118	70
125 WS_F	DTC875	2006	Ford	Territory	Unknown	Lam	WS	Lam/F	Green	2.05	Float	63.7	1.52022	63.18	1.52073	51
126 R	DAM709	2005	Mitsubishi	Colt	Japan	T	Rear	Rear	Grey	3.12	Float	64.97	1.51976	60.83	1.5216	184
127 R	CPM600	2005	Nissan	Primera	Japan	T	Rear	Rear	Green	3.18	Float	70.52	1.51803	65.64	1.51983	180
128 WS_F	BPJ407	2003	Holden	Astra	Germany	Lam	WS	Lam/F	Blue/Green	2.1	Float	65.41	1.51991	63.31	1.52068	77
129 LRQ	DFN777	2006	Audi		Germany	T	LRQ	LRQ	Green	2.85	Float	62.22	1.52077	57.26	1.5226	183
130 WS_F	S6V10	2006	Audi	S6 V10	Germany	Lam	WS	Lam/F	Green	2.13	Float	69.51	1.5184	67.33	1.51888	48
130 WS_B	S6V10	2006	Audi	S6 V10	Germany	Lam	WS	Lam/B	Clear	2.12	Float	68.67	1.5184	67.7	1.51907	67
131 LR	S6V10	2006	Audi	S6 V10	Germany	T	LR	LR	Green	3.13	Float	54.37	1.52365	50.15	1.52521	156
132 WS_F	CAQ640	2004	Holden	Commodore	Australia	Lam	WS	Lam/F	Green	2.23	Float	62.69	1.52091	61.03	1.52152	61
132 WS_B	CAQ640	2004	Holden	Commodore	Australia	Lam	WS	Lam/B	Green	2.24	Float	61.88	1.5209	59.93	1.52161	71
133 R	DPP697	2006	Ford	Focus	Germany	T	Rear	Rear	Green	3.21	Float	60.93	1.52125	55.69	1.5228	155
134 WS_F	CKZ273	2002	Nissan	Navara	Japan	Lam	WS	Lam/F	Green	2.34	Float	63.26	1.52039	61.83	1.52091	52
134 WS_B	CKZ273	2002	Nissan	Navara	Japan	Lam	WS	Lam/B	Green	2	Float	65.53	1.51987	63.99	1.52043	56
135 LF	CKZ273	2002	Nissan	Navara	Japan	T	LF	LF	Green	3.35	Float	66.77	1.51941	61.42	1.52138	197
136 WS_F	DKJ849	2006	Ford	Fiesta	Belgium	Lam	WS	Lam/F	Blue/Green	2.08	Float	62.61	1.52094	60.71	1.52164	70
136 WS_B	DKJ849	2006	Ford	Fiesta	Belgium	Lam	WS	Lam/B	Blue/Green	2.08	Float	62.73	1.5209	60.7	1.52164	74
137 R	DES851	2006	Hyundai	Getz	South Korea	T	Rear	Rear	Pale Green	3.23	Float	68.8	1.51834	64.67	1.51986	152
138 WS_F	DEY935	2006	Kia	Sportage	South Korea	Lam	WS	Lam/F	Pale Green	2.09	Float	53.86	1.52416	52.25	1.52475	59

Sheet ID	Registration Number	Year	Make	Model	Country	Lam /non	Pane	Origin	Colour	Width	Float	Match Temp	RI	Match Temp (Post Annealed)	RI (Post Annealed)	Delta RI
138 WS_B	DEY935	2006	Kia	Sportage	South Korea	Lam	WS	Lam/B	Clear	1.73	Float	54.02	1.5241	52.11	1.5248	70
139 WS_F	CHJ850	2004	Toyota	Hilux	Japan	Lam	WS	Lam/F	Clear	?	NOS	64.61	1.52021	62.91	1.52083	62
139 WS_B	CHJ850	2004	Toyota	Hilux	Japan	Lam	WS	Lam/B	Clear	?	NOS	64.61	1.51989	62.13	1.52081	92
140 WS_F	BQK185	2003	Mitsubishi	Lancer	Japan	Lam	WS	Lam/F	Green	2.11	Float	63.87	1.52048	62.34	1.52104	56
140 WS_B	BQK185	2003	Mitsubishi	Lancer	Japan	Lam	WS	Lam/B	Green	2.11	Float	63.06	1.52046	61.6	1.52099	53
141 RF	BQK185	2003	Mitsubishi	Lancer	Japan	T	RF	RF	Pale Green	3.35	Float	66.03	1.51969	61.67	1.52129	160
142 WS_F	AQD743	2002	Holden	VU Ute	Australia	Lam	WS	Lam/F	Green	2.5	Float	59.8	1.52166	58.31	1.5222	54
142 WS_B	AQD743	2002	Holden	VU Ute	Australia	Lam	WS	Lam/B	Green	2.07	Float	59.26	1.52186	58.09	1.52229	43
143 RF	AQD743	2002	Holden	VU Ute	Australia	T	RF	RF	Green	3.94	Float	62.22	1.52077	57.52	1.52249	172
144 RRQ	AQD743	2002	Holden	VU Ute	Australia	T	RRQ	RRQ	Green	2.44	Float	63.4	1.52065	61.89	1.5212	144
145 WS_F	DDJ153	2006	Toyota	Corolla	Japan	Lam	WS	Lam/F	Green	1.97	Float	65.76	1.51947	63.59	1.52026	79
145 WS_B	DDJ153	2006	Toyota	Corolla	Japan	Lam	WS	Lam/B	Green	2.02	Float	65.85	1.51944	63.98	1.52012	68
146 WS_F	SPLTNZ	2002	Nissan	March	Unknown	Lam	WS	Lam/F	Green	1.99	Float	65.63	1.51983	64.04	1.52041	58
146 WS_B	SPLTNZ	2002	Nissan	March	Unknown	Lam	WS	Lam/B	Green	1.77	Float	65.77	1.51978	63.93	1.52046	68
147 WS_F	CRF413	2002	Holden	VX Commodore	Australia	Lam	WS	Lam/F	Green	2.27	Float	58.18	1.52257	59.12	1.52223	34
147 WS_B	CRF413	2002	Holden	VX Commodore	Australia	Lam	WS	Lam/B	Green	2.28	Float	59.47	1.52178	57.87	1.52237	59
148 WS_F	DMN248	2006	Holden	Barina	South Korea	Lam	WS	Lam/F	Green	2.15	Float	64.87	1.51979	63.85	1.52017	38
148 WS_B	DMN248	2006	Holden	Barina	South Korea	Lam	WS	Lam/B	Clear	2.06	Float	63.37	1.52066	62.22	1.52108	42
149 WS_F	ALH449	2002	Ford	Mondeo	Belgium	Lam	WS	Lam/F	Blue/Green	2.05	Float	62.86	1.52085	61.67	1.52128	43
149 WS_B	ALH449	2002	Ford	Mondeo	Belgium	Lam	WS	Lam/B	Green	2.04	Float	63.28	1.5207	61.77	1.52125	55
150 WS_F	CJF699	2004	Holden	Rodeo	Thailand	Lam	WS	Lam/F	Green	1.99	Float	66.69	1.51944	64.84	1.52012	68

Sheet ID	Registration Number	Year	Make	Model	Country	Lam /non	Pane	Origin	Colour	Width	Float	Match Temp	RI	Match Temp (Post Annealed)	RI (Post Annealed)	Delta RI
150 WS_B	CJF699	2004	Holden	Rodeo	Thailand	Lam	WS	Lam/B	Green	2.05	Float	66.08	1.51935	64.21	1.52004	69
151 RF	CJF699	2004	Holden	Rodeo	Thailand	T	RF	RF	Pale Green	3.34	Float	68.7	1.51839	63.97	1.52012	173
152 WS_F	MUMSZ1	2003	Toyota	Hilux	Japan	Lam	WS	Lam/F	Pale Green	2.01	Float	62.7	1.52059	61.16	1.52116	57
152 WS_B	MUMSZ1	2003	Toyota	Hilux	Japan	Lam	WS	Lam/B	Pale Green	2.04	Float	63.89	1.52047	61.68	1.52128	81
153 WS_F	DFT275	2006	Toyota	Hiace	Japan	Lam	WS	Lam/F	Blue/Green	2.01	Float	63.97	1.52012	62.15	1.52079	67
153 WS_B	DFT275	2006	Toyota	Hiace	Japan	Lam	WS	Lam/B	Green? (black backing)	2.05	Float	63.18	1.52041	60.43	1.52143	102
154 RF	DDJ153	2006	Toyota	Corolla	Japan	T	RF	RF	Green	3.49	Float	68.01	1.51863	63.6	1.52026	163
155 WS_F	DEQ185	2006	Kia	K2700	South Korea	Lam	WS	Lam/F	Blue/Green	2.09	Float	52.81	1.52424	50.88	1.52494	70
155 WS_B	DEQ185	2006	Kia	K2700	South Korea	Lam	WS	Lam/B	Blue/Green	2.11	Float	53.37	1.52403	51.98	1.52485	82
156 WS_F	DKA49	2006	Ford	Mondeo	Belgium	Lam	WS	Lam/F	Green	2.07	Float	57.32	1.52257	56.17	1.52299	42
156 WS_B	DKA49	2006	Ford	Mondeo	Belgium	Lam	WS	Lam/B	Green	2.05	Float	57.1	1.52265	56.5	1.52287	22
157 WS_F	DUQ622	2006	Toyota	Prado	Japan	Lam	WS	Lam/F	Green	2.22	Float	63.69	1.52023	62.03	1.52083	60
157 WS_B	DUQ622	2006	Toyota	Prado	Japan	Lam	WS	Lam/B	Green	2.21	Float	63.68	1.52055	62.24	1.52108	53
158 LF	DUQ622	2006	Toyota	Prado	Japan	T	LF	LF	Green	4.38	Float	63.36	1.52066	59.62	1.52204	138
159 WS_F	CS360	2003	Ferrari	360	Italy	Lam	WS	Lam/F	Blue/Green	2.07	Float	64.14	1.52037	62.31	1.52105	68
159 WS_B	CS360	2003	Ferrari	360	Italy	Lam	WS	Lam/B	Clear	1.59	Float	65.05	1.51973	62.97	1.52049	76
160 LRQ	CS360	2003	Ferrari	360	Italy	T	LRQ	LRQ	Pale Green	3.18	Float	62.49	1.52067	57.49	1.52251	184
161 WS_F	CRB356	2005	Ford	Territory	Thailand	Lam	WS	Lam/F	Clear	?	NOS	61.28	1.52111	59.55	1.52175	64
161 WS_B	CRB356	2005	Ford	Territory	Thailand	Lam	WS	Lam/B	Clear	?	NOS	61.17	1.52115	59.74	1.52168	53
162 RRQ	CRB356	2005	Ford	Territory	Thailand	T	RRQ	RRQ	Green	3.96	Float	67.68	1.51908	63.65	1.52056	148
167 WS_F	DLP420	2004	Dodge	RAM 2500	USA	Lam	WS	Lam/F	Blue/Green	2.21	Float	63.9	1.52015	62.4	1.5207	55

Sheet ID	Registration Number	Year	Make	Model	Country	Lam /non	Pane	Origin	Colour	Width	Float	Match Temp	RI	Match Temp (Post Annealed)	RI (Post Annealed)	Delta RI
167 WS_B	DLP420	2004	Dodge	RAM 2500	USA	Lam	WS	Lam/B	Blue/Green	2.21	Float	63.57	1.52027	62.55	1.52065	38
168 LRQ	CJE800	2004	Nissan	Pulsar	England	T	LRQ	LRQ	Green	3.14	Float	66	1.51969	61.39	1.52139	170
169 R	CJE800	2004	Nissan	Pulsar	England	T	Rear	Rear	Green	3.13	Float	64.64	1.52019	60.33	1.52178	159
170 WS_F	BLM778	2003	Holden	Commodore	Australia	Lam	WS	Lam/F	Blue/Green	2.26	Float	62.39	1.52102	60.85	1.52159	57
170 WS_B	BLM778	2003	Holden	Commodore	Australia	Lam	WS	Lam/B	Clear	1.47	Float	62.03	1.52115	60.7	1.52164	49
171 WS_F	BZM651	2004	Ford	Explorer	USA	Lam	WS	Lam/F	Green	3.15	Float	64.11	1.52007	62.57	1.52064	57
171 WS_B	BZM651	2004	Ford	Explorer	USA	Lam	WS	Lam/B	Green	2.15	Float	64.92	1.52009	64.56	1.52022	13
172 WS_F	CCW390	2004	Mazda	Mazda3	Japan	Lam	WS	Lam/F	Blue/Green	1.96	Float	65.39	1.51992	64.39	1.52028	36
172 WS_B	CCW390	2004	Mazda	Mazda3	Japan	Lam	WS	Lam/B	Blue/Green	1.97	Float	66.12	1.51965	64.32	1.52031	66
173 WS_B	CYF242	2005	Toyota	Echo	Japan	Lam	WS	Lam/B	Green	1.86	Float	64.21	1.52003	61.95	1.52087	84
173 WS_F	CYF242	2005	Toyota	Echo	Japan	Lam	WS	Lam/F	Green	2	Float	66.61	1.51947	64.74	1.52016	69
174 WS_B	CME430	2005	Hyundai	Tucson	South Korea	Lam	WS	Lam/B	Blue/Green	2.14	Float	55.85	1.52343	53.07	1.52413	70
174 WS_F	CME430	2005	Hyundai	Tucson	South Korea	Lam	WS	Lam/F	Blue/Green	2.14	Float	55.76	1.52346	54	1.5241	64
175 RF	?	2006	Toyota	Hilux	Unknown	T	RF	RF	Green	3.48	Float	68.87	1.51864	64.44	1.52027	163

6.2 Plackett-Burman run sequence

Standard Order	Run Order	Spot Diameter (um)	Laser Power (%)	Carrier Gas - He (ml/min)	Nebuliser Gas - Ar (ml/min)	Frequency (Hz)	Ablation time (sec)	Depth (um)
Day 1								
17	1	60	50	0.9	0.6	8	60	5
28	2	60	90	1	0.65	8	50	7
25	3	60	50	0.9	0.65	10	50	7
12	4	60	50	1	0.6	10	60	7
20	5	50	50	0.9	0.6	8	50	5
35	6	50	50	0.9	0.65	8	60	5
21	7	60	50	1	0.65	8	50	5
14	8	50	50	1	0.6	10	50	7
5	9	60	50	0.9	0.65	10	50	7
29	10	50	90	1	0.65	10	50	5
23	11	50	90	1	0.6	10	60	5
10	12	60	50	1	0.65	10	60	5
36	13	50	50	0.9	0.6	10	50	7
6	14	60	90	0.9	0.6	10	60	5
8	15	60	90	1	0.65	8	50	7
22	16	60	90	0.9	0.65	10	50	5
18	17	60	90	0.9	0.6	8	50	7
13	18	50	90	0.9	0.65	8	60	7
16	19	50	50	0.9	0.6	10	50	7
11	20	50	90	0.9	0.65	10	60	7

Standard Order	Run Order	Spot Diameter (um)	Laser Power (%)	Carrier Gas - He (ml/min)	Nebuliser Gas - Ar (ml/min)	Frequency (Hz)	Ablation time (sec)	Depth (um)
Day 2								
40	21	50	50	0.9	0.6	8	50	5
24	22	50	50	1	0.65	8	60	7
3	23	50	90	1	0.6	10	60	5
2	24	60	90	0.9	0.65	10	50	5
31	25	50	90	0.9	0.65	10	60	7
27	26	60	90	1	0.6	8	60	7
33	27	50	90	0.9	0.65	8	60	7
30	28	60	50	1	0.65	10	60	5
9	29	50	90	1	0.65	10	50	5
19	30	50	90	1	0.6	8	50	5
38	31	60	90	0.9	0.6	8	50	7
26	32	60	90	0.9	0.6	10	60	5
37	33	60	50	0.9	0.6	8	60	5
4	34	50	50	1	0.65	8	60	7
1	35	60	50	1	0.65	8	50	5
15	36	50	50	0.9	0.65	8	60	5
34	37	50	50	1	0.6	10	50	7
32	38	60	50	1	0.6	10	60	7
39	39	50	90	1	0.6	8	50	5
7	40	60	90	1	0.6	8	60	7

6.3 Main effects plots for Plackett-Burman test

The individual main effects plots for each element are located on the electronic media.

6.4 Normal plot of the standardised effects for Plackett-Burman test

The individual normal plot of the standardised effects for each element are located on the electronic media.

6.5 Quality control charts using NIST 612 as calibration standard

The individual control charts for each element are located on the electronic media.

6.6 Quality control charts using FGS 2 as calibration standard

The individual control charts for each element are located on the electronic media.

6.7 Contour plots for Toyota Corolla side window

The contour plots for the Toyota Corolla side window are located on the electronic media.

6.8 Surface plots for Toyota Corolla side window

The surface plots for the Toyota Corolla side window are located on the electronic media.

6.9 Contour plots for Mitsubishi Cedia side window

The contour plots for the Mitsubishi Cedia side window are located on the electronic media.

6.10 Contour plots for Holden Commodore windscreen

The contour plots for the Holden Commodore windscreen are located on the electronic media.

6.11 Surface plots for Mitsubishi Cedia side window

The surface plots for the Mitsubishi Cedia side window are located on the electronic media.

6.12 Surface plots for Holden Commodore windscreen

The surface plots for the Holden Commodore windscreen are located on the electronic media.

6.13 Summary of range overlap method

The following table shows the samples that were indistinguishable using the range overlap method and lists the samples which matched each recovered sample.

Elemental Composition

- The samples being compared to the database are called the recovered sample; the samples in the database are referred to as the control samples.
- If the front pane matched the back pane of a windscreen (shown in bold type) the back pane was not included in the tally of samples that matched that windscreen, and vice versa. In addition, if both the front and back panes matched another sample, they were only counted as one sample (shown underlined).
- In cases where indistinguishable front or back panes had a different relativity to other samples, the pane that matched more samples was used for analysis of the type II error. The other sample has an *.
- The percentage value for elemental composition is for the 204 individual samples due to the removal of 40 windscreen samples.

RI

- The samples were separated into laminated and tempered groups before the RI ranges were compared.
- The percentage values for RI matches are for laminated (162 samples) or tempered (82 samples), not the total database.

Sheet ID (Recovered sample)	**Country of origin**	**Samples that match RI**	**WS pairs**	**Samples that match elemental composition**	**Sheet ID of samples which are indistinguishable by elemental composition (Control samples):**						
1 LF	Australia	14 (16.47 %)		8 (3.92 %)	13	42F	66	87F&B	110	120	123
					132F&B						
2 WS_B	Australia	3 (1.85 %)	P	0							
2 WS_F	Australia	32 (19.75 %)	P	0							
3 RR	Japan	6 (7.05 %)		0							
4 LF	Japan	20 (23.53 %)		0							
5 RF	Japan	22 (25.88 %)		0							
6 WS_B	Japan	20 (12.35 %)	**P**	*****	**6F**						
6 WS_F	Japan	7 (4.32 %)	**P**	**0**	**6B**						
7 WS_B	Japan	0	P	0							
7 WS_F	Japan	6 (3.70 %)	P	0							
8 RRQ	Australia	8 (9.41 %)		0							
9 WS_B	Australia	4 (2.7 %)	**P**	*****	**9F**						
9 WS_F	Australia	5 (3.09 %)	**P**	**0**	**9B**						
11 WS_F	Australia	37 (22.84 %)		9 (4.41 %)	14F	38F&B	52	62	66	68F&B	69B
					122B	161F					
12 WS_F	Japan	42 (25.93 %)		0							

13 RF	Australia	17 (20.0 %)		11 (5.39 %)	1	42	66	68F	69F	87F&B	101F&B
					122	123	132F&B	144			
14 WS_F	Australia	32 (19.75 %)	**P**	**6 (2.94 %)**	11	**14B**	42F	69F	76	107	121
14 WS_B	Australia	25 (15.43 %)	**P**	*		**14F**					
15 WS_F	Japan	41 (25.30 %)	P	0							
15 WS_B	Japan	29 (17.90 %)	P	0							
16 R	Japan	15 (17.65 %)		0							
17 WS_F	Germany	32 (19.75 %)	P	0							
17 WS_B	Germany	32 (19.75 %)	P	0							
18 WS_B	Japan	25 (15.43 %)	P	0							
18 WS_F	Japan	26 (16.05 %)	P	0							
19 LF	Japan	0		0							
20 WS_F	Japan	41 (25.30 %)		0							
21 RRQ	Japan	5 (5.88 %)		0							
22 WS_B	Japan	37 (22.84 %)	P	0							
22 WS_F	Japan	36 (22.22 %)	P	0							
23 WS_F	Japan	37 (22.84 %)		0							
24 LF	Japan	19 (22.35 %)		0							
25 LF	Australia	19 (22.35 %)		0							
26 LRQ	USA	20 (23.53 %)		0							
27 R	Japan	21 (24.70 %)		0							
28 WS_B	Japan	38 (23.46 %)	P	0							

28 WS_F	Japan	37 (22.84 %)	P	0							
29 R	Japan	5 (5.88 %)		0							
30 R	Japan	9 (10.59 %)		0							
31 LR	Japan	5 (5.88 %)		0							
32 LF	Japan	15 (17.65 %)		0							
33 LF	Unknown	20 (23.53 %)		0							
35 WS_F	England	38 (23.46 %)	P	1 (0.49 %)	171F						
35 WS_B	England	1 (0.62 %)	P	0							
36 R	Japan	15 (17.65 %)		0							
37 WS_B	Japan	18 (11.11 %)	P	1 (0.49 %)	172F						
37 WS_F	Japan	23 (14.20 %)	P	0							
38 WS_B	Australia	31 (19.14 %)	**P**	**7 (3.43 %)**	11F	**38F**	61	62	69B	80	122B
					161F						
38 WS_F	Australia	35 (21.60 %)	**P**	*****	11F	**38B**		62	69B	80	
39 WS_F	Japan	35 (21.60 %)	P	0							
40 WS_B	Japan	4 (2.7 %)	P	0							
40 WS_F	Japan	4 (2.7 %)	P	0							
41 WS_B	Japan	0	P	0							
41 WS_F	Japan	3 (1.85 %)	P	0							
42 WS_F	Japan	4 (2.7 %)		5 (2.45 %)	1	13	14B	66	132B		
43 WS_B	Japan	31 (19.14 %)	P	0							
43 WS_F	Japan	29 (17.90 %)	P	0							

44 R	Unknown	9 (10.59 %)		0							
45 R	Japan	5 (5.88 %)		0							
46 LF	Thailand	0		0							
47 WS_B	Thailand	27 (16.67 %)	P	0							
47 WS_F	Thailand	23 (14.20 %)	P	0							
48 WS_B	France	38 (23.46 %)	P	0							
48 WS_F	France	29 (17.90 %)	P	0							
49 WS_B	Unknown	27 (16.67 %)	P	1 (0.49 %)	65B						
49 WS_F	Unknown	25 (15.43 %)	P	0							
50 WS_B	Australia	24 (14.81 %)	**P**	*	**50F**	106F&B					
50 WS_F	Australia	5 (3.09 %)	**P**	**1 (0.49 %)**	**50B**	106F&B					
51 R	Unknown	5 (5.88 %)		0							
52 RF	Australia	10 (11.76 %)		7 (3.43 %)	11	66	68F&B	69F&B	80	101B	122B
53 RF	Japan	2 (2.35 %)		0							
54 WS_B	Japan	41 (25.30 %)	**P**	*	**54F**						
54 WS_F	Japan	35 (21.60 %)	**P**	**0**	**54B**						
55 LF	Australia	22 (25.88 %)		0							
56 WS_B	Germany	24 (14.81 %)	**P**	*	**56F**						
56 WS_F	Germany	29 (17.90 %)	**P**	**0**	**56B**						
57 RRQ	Japan	18 (21.18 %)		0							
58 WS_B	Japan	32 (19.75 %)	**P**	*	**58F**						
58 WS_F	Japan	32 (19.75 %)	**P**	**0**	**58B**						

59 R	France	17 (20.0 %)		0							
60 R	Japan	10 (11.76 %)		0							
61 RRQ	Australia	14 (16.47 %)		2 (0.98 %)	38B	161F					
62 LF	Unknown	20 (23.53 %)		9 (4.41 %)	11	38F&B	66	68F&B	69F&B	120	122F
					144	161B					
63 WS_F	Unknown	28 (17.28 %)		0							
64 R	Spain	3 (3.53 %)		0							
65 WS_B	Japan	26 (16.05 %)	P	1 (0.49 %)	49B						
65 WS_F	Japan	23 (14.20 %)	P	0							
66 R	Australia	22 (25.88 %)		17 (8.33 %)	1	11	13	42F	52	62	68F&B
					69F&B	87F&B	101F&B	102	110	120	122F&B
					123	132F&B	144				
67 WS_B	Australia	17 (10.49 %)	**P**	*****	**67F**						
67 WS_F	Australia	10 (6.17 %)	**P**	**0**	**67B**						
68 WS_B	Australia	27 (16.67 %)	**P**	*****	11	52	62	66	**68F**	69F	87F&B
					101F	110	120	122F	123		
68 WS_F	Australia	27 (16.67 %)	**P**	**13 (6.37 %)**	11	13	52	62	66	**68B**	69F&B
					87F&B	101F&B	102	110	120	122F&B	123
69 WS_B	Australia	35 (21.60 %)	**P**	*	11	38F&B	52	62	66	68F	**69F**
					76	80	120	122F	144	161	
69 WS_F	Australia	29 (17.90 %)	**P**	12 (5.88 %)	13	14F	52	62	66	68F&B	**69B**
					76	87F	101F&B	120	121	161F&B	

70 WS_B	France	31 (19.14 %)	P	0						
70 WS_F	France	7 (4.32 %)	P	0						
72 WS_F	South Korea	36 (22.22 %)		0						
73 WS_B	Germany	5 (3.09 %)	P	0						
73 WS_F	Germany	27 (16.67 %)	P	0						
74 RF	Unknown	5 (5.88 %)		0						
75 WS_B	Japan	29 (17.90 %)	P	0						
75 WS_F	Japan	29 (17.90 %)	P	0						
76 LF	Australia	21 (24.70 %)		8 (3.92 %)	14F 161B	68F&B	102	110	119	122	132
77 LR	Japan	1 (1.18 %)		0						
78 WS_B	Unknown	6 (3.70 %)	P	0						
78 WS_F	Unknown	5 (3.09 %)	P	1 (0.49 %)	174F&B					
79 LR	South Korea	1 (1.18 %)		0						
80 RR	Australia	21 (24.70 %)		4 (1.96 %)	38F&B	52	69B	161F		
81 WS_B	Japan	25 (15.43 %)	P	0						
81 WS_F	Japan	25 (15.43 %)	P	0						
82 RF	Japan	15 (17.65 %)		0						
83 RL	Japan	5 (5.88 %)		0						
84 WS_B	Japan	33(20.37 %)	P	0						

84 WS_F	Japan	30 (18.52 %)	P	0							
85 LRQ	Japan	14 (16.47 %)		0							
86 RRQ	Japan	6 (7.05 %)		0							
87 WS_B	Australia	25 (15.43 %)	**P**	*	1	13	66	68F&B	69F	**87F**	101F&B
					102	110	122F&B	123	161B		
87 WS_F	Australia	26 (16.05 %)	**P**	12 (5.88 %)	1	13	66	68F&B	69F	**87B**	101F&B
					110	120	121	122F&B	123	132B	144
					161B						
88 RF	Australia	20 (23.53 %)		0							
89 R	Japan	12 (14.12 %)		0							
90 WS_B	Japan	41 (25.30 %)	**P**	*	**90F**						
90 WS_F	Japan	41 (25.30 %)	**P**	0	**90B**						
91 WS_B	Thailand	27 (16.67 %)	**P**	*	**91F**						
91 WS_F	Thailand	28 (17.28 %)	**P**	0	**91B**						
92 LF	Thailand	9 (10.59 %)		0							
93 RF	South Korea	3 (3.53 %)		0							
94 WS_B	South Korea	23 (14.20 %)	P	0							
94 WS_F	South Korea	37 (22.84 %)	P	0							

95 R	Japan	19 (22.35 %)		0							
96 WS_B	England	4 (2.7 %)	P	0							
96 WS_F	England	7 (4.32 %)	P	0							
97 LF	Australia	16 (9.88 %)		0							
98 WS_B	Australia	37 (22.84 %)	**P**	*	**98F**						
98 WS_F	Australia	37 (22.84 %)	**P**	0	**98B**						
99 WS_B	Japan	23 (14.20 %)	**P**	*	**99F**						
99 WS_F	Japan	31 (19.14 %)	**P**	0	**99B**						
100 RF	Australia	15 (17.65 %)		0							
101 WS_F	Australia	29 (17.90 %)	**P**	*	13	66	68F&B	69F	87F&B	**101F**	102
					110	122F	123	144			
101 WS_B	Australia	28 (17.28 %)	**P**	11 (5.39 %)	13	52	66	68F	69F	87F&B	**101B**
					120	122F	123	161B			
102 RRQ	Australia	14 (16.47 %)		14 (6.86 %)	66	69B	76	87F&B	101F	110	120
					121	122F&B	123	125F&B	125B	132B	161B
103 WS_F	Japan	28 (17.28 %)	**P**	*	**103B**						
103 WS_B	Japan	33(20.37 %)	**P**	0	**103F**						
104 LF	Japan	10 (11.76 %)		0							
105 WS_F	Japan	37 (22.84 %)	**P**	*	**105B**						
105 WS_B	Japan	35 (21.60 %)	**P**	0	**105F**						
106 WS_F	Australia	28 (17.28 %)	**P**	*	50F&B	**106B**					

106 WS_B	Australia	32 (19.75 %)	**P**	1 (0.49 %)	50F&B	**106F**					
107 RR	Australia	21 (24.70 %)		1 (0.49 %)	14F						
108 WS_F	Japan	38 (23.46 %)		0							
109 R	Japan	14 (16.47 %)		0							
110 R	Australia	22 (25.88 %)		13 (6.37 %)	1	66	68F&B	76	87F&B	101F	102
					120	121	122F&B	123	132F&B	161B	
111 RF	South Africa	18 (21.18 %)		0							
112 WS_F	South Korea	37 (22.84 %)	P	0							
112 WS_B	South Korea	28 (17.28 %)	P	0							
113 WS_F	Japan	26 (16.05 %)	**P**	*	**113B**	145F&B					
113 WS_B	Japan	23 (14.20 %)	**P**	1 (0.49 %)	**113F**	145F&B					
114 R	England	6 (7.05 %)		0							
115 RF	Germany	15 (17.65 %)		0							
116 RF	South Korea	2 (2.35 %)		0							
117 R	Japan	19 (22.35 %)		0							
118 WS_F	Japan	18 (11.11 %)	**P**	*	**118B**						
118 WS_B	Japan	18 (11.11 %)	**P**	0	**118F**						
119 RR	Australia	22 (25.88 %)		2 (0.98 %)	76	121					

120 R	Australia	16 (14.11 %)		10 (4.90 %)	62	66	68F&B	69F&B	87F	101B	102
					110	122F&B	123				
121 LF	Australia	21 (24.70 %)		11 (5.39 %)	1	13	69F	76	87F	102	110
					119	123	132B	161B			
122 WS_F	Australia	32 (19.75 %)	**P**	11 (5.39 %)	13	52	62	66	68F&B	69B	87F&B
					101F&B	102	110	120	**122B**		
122 WS_B	Australia	32 (19.75 %)	**P**	*	11	38B	66	68F	87F&B	102	110
					120	**122F**	123				
123 RRQ	Australia	21 (24.70 %)		15 (7.35 %)	1	13	66	68F&B	87F&B	101F&B	102
					110	120	121	122B	125B	132B	144
					161B						
124 RF	Unknown	14 (16.47 %)		0							
125 WS_B	Unknown	39 (24.07 %)	**P**	2 (0.98 %)	102	123	**125F**				
125 WS_F	Unknown	35 (21.60 %)	**P**	*	102		**125B**				
126 R	Japan	8 (9.41 %)		0							
127 R	Japan	1 (1.18 %)		0							
128 WS_F	Germany	23 (14.20 %)		0							
129 LRQ	Germany	7 (8.23 %)		0							
130 WS_F	Germany	2 (1.23 %)	**P**	0	**130B**						
130 WS_B	Germany	2 (1.23 %)	**P**	*	**130F**						
131 LR	Germany	1 (1.18 %)		0							
132 WS_F	Australia	24 (14.81 %)	**P**	*	1	13	66	110	**132B**		

132 WS_B	Australia	25 (15.43 %)	**P**	10 (4.90 %)	1	13	42	66	76	87F	102
					110	121	123	**132F**			
133 R	Germany	1 (1.18 %)		0							
134 WS_F	Japan	41 (25.30 %)	P	0							
134 WS_B	Japan	26 (16.05 %)	P	0							
135 LF	Japan	11 (12.94 %)		0							
136 WS_F	Belgium	29 (17.90 %)	**P**	0	**136B**						
136 WS_B	Belgium	25 (15.43 %)	**P**	*	**136B**						
137 R	South Korea	3 (3.53 %)		0							
138 WS_F	South Korea	3 (1.85 %)	P	0							
138 WS_B	South Korea	3 (1.85 %)	P	0							
139 WS_F	Japan	34 (20.99 %)	**P**	0	**139B**						
139 WS_B	Japan	24 (14.81 %)	**P**	*	**139F**						
140 WS_F	Japan	39 (24.07 %)	**P**	0	**140B**						
140 WS_B	Japan	41 (25.30 %)	**P**	*	**140F**						
141 RF	Japan	6 (7.05 %)		0							
142 WS_F	Australia	5 (3.09 %)	**P**	0	**142B**						
142 WS_B	Australia	5 (3.09 %)	**P**	*	**142F**						
143 RF	Australia	7 (8.23 %)		0							

144 RRQ	Australia	6 (7.05 %)		7 (3.43 %)	13	62	66	69B	87F	101F	123
145 WS_F	Japan	23 (14.20 %)	**P**	1 (0.49 %)	113F&B	**145B**					
145 WS_B	Japan	23 (14.20 %)	**P**	*	113F&B	**145F**					
146 WS_B	Unknown	25 (15.43 %)	P	0							
146 WS_F	Unknown	25 (15.43 %)	P	0							
147 WS_B	Australia	4 (2.7 %)	**P**	*	**147F**						
147 WS_F	Australia	5 (3.09 %)	**P**	0	**147B**						
148 WS_F	South Korea	25 (15.43 %)	P	0							
148 WS_B	South Korea	28 (17.28 %)	P	0							
149 WS_B	Belgium	24 (14.81 %)	**P**	*	**149F**						
149 WS_F	Belgium	30 (18.52 %)	**P**	0	**149B**						
150 WS_F	Thailand	23 (14.20 %)	P	0							
150 WS_B	Thailand	18 (11.11 %)	P	0							
151 RF	Thailand	5 (5.88 %)		0							
152 WS_F	Japan	28 (17.28 %)	**P**	0	**152B**						
152 WS_B	Japan	40 (24.69 %)	**P**	*	**152F**						
153 WS_F	Japan	31 (19.14 %)	P	0							
153 WS_B	Japan	42 (25.93 %)	P	0							
154 RF	Japan	6 (7.05 %)		0							
155 WS_F	South	3 (1.85 %)	P	0							

	Korea										
155 WS_B	South	4 (2.7 %)	P	0							
	Korea										
156 WS_F	Belgium	4 (2.7 %)	**P**	*****	**156B**						
156 WS_B	Belgium	4 (2.7 %)	**P**	0	**156F**						
157 WS_F	Japan	37 (22.84 %)	P	0							
157 WS_B	Japan	32 (19.75 %)	P	0							
158 LF	Japan	9 (10.59 %)		0							
159 WS_F	Italy	42 (25.93 %)	P	0							
159 WS_B	Italy	23 (14.20 %)	P	0							
160 LRQ	Italy	8 (9.41 %)		0							
161 WS_F	Thailand	35 (21.60 %)	**P**	*	11	38	61	62	69F&B	80	**161B**
161 WS_B	Thailand	35 (21.60 %)	**P**	7 (3.43 %)	69F	76	87F&B	101B	102	110	123
					161F						
162 RRQ	Thailand	15 (17.65 %)		0							
167 WS_F	USA	31 (19.14 %)	**P**	0	**167B**						
167 WS_B	USA	39 (24.07 %)	**P**	*	**167F**						
168 LRQ	England	6 (7.05 %)		0							
169 R	England	22 (25.88 %)		0							
170 WS_F	Australia	35 (21.60 %)	P	0							
170 WS_B	Australia	35 (21.60 %)	P	0							
171 WS_F	USA	28 (17.28 %)	**P**	1 (0.49 %)	35F	**171F**					

171 WS_B	USA	30 (18.52 %)	**P**	*		**171B**
172 WS_F	Japan	23 (14.20 %)	**P**	1 (0.49 %)	37B	**172B**
172 WS_B	Japan	27 (16.67 %)	**P**	*		**172F**
173 WS_B	Japan	31 (19.14 %)	P	0		
173 WS_F	Japan	23 (14.20 %)	P	0		
174 WS_B	South Korea	5 (3.09 %)	**P**	1 (0.49 %)	78F	**174F**
174 WS_F	South Korea	5 (3.09 %)	**P**	*	78F	**174B**
175 RF	Unknown	6 (7.05 %)		0		